



Curtin University

# *Computer Vision and Deep Learning Techniques for Vibration based Structural Health Monitoring*

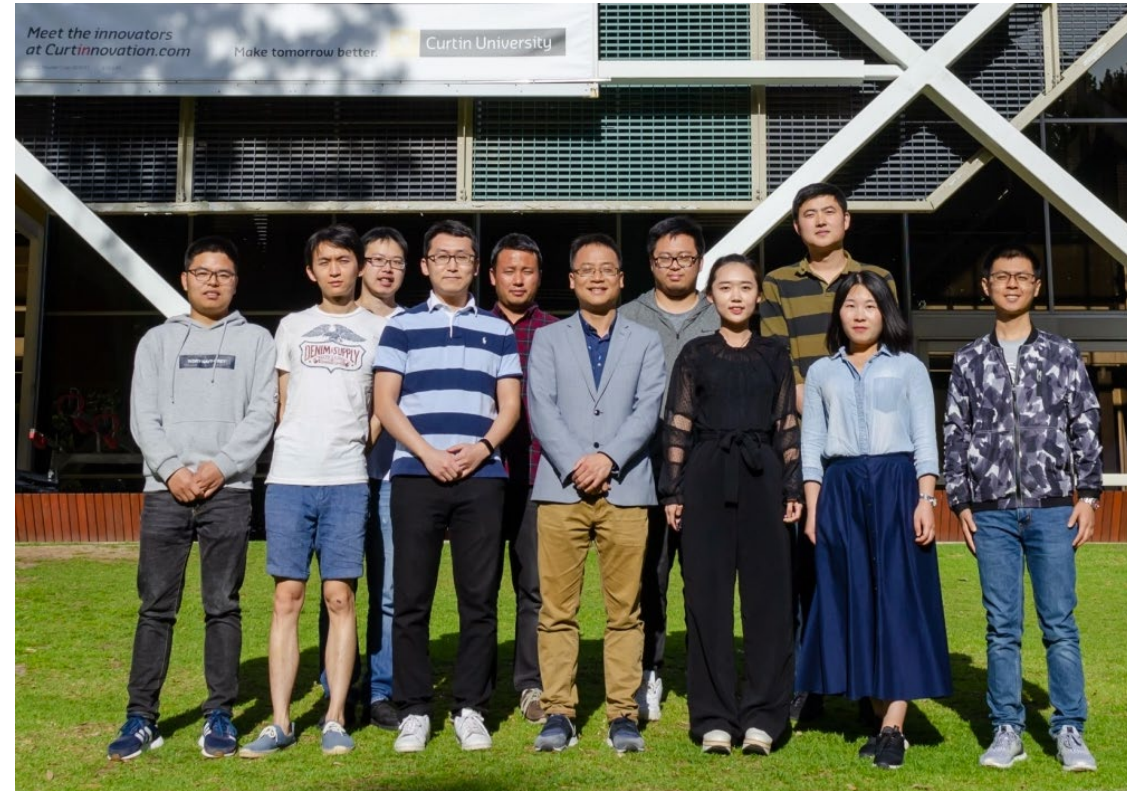
**Dr Jun Li, ARC Future Fellow, Associate Professor**

**Centre for Infrastructural Monitoring and Protection**

**School of Civil and Mechanical Engineering, Curtin University, Australia**

# Acknowledgements

- Collaborators: Prof. Hong Hao, Prof. Ling Li, Dr Senjian An, Curtin University
- Team members, research fellows: Dr Ruhua Wang, Dr Zhen Peng,
- Former and current PhD students: Dr C.S. Nadith Pathirage, Dr Gao Fan, Dr Zhenghao Ding, Mr Dong Tan, etc
- ARC research grants, Future Fellowship, Discovery Projects, etc



# OUTLINE

1. Background
2. Review on Vision and Artificial Intelligence (AI) in SHM
3. Target-free vision-based displacement measurement
4. Deep learning (GAN) for response reconstruction
5. Novel data analytics for condition monitoring
6. Engineering applications
7. Conclusions





# 1. Background

Risk in new constructions and ageing infrastructure



Risks in new design, new construction technologies, behavior understanding of new structural forms and materials

Risks in aged bridges in the regular maintenance and inspection to cater for the growing traffic demand with the decreasing load carrying capacity

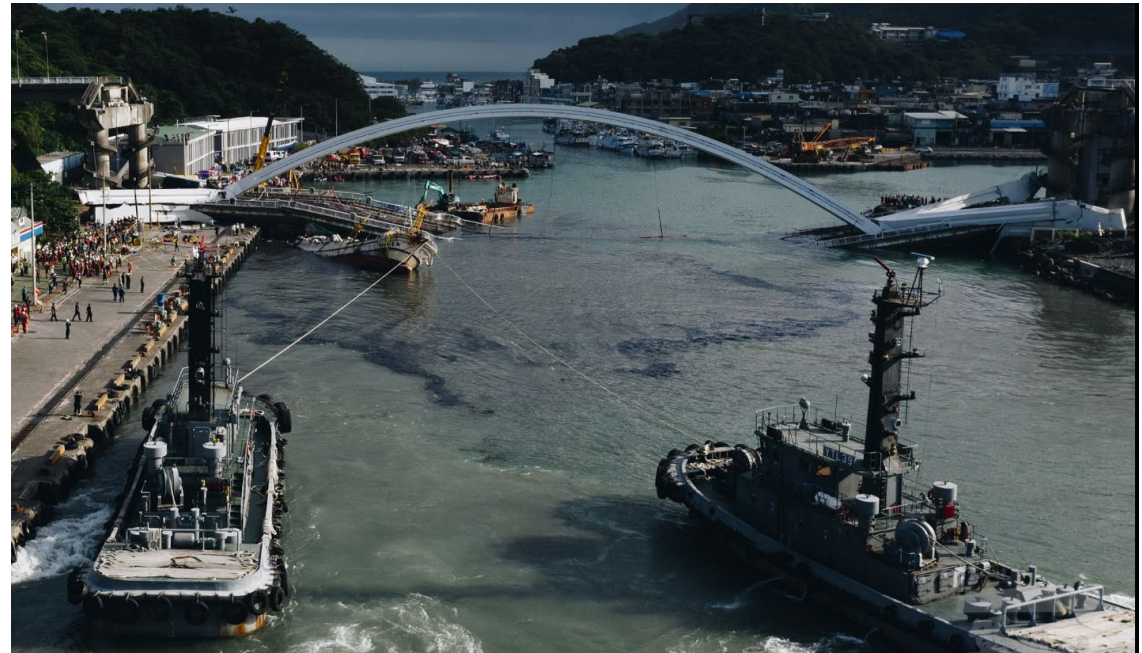




- Bridge safety are essential for society and community
- Maintenance for ageing infrastructure is important and could be expensive

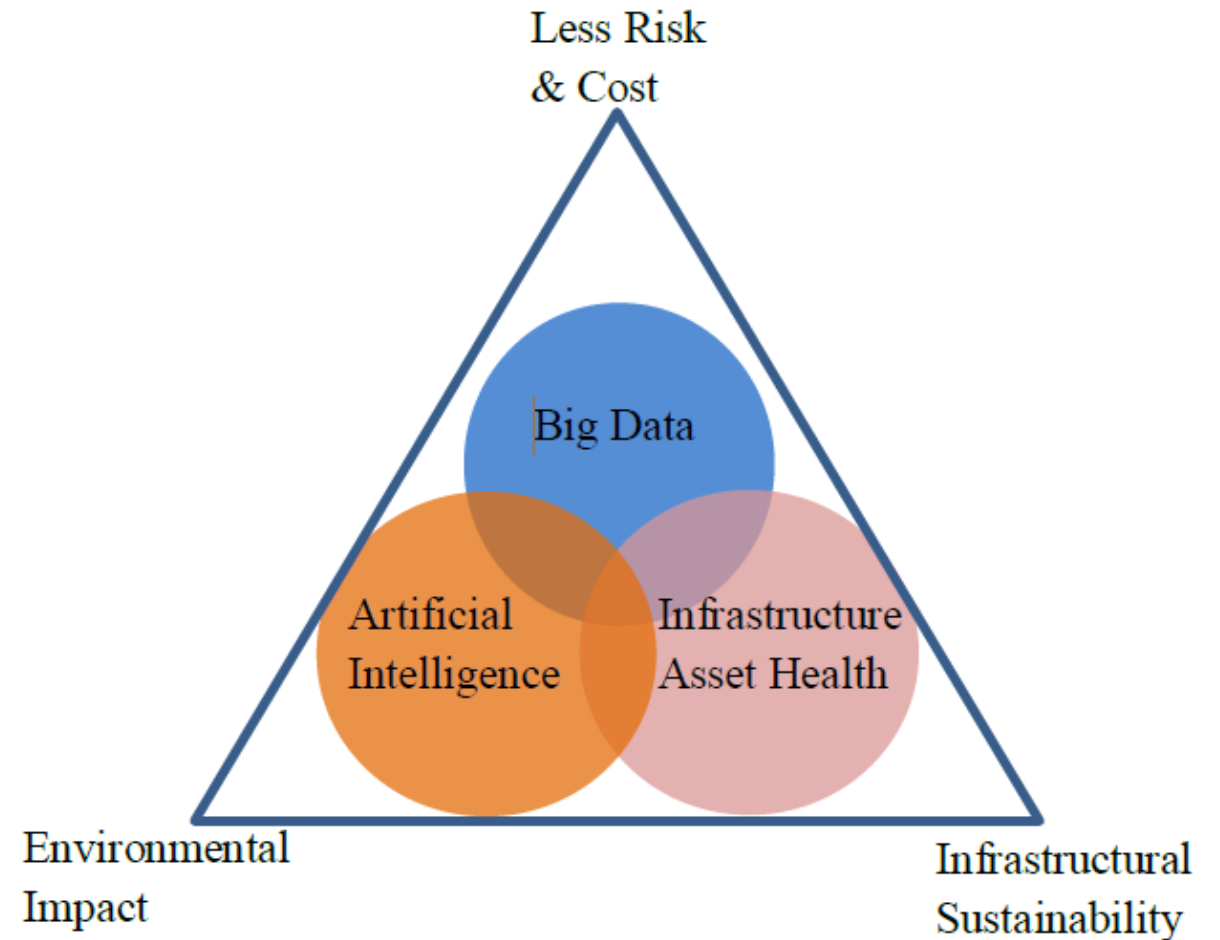
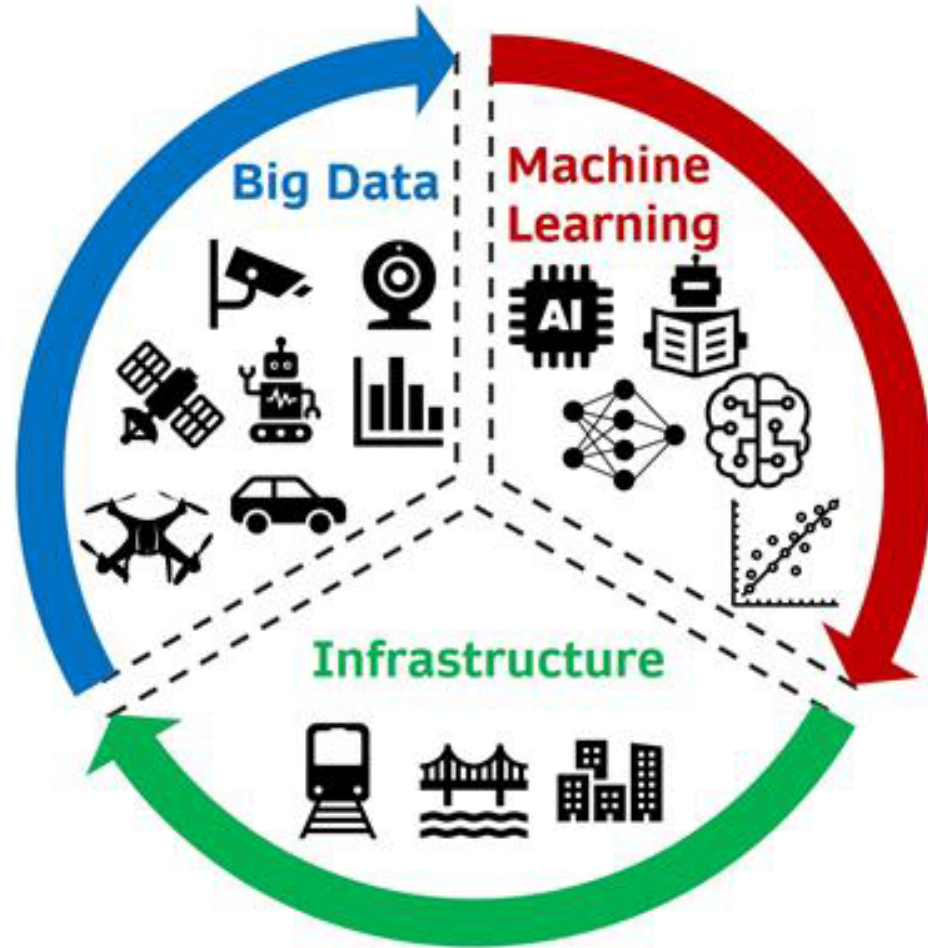


The Morandi bridge tragedy killed 43 and left 600 homeless – but also dealt a hammer blow to Italy’s engineering legacy. *The Guardian*. (2018)



Total collapse of Nanfang'ao Bridge in Taiwan, in 2019, caused 4 dead and 10 injured.

# Civil engineering structures & AI & Big data

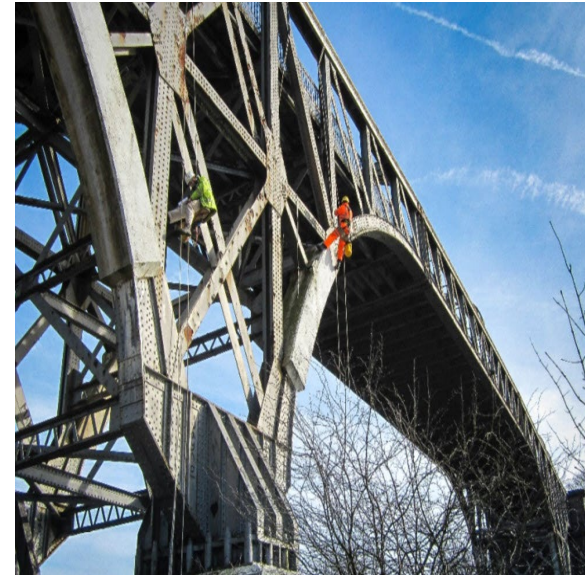


<https://www.frontiersin.org/research-topics/16803/machine-learning-methods-and-big-data-analytics-in-structural-health-monitoring#overview>



# Bridge Inspection

- Time consuming and costly (Chase and Edwards 2011, Sanford et al. 1999)
- Subjective and not always reliable (Phares et al. 2004, Moore et al. 2001)
- Hard to conduct the assessment of inaccessible part of the structure
- Not allowing rapid and quantitative based decision regarding repairs (Metni and Hamel 2007)

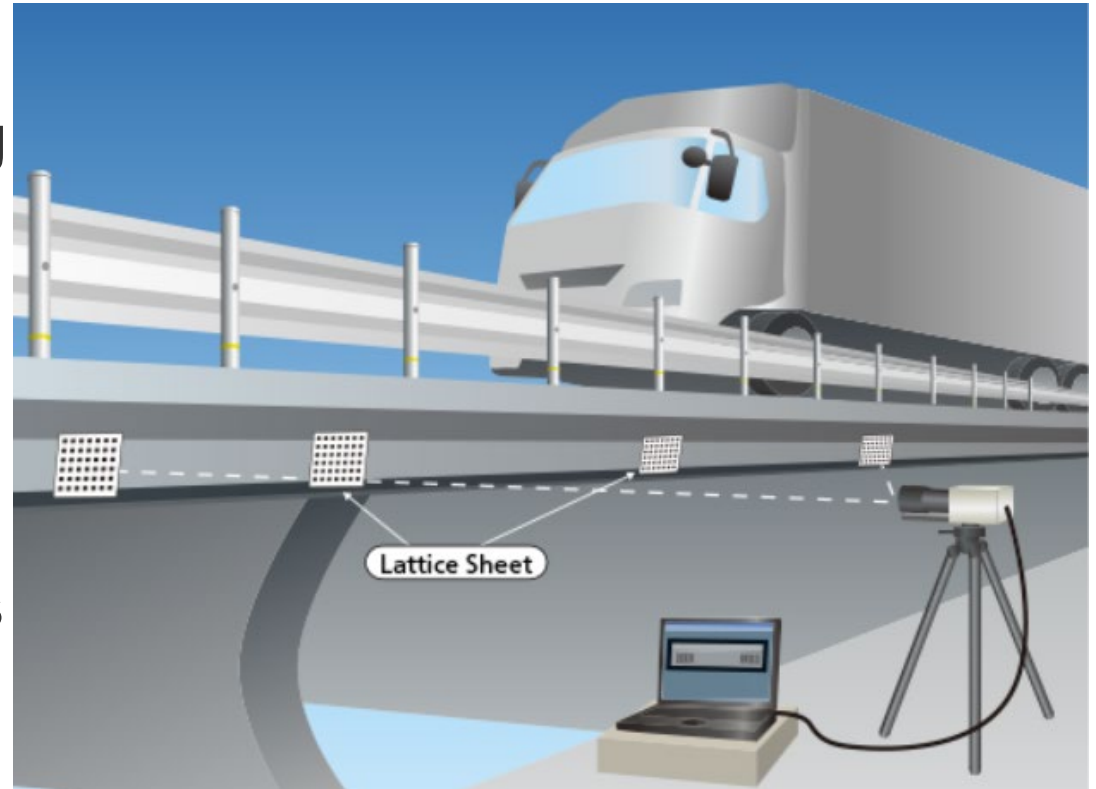


- Require lane closure and traffic control measure
- Traffic control and access unit consume 40-50% of the budget and mobilization of inspection units need 40-50% of the overall time (Highway IDEA project, Choset 2000)



# Needs to develop cost effective methods

- As the bridges age and continue to deteriorate, not updating the traditional inspection methods pose a risk to the traveling public and a nations economic viability.
- Needs to reduce lane closures and traffic disruptions, and dangers to personnel.
- Non-Contact vision and image based techniques can provide cost effective methods for bridge inspection
- Vibration displacement responses can be used to assess the health condition and serviceability of bridges

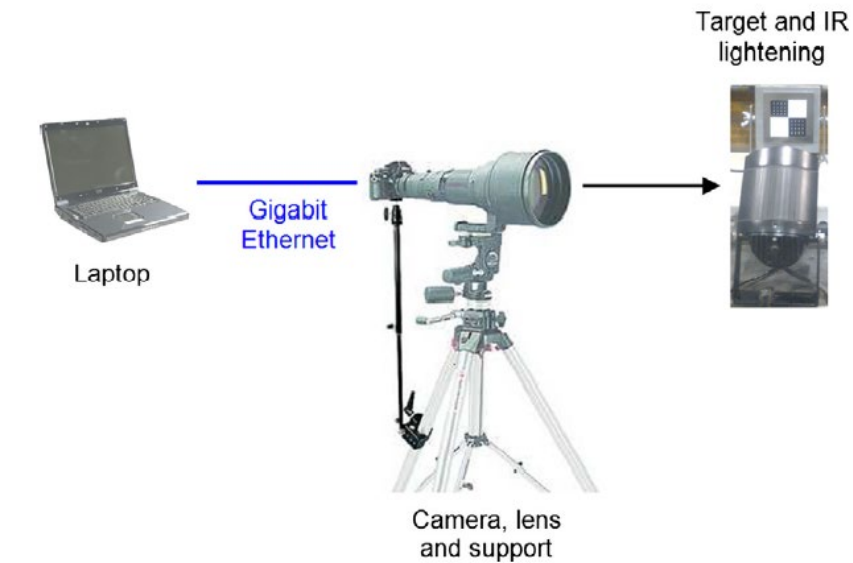


Target based or Target free?

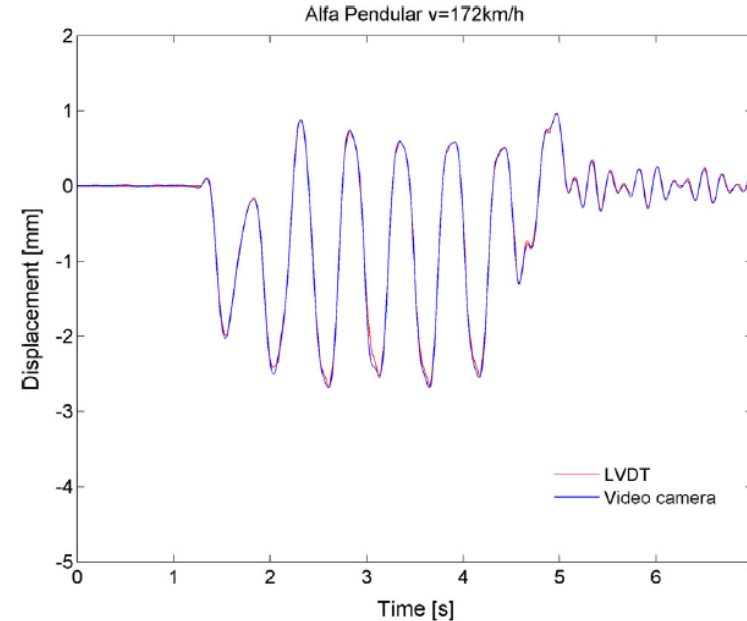
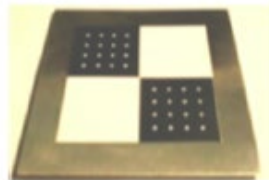
# 2 Vision sensing and AI techniques for SHM

## (a) Vision Based Method

Artificial targets on structures required



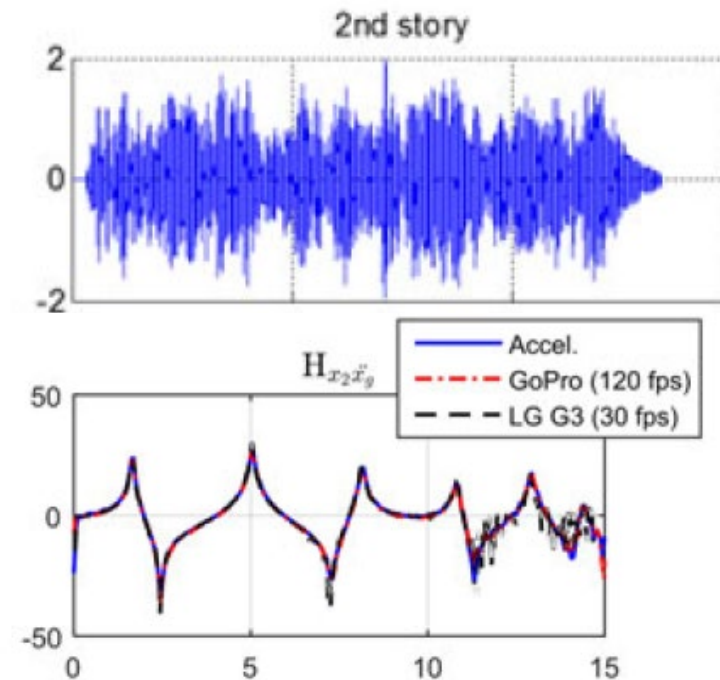
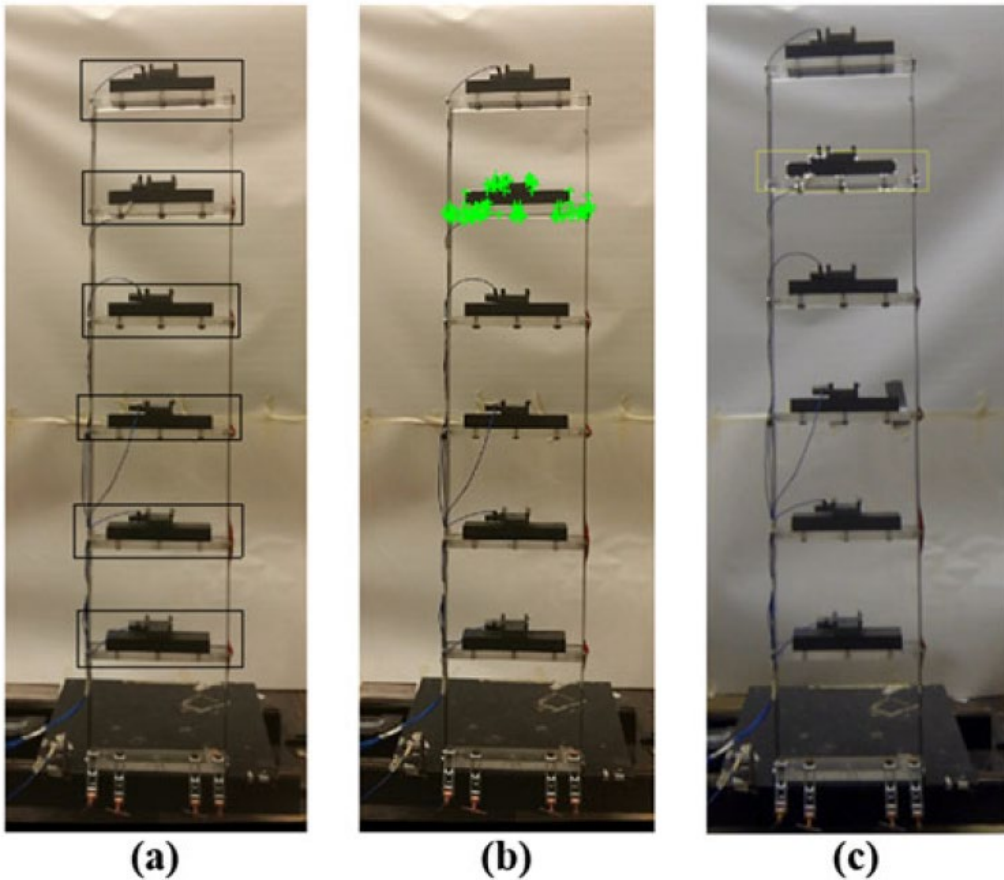
Precision target



- Digital image correlation (DIC) techniques are used;
- Vibration measurements under significant vibrations;
- Environmental conditions, artificial lights may also be required.

# Target-free Computer Vision Based Method

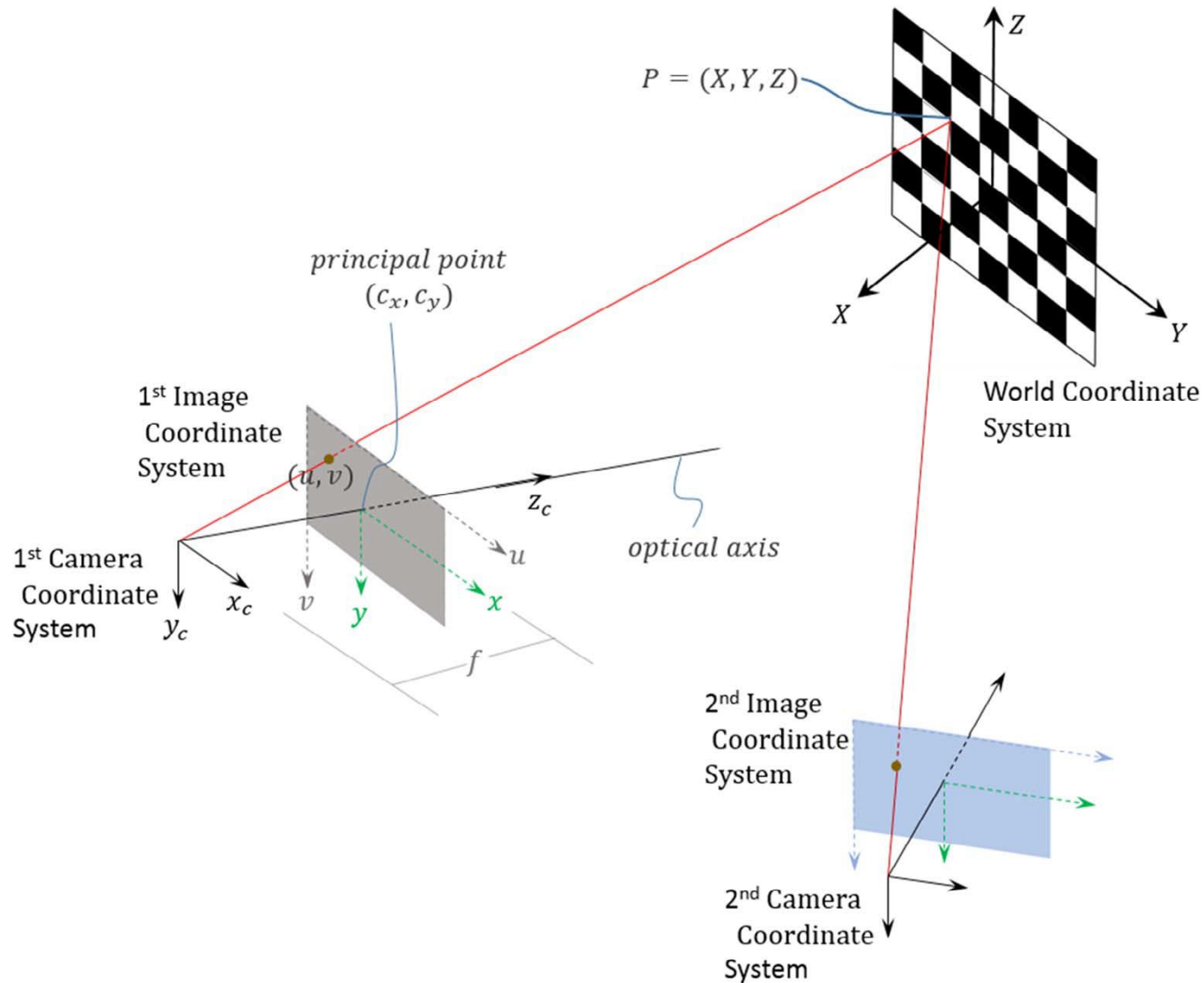
- Using structural natural features and component textures



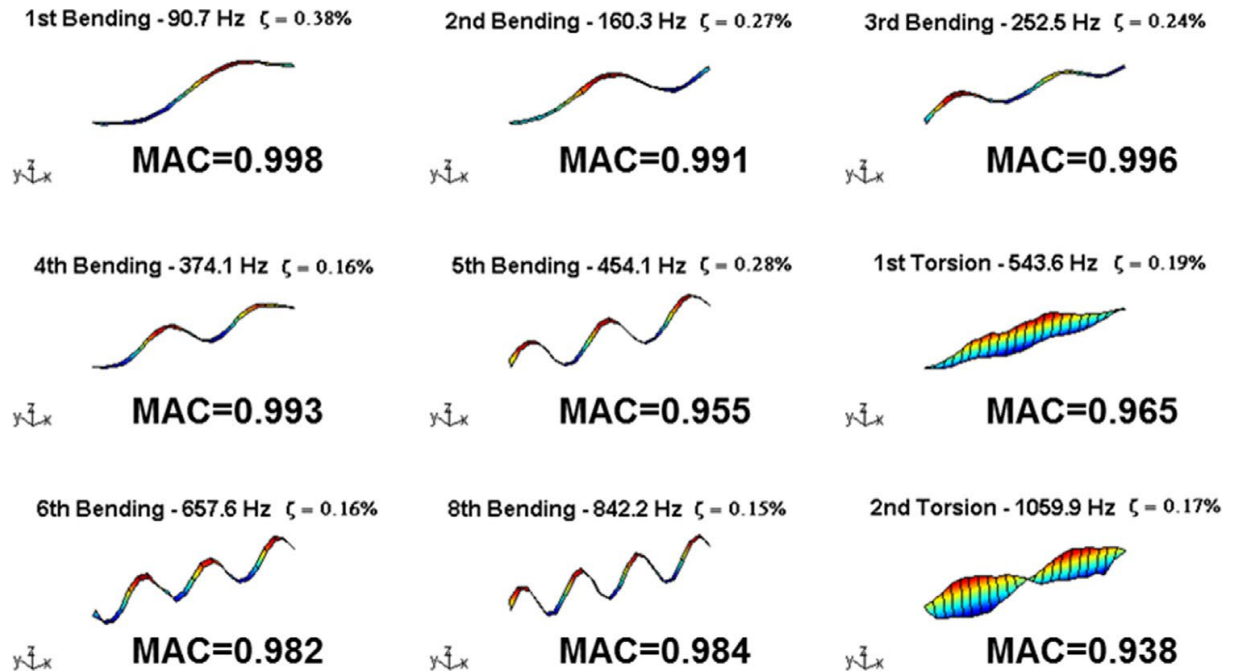
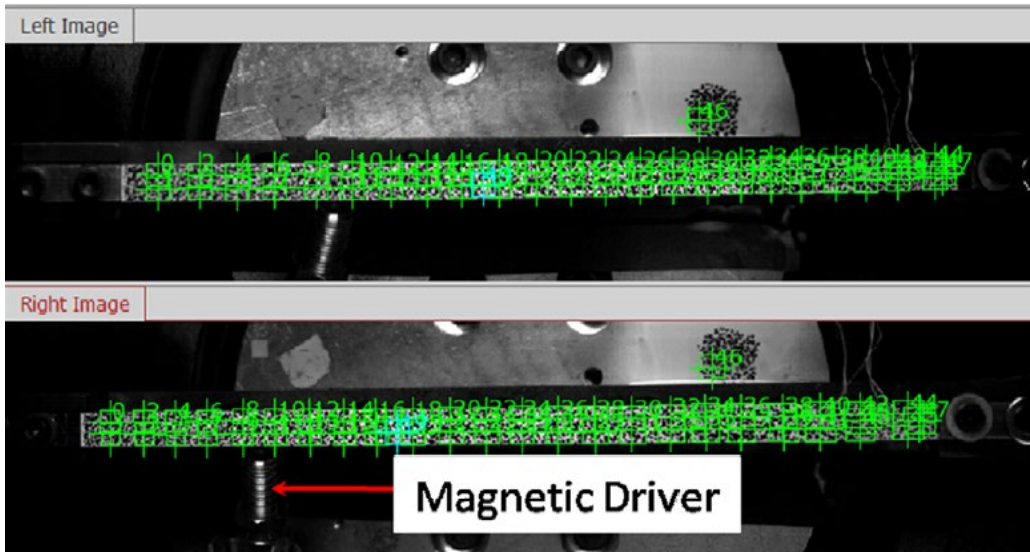
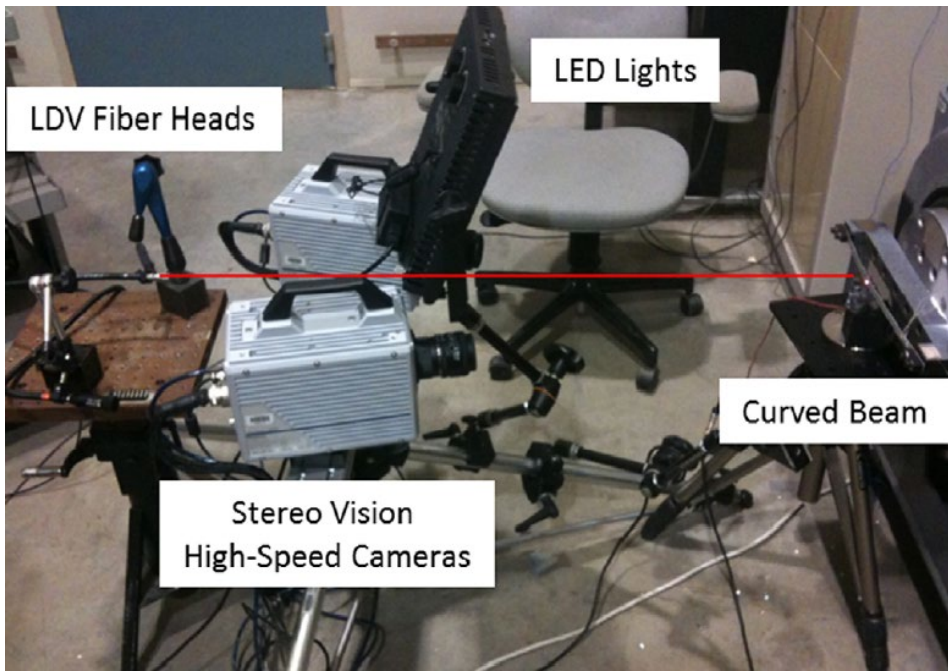
- Displacement measurements under uni-axial vibrations
- Accuracy affected by the used consumer grade cameras and frame rate



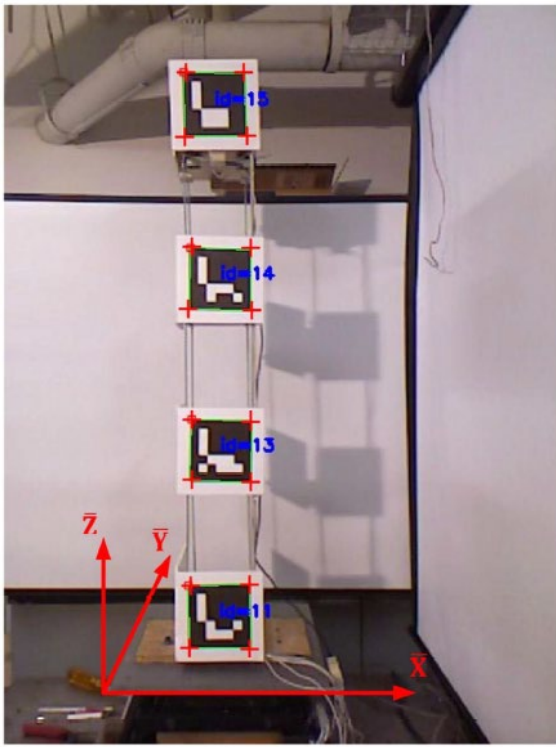
- 3D measurement



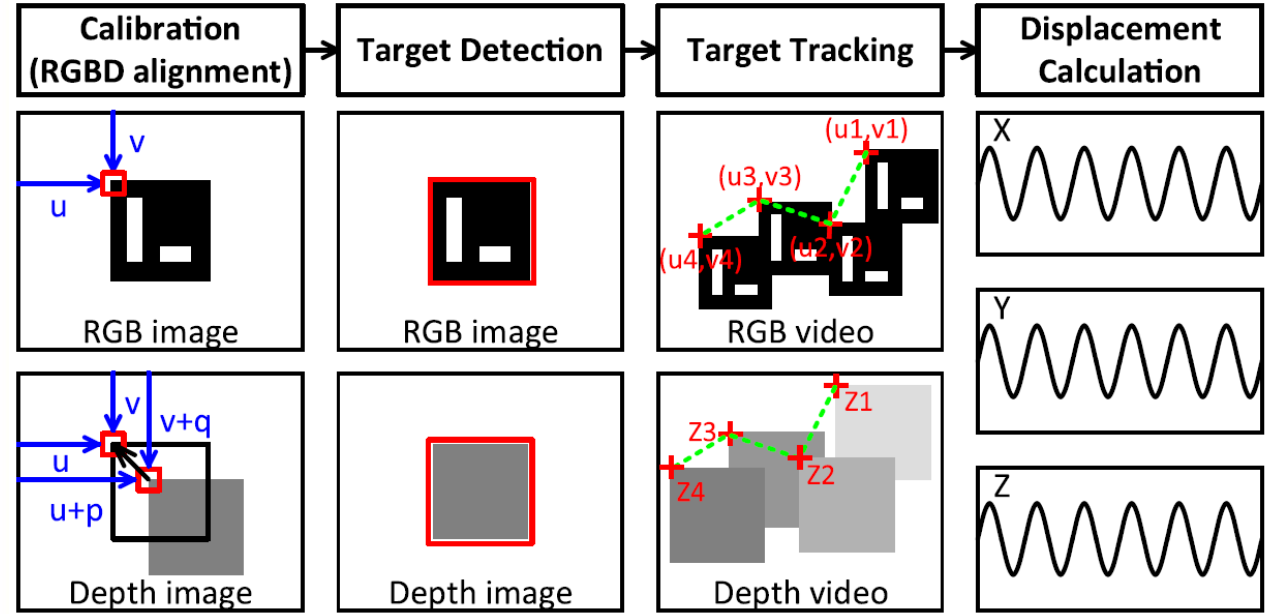
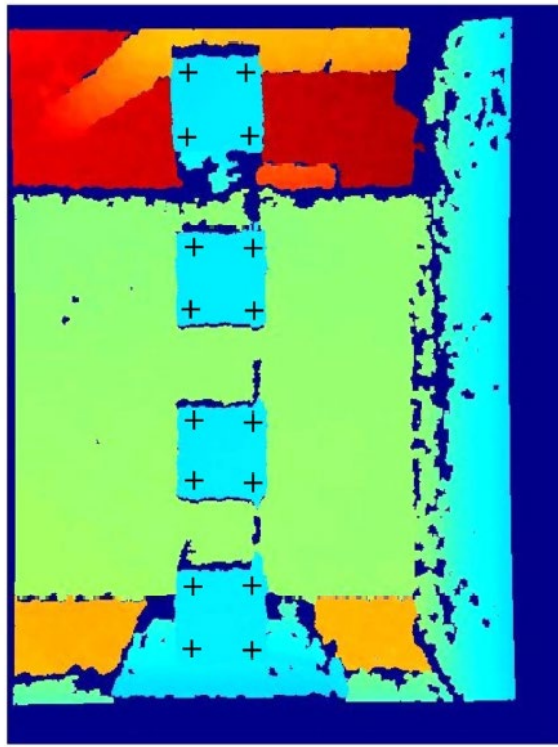
- Most vision based methods focus on 1D or 2D displacement measurement;
- In-plane measurement accuracy is sensitive to out-of-plane motion;
- Accuracy of 3D vibration displacement measurement is a significant challenge



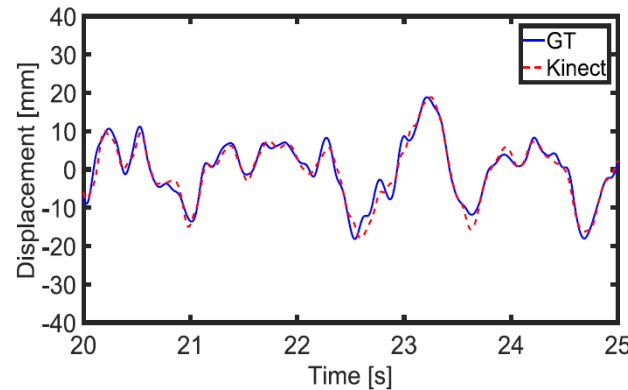
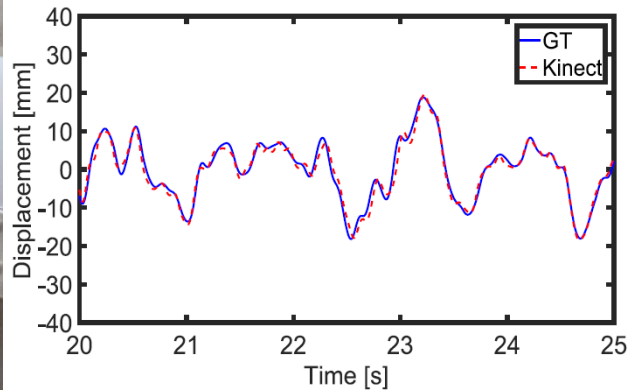
- A camera angle between 20° and 30° is ideal;
- Speckle pattern with white spray paint base and black permanent marker dots;
- Out-of-plane movement at 6.38mm – 4.70mm;



(a)



Cameras with depth sensing capabilities  
 markers used  
 640\*480@30fps



Abdelbarr et al., SMS, 2017

Curtin University is a trademark of Curtin University of Technology  
 CRICOS Provider Code 00301J



# Motion magnification for vibration measurement

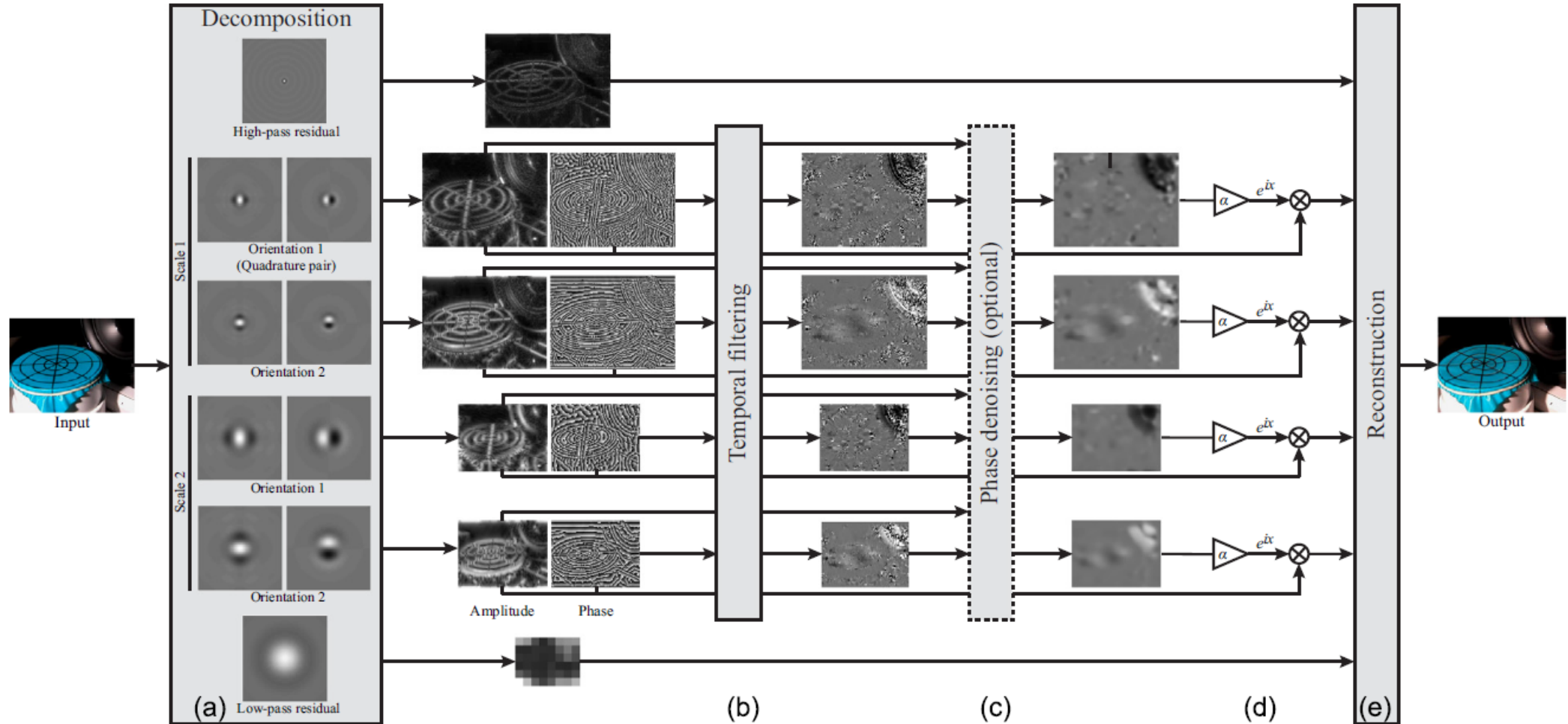
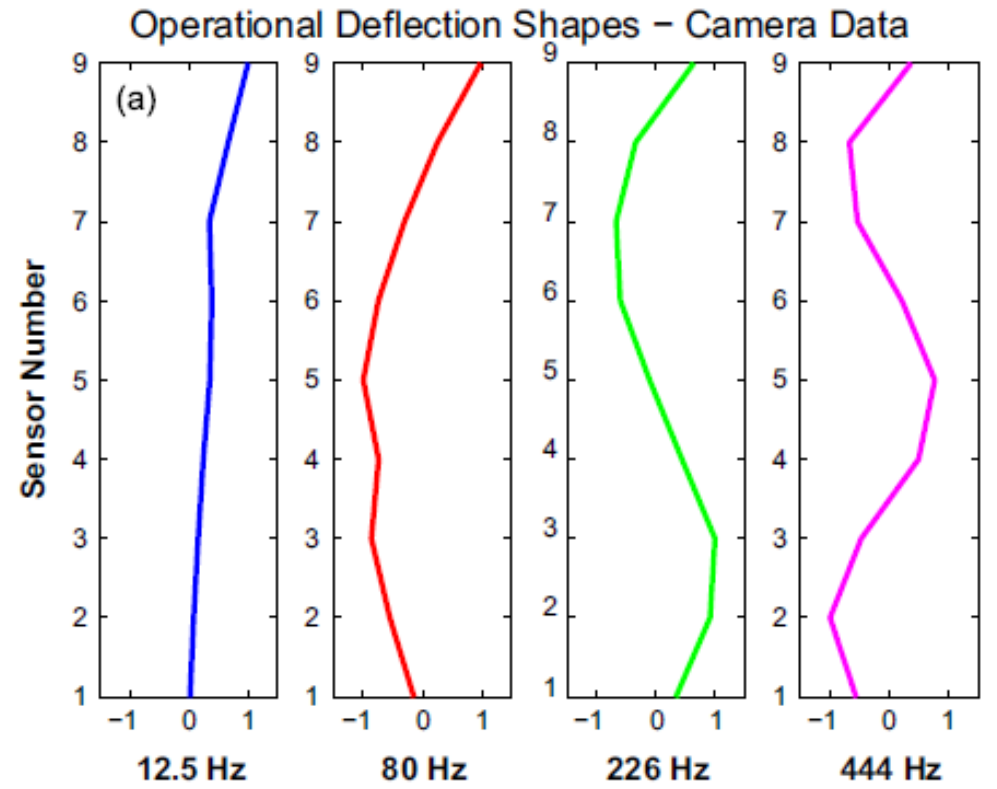
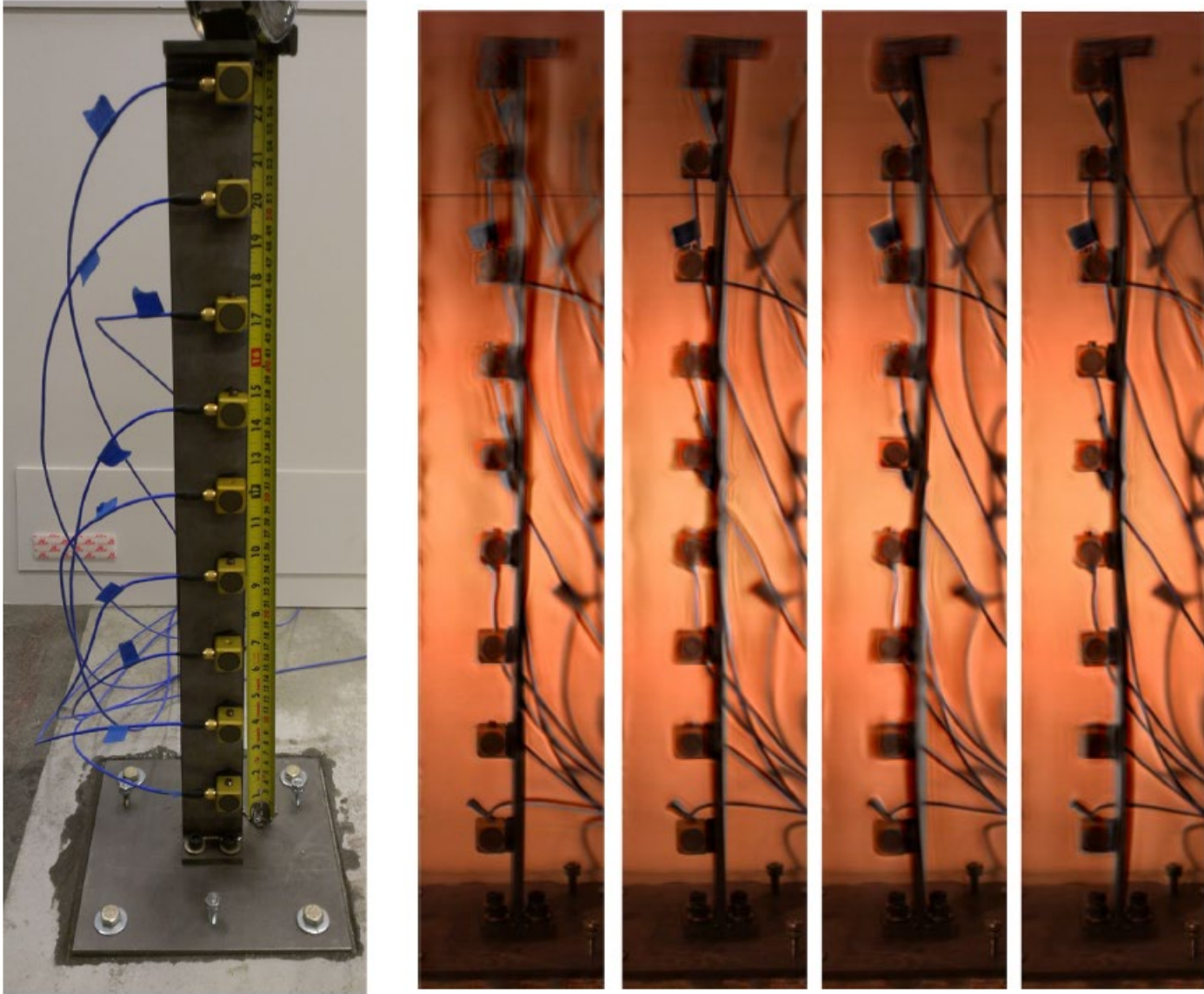


**Fig. 1.** Motion magnification processing workflow: (a) complex steerable pyramid filters decompose the video into amplitude and phase at different scales, (b) the decomposed phases are bandpass filtered in frequency, (c) amplitude-weighted smoothing is applied, (d) the bandpassed phases are amplified or attenuated, and (e) the video is reconstructed [14].

(a)



# Challenges in vision-based 3D displacement measurement

## 1. **3D** displacement measurement

- *Only 2D displacement can be obtained by a single camera*
- *Depth direction displacement measurement is difficult*

## 2. **Subtle displacement (less than 1mm level)** measurement

- *Difficult to measure by traditional sensors owing to uncertainties*
- *Leading to image features tracking and matching failure*
- *Motion magnification only applicable to 1D or 2D with a camera*

## 3. **Target-free** displacement measurement

- *Need hundreds pairs of matched key points to properly calibrate stereo cameras.*
- *The accuracy of triangulation algorithm will be impacted by wrong matched features*



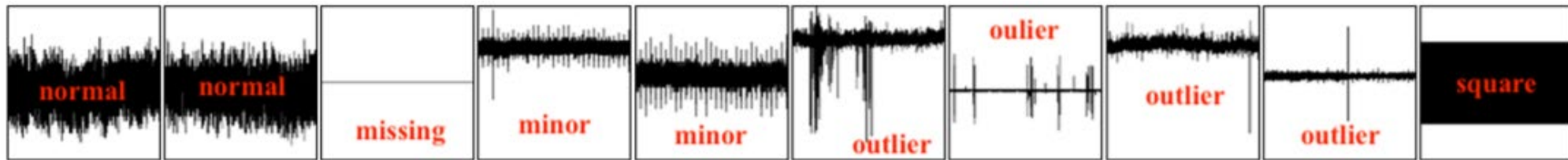
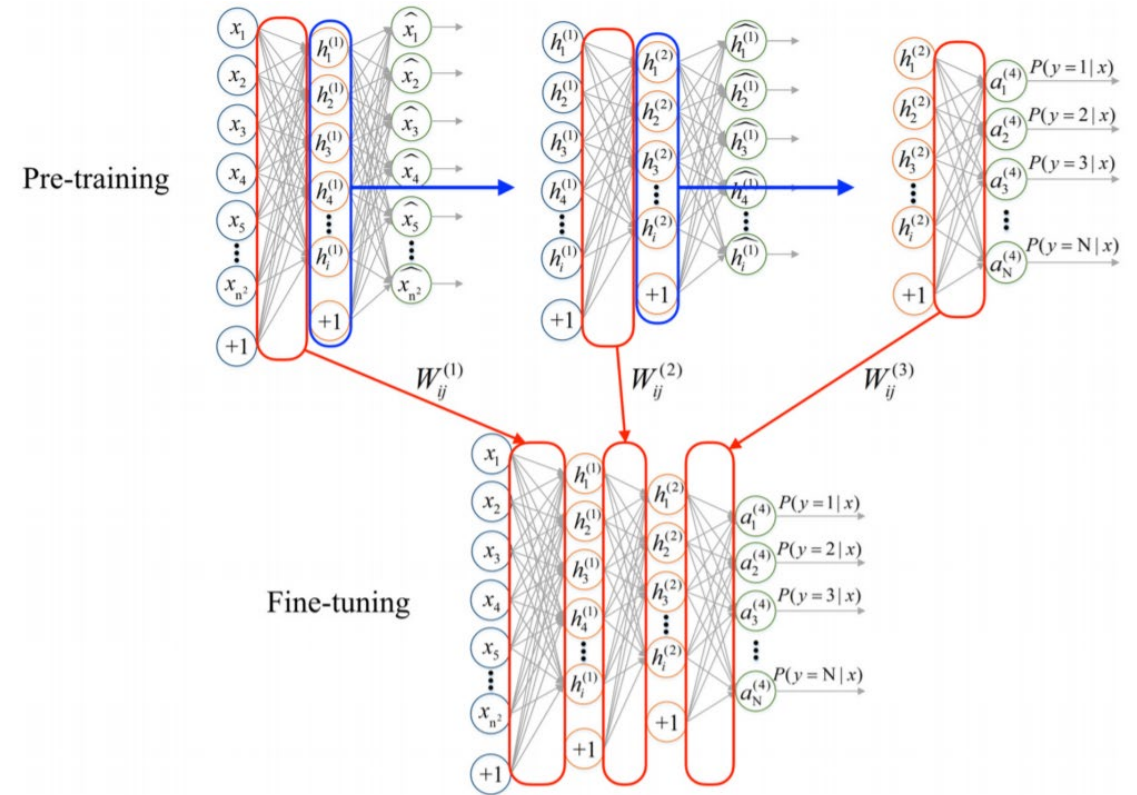
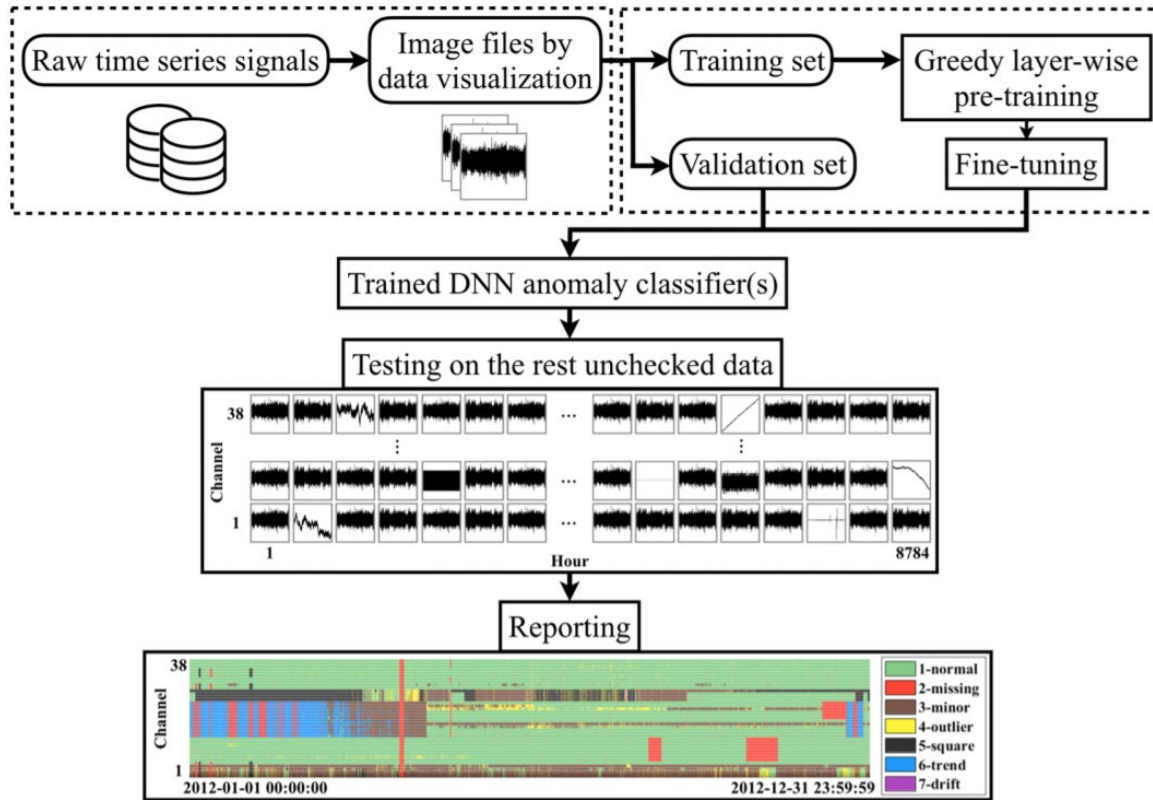
## (b) AI in SHM

### *Machine learning*

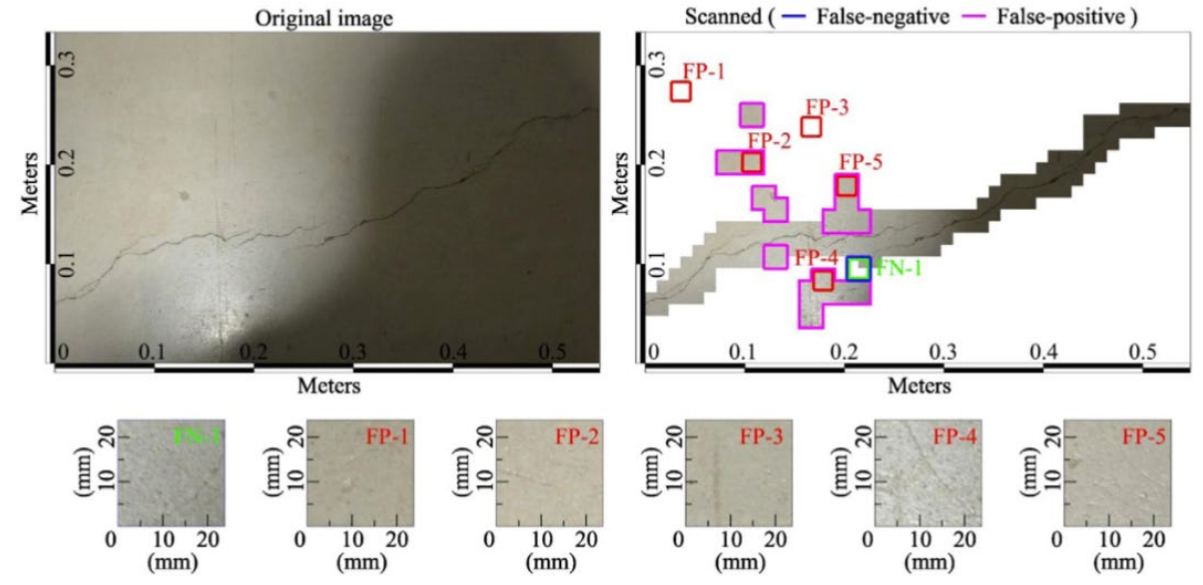
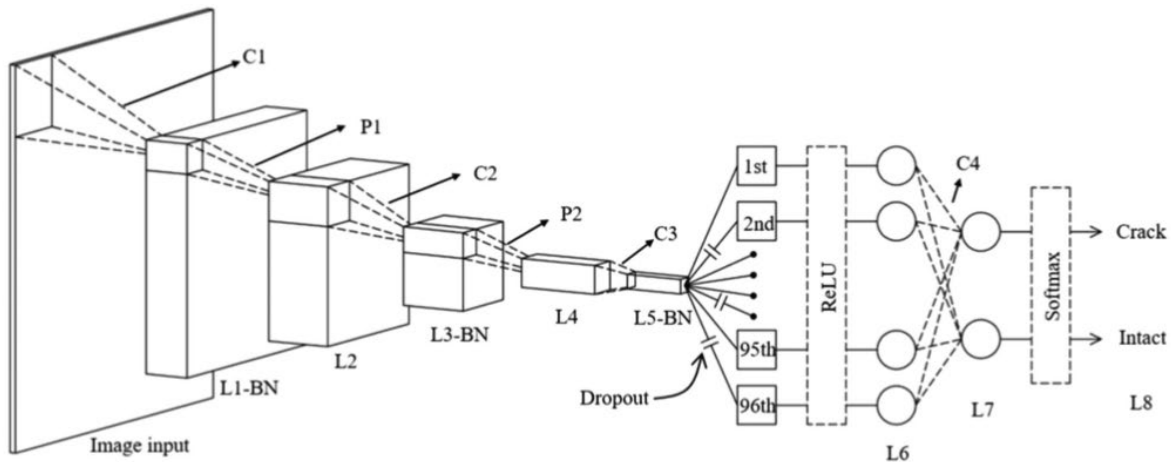
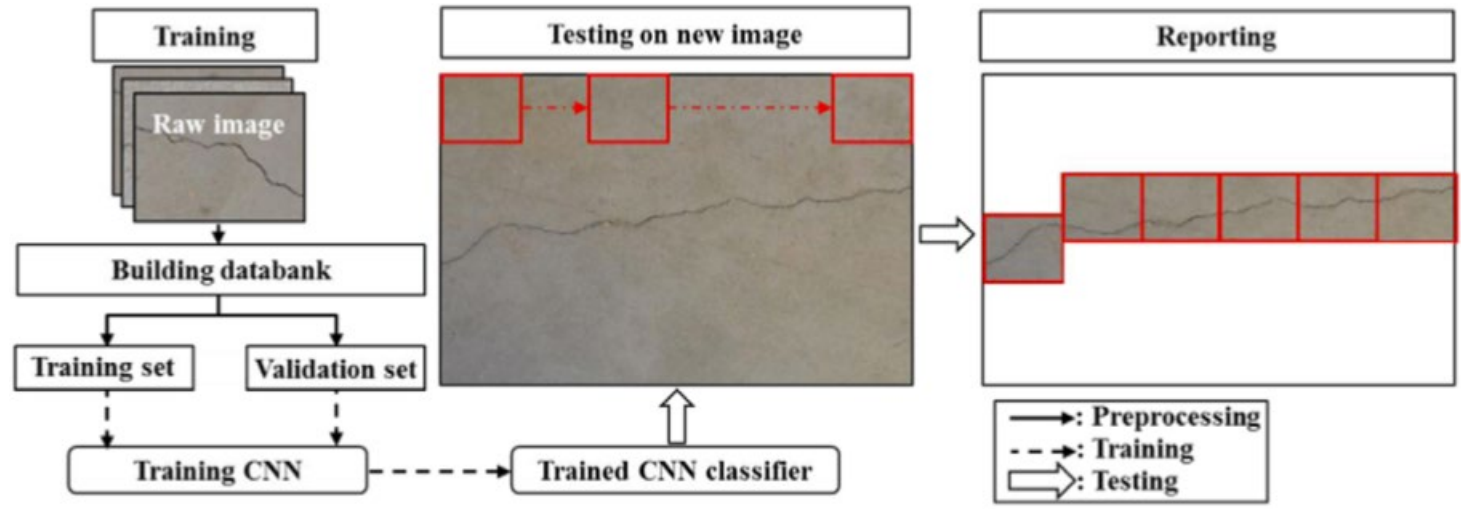
- Explores the study and construction of algorithms that can learn from and make predictions on data
- Operates by building a model from example inputs in order to make data-driven predictions or decisions, rather than following strictly static program instructions.

CNN, RNN, Artificial Neural Network, Genetic Algorithms, Support Vector Machines, Clustering, Sparse Dictionary Learning, Decision Tree, Transfer learning, GAN,...

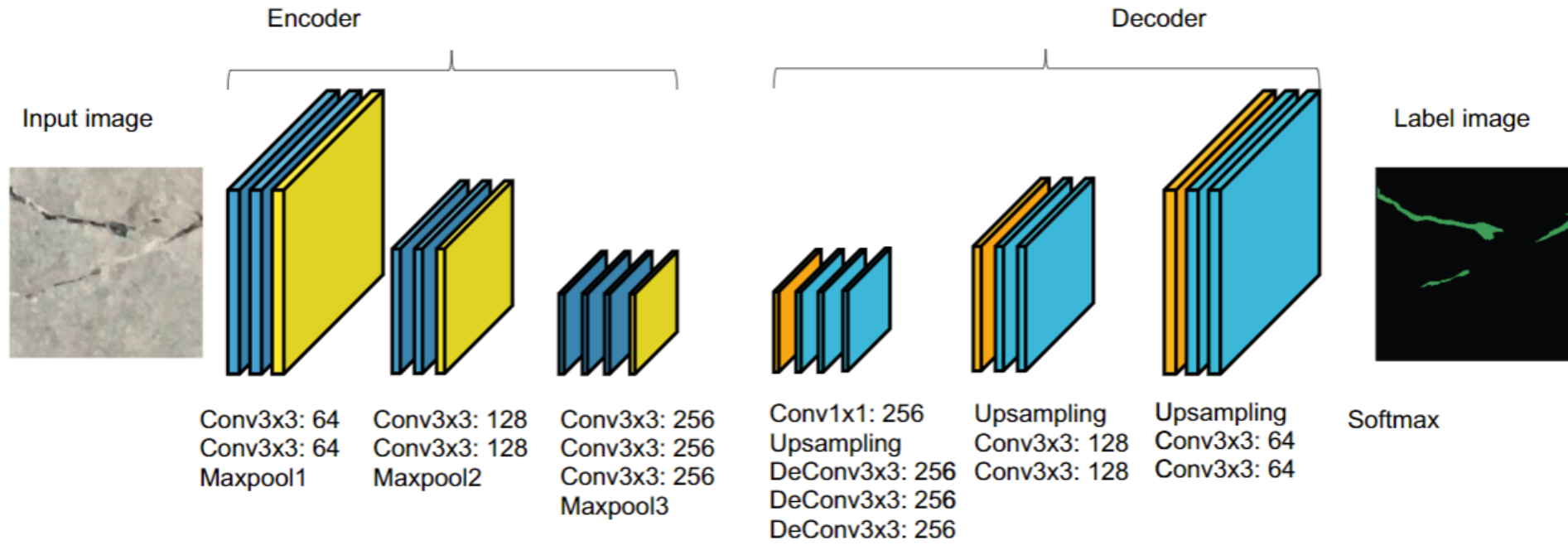
# Data abnormality detection



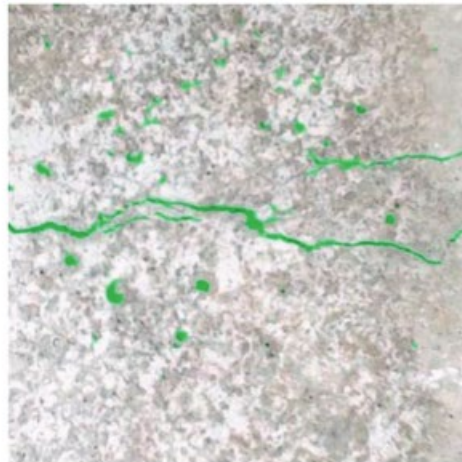
# Crack detection







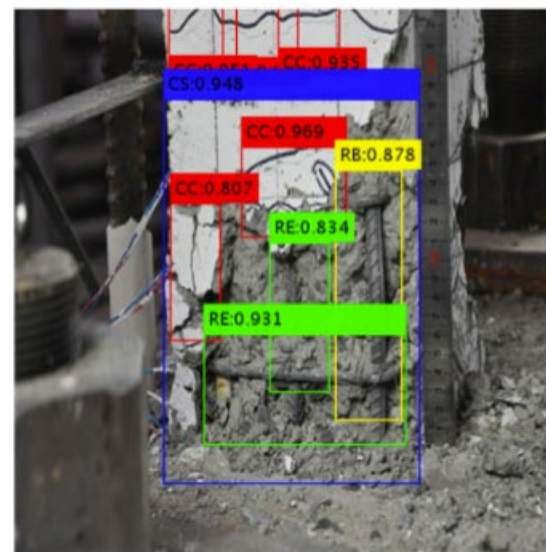
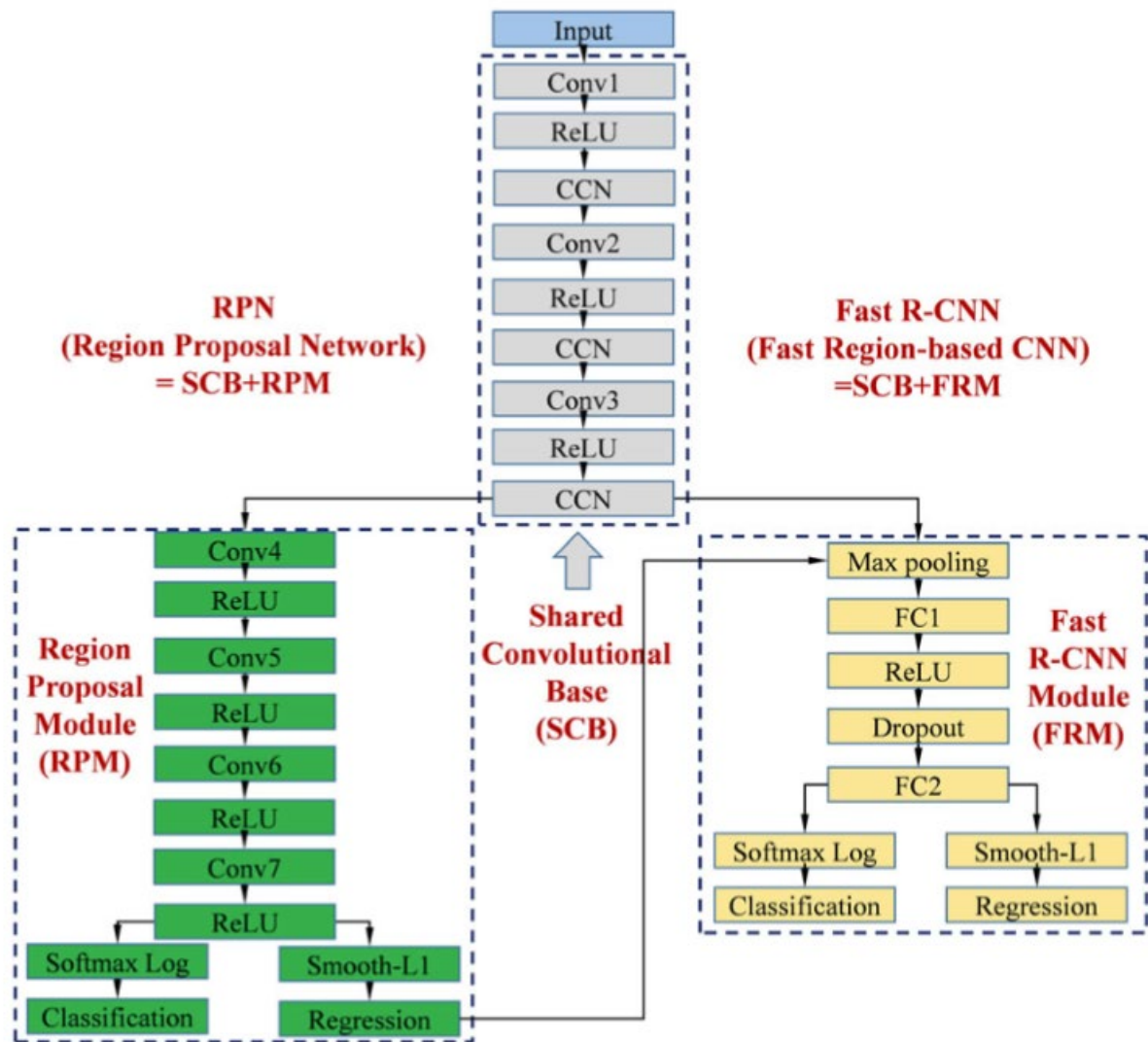
(a) Original image



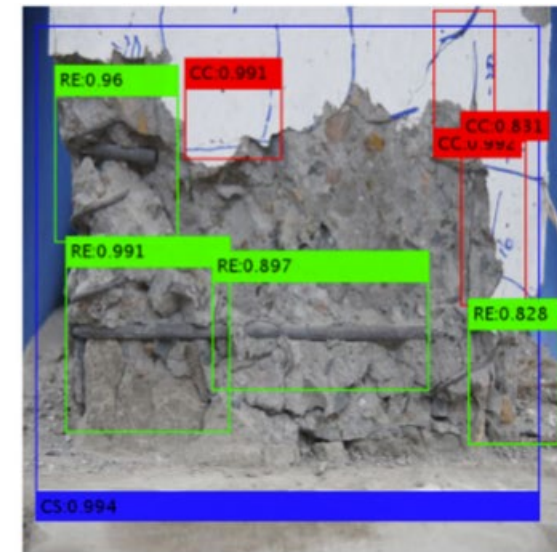
(b) Segmented image

Dung and Anh, Automation in Construction 2019

# Damage type detection



a) Identified damage types: CC, CS, RE and RB

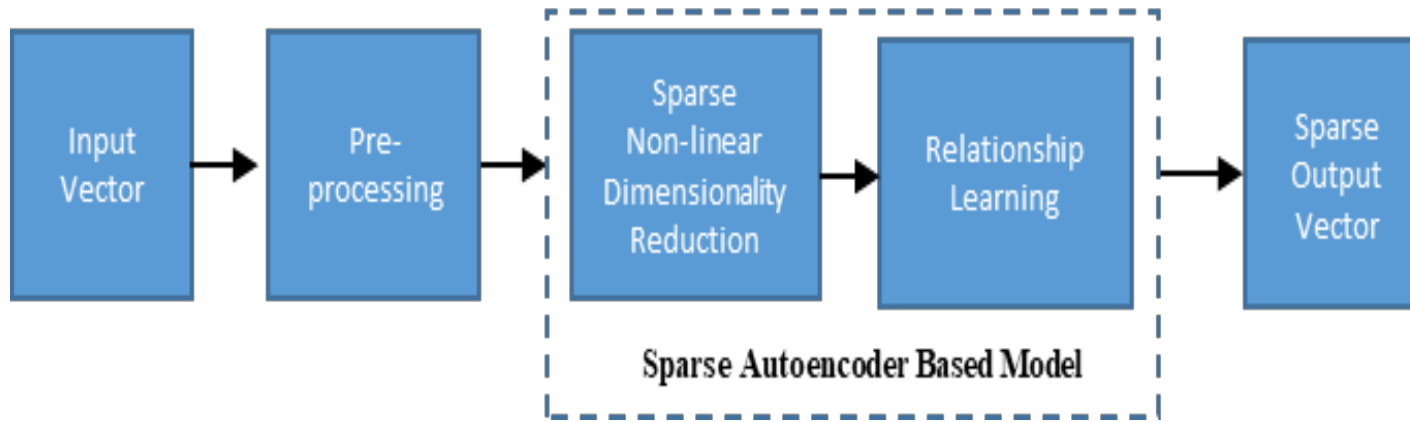


(b) Identified damage types: CC, CS and RE

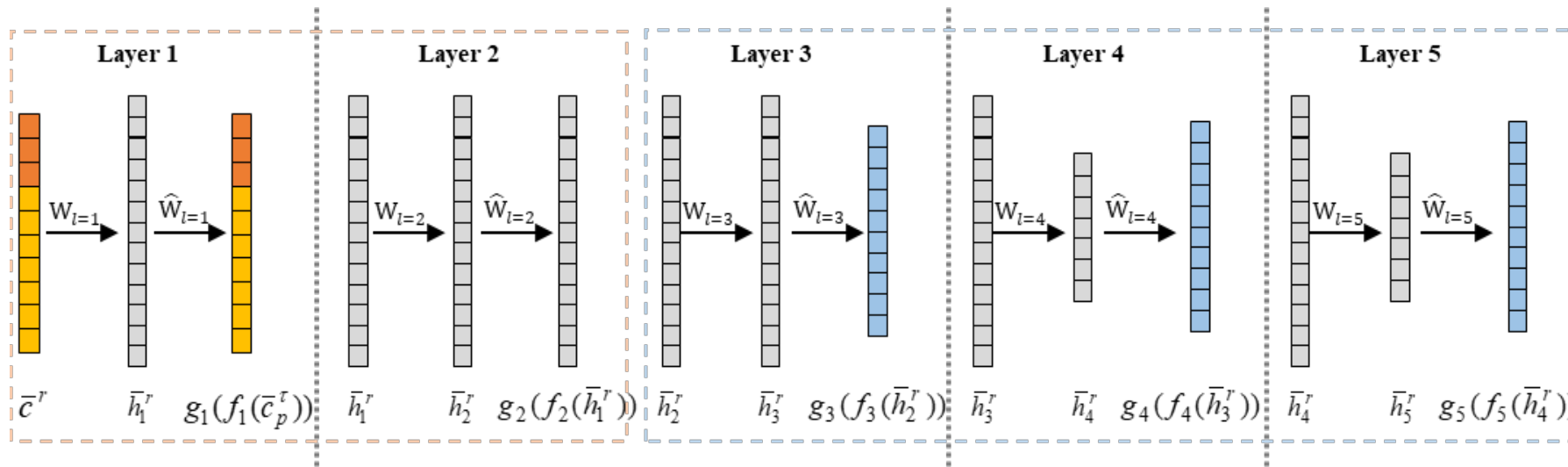
Xu et al. 2019, SCHM, 19, e2313.

# Structural damage identification

## Sparse Autoencoder Framework (SAF)

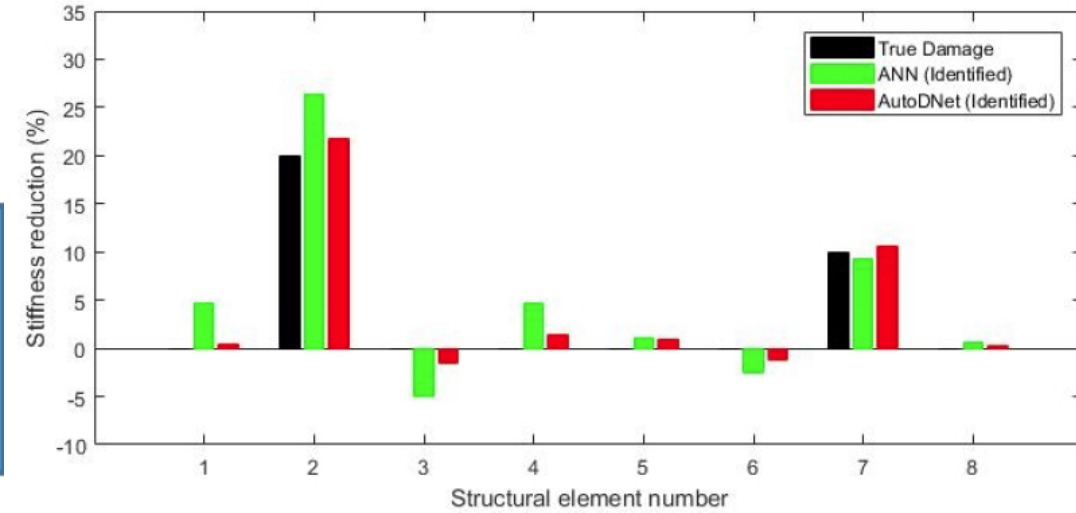


Layer wise Pre-Training



sparse non-linear dimensionality reduction

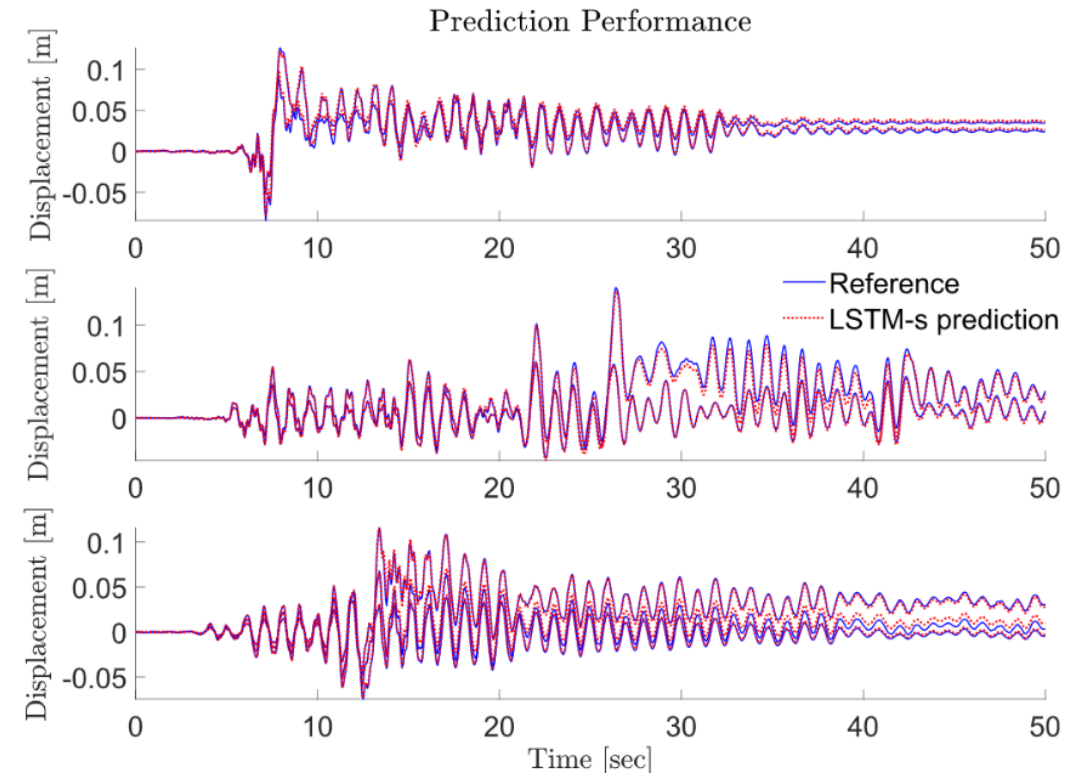
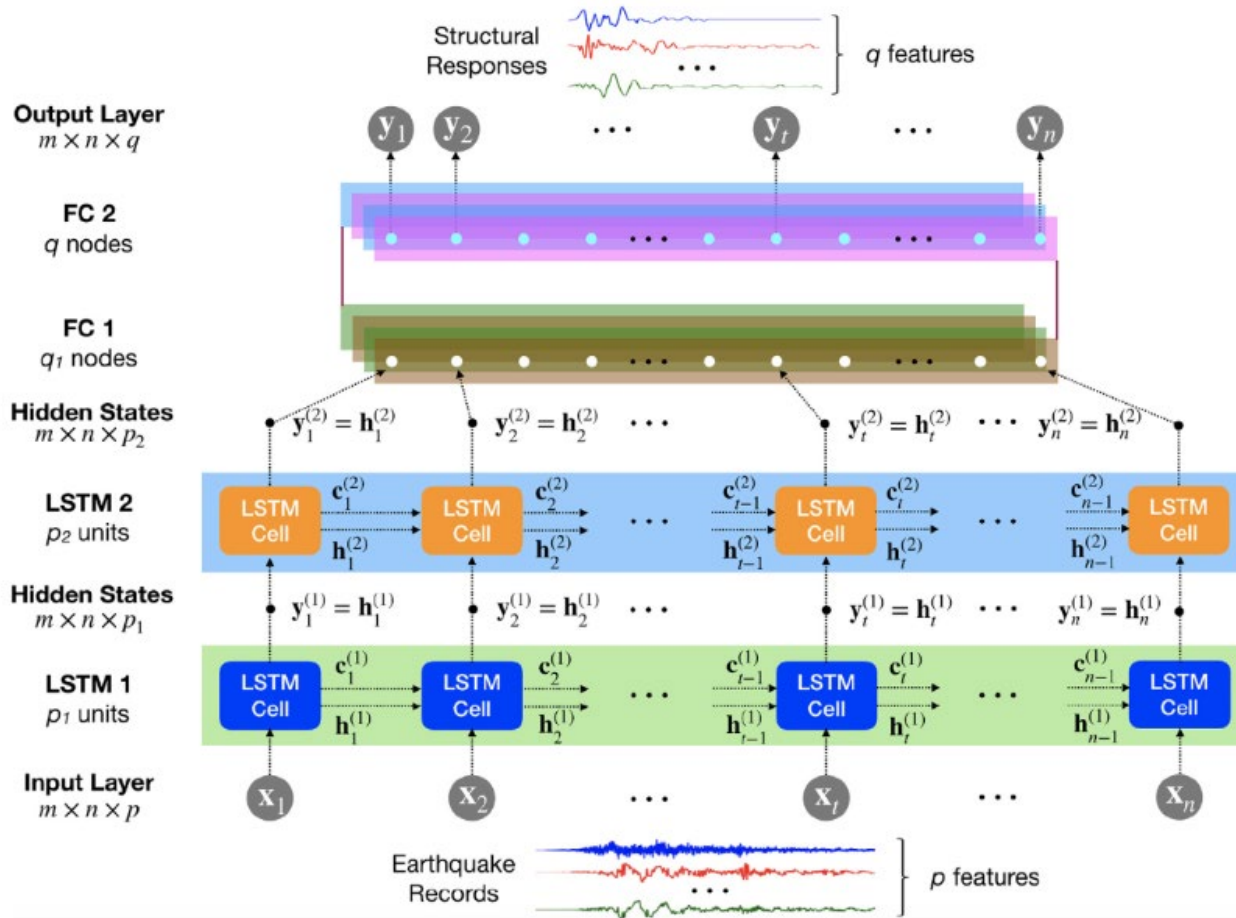
Non-linear mapping network



Pathirage, et al., 2018, *ES*, 172: 13-28.



# Response modelling and prediction



Zhang et al., 2019, *Computers and Structures*, 220: 55-68.

# 3. Target-free vision based displacement measurement

## 3.1 Methodology

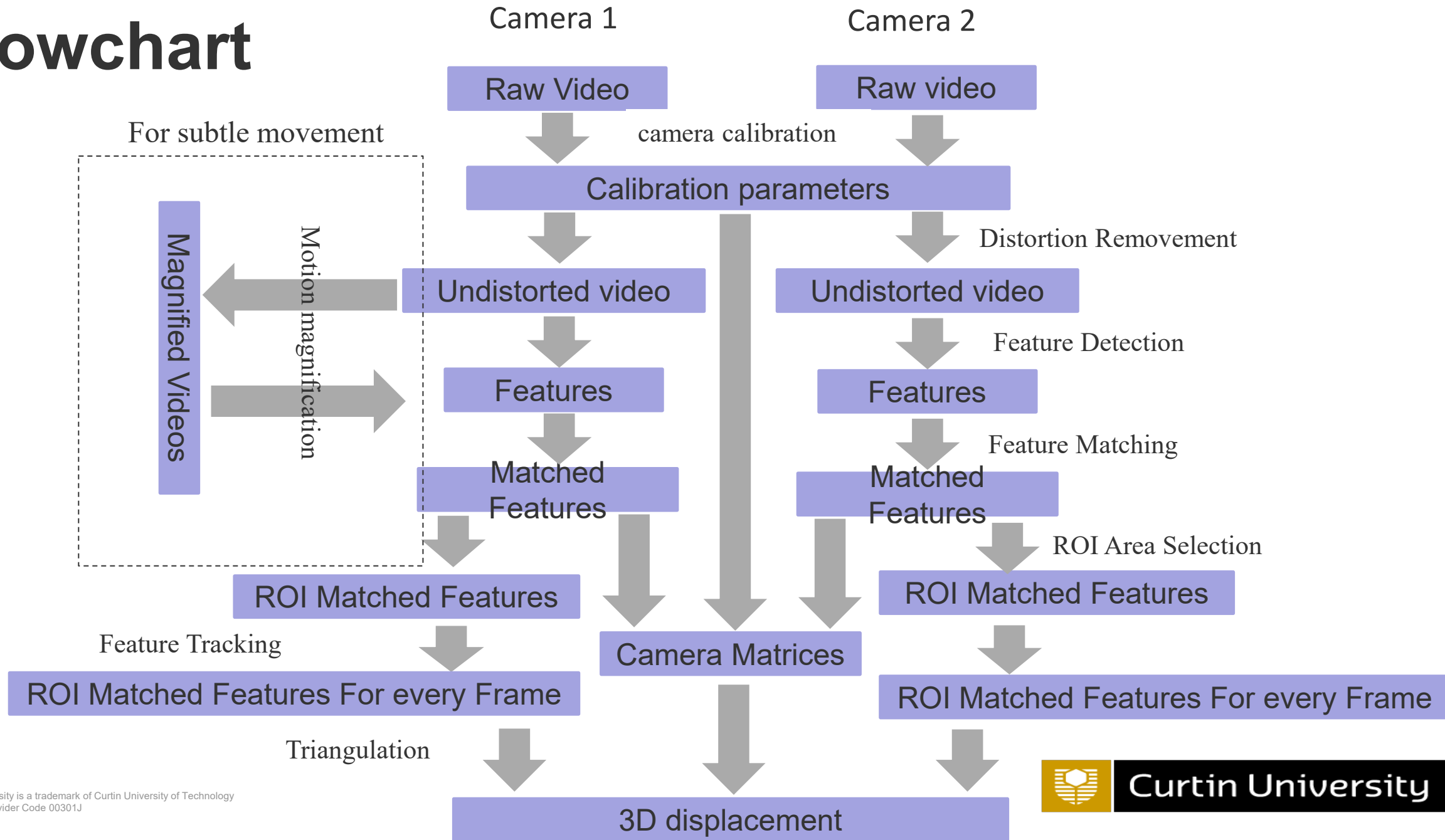
- Apply **videogrammetry technology** on civil engineering to capture the 3D movement of civil structures using **two** cameras without any **artificial targets**
- Videogrammetry is a measurement technology in which the 3D coordinates of points on an object are determined by two or more videos taken from different angles



24



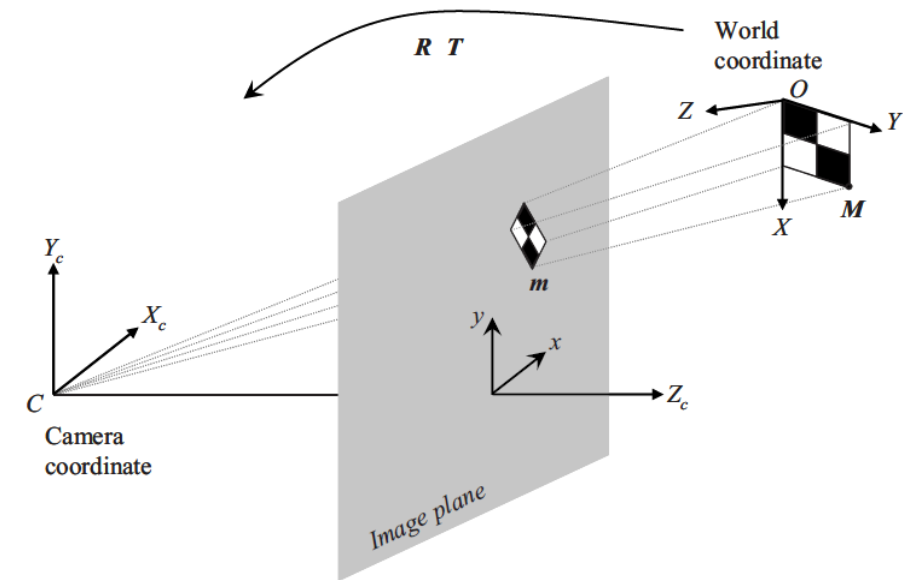
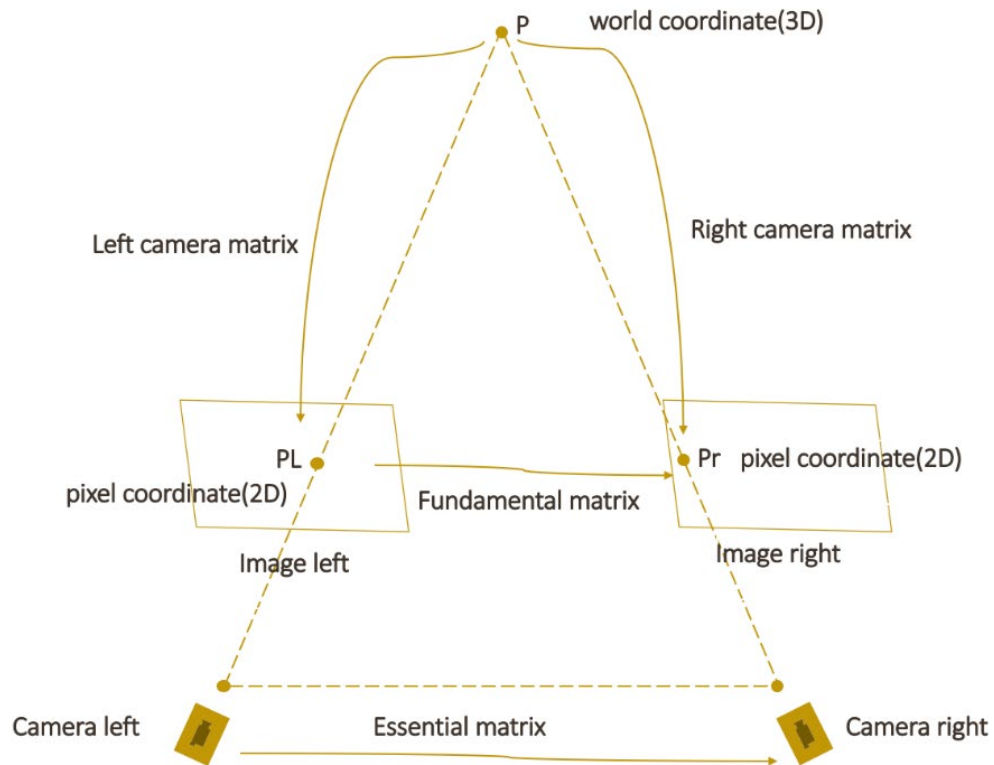
# Flowchart





# Camera Stereo Calibration

- To estimate the conversion factor from pixel to engineering unit, i.e. mm
- To estimate the camera matrixes of two cameras
- To remove the radial distortion of lens



An object in the world coordinate is converted to the image coordinate by a camera matrix.

# Feature Detection

## Traditional methods:

- **SIFT:** Lowe G. **SIFT-the scale invariant feature transform**[J]. Int. J, 2004.
- **SURF:** Bay H, Tuytelaars T, Van Gool L. **Surf: Speeded up robust features**, 2006.
- **KAZE:** Alcantarilla P F, Bartoli A, Davison A J. **KAZE features**, 2012.

Traditional  
Computer Vision

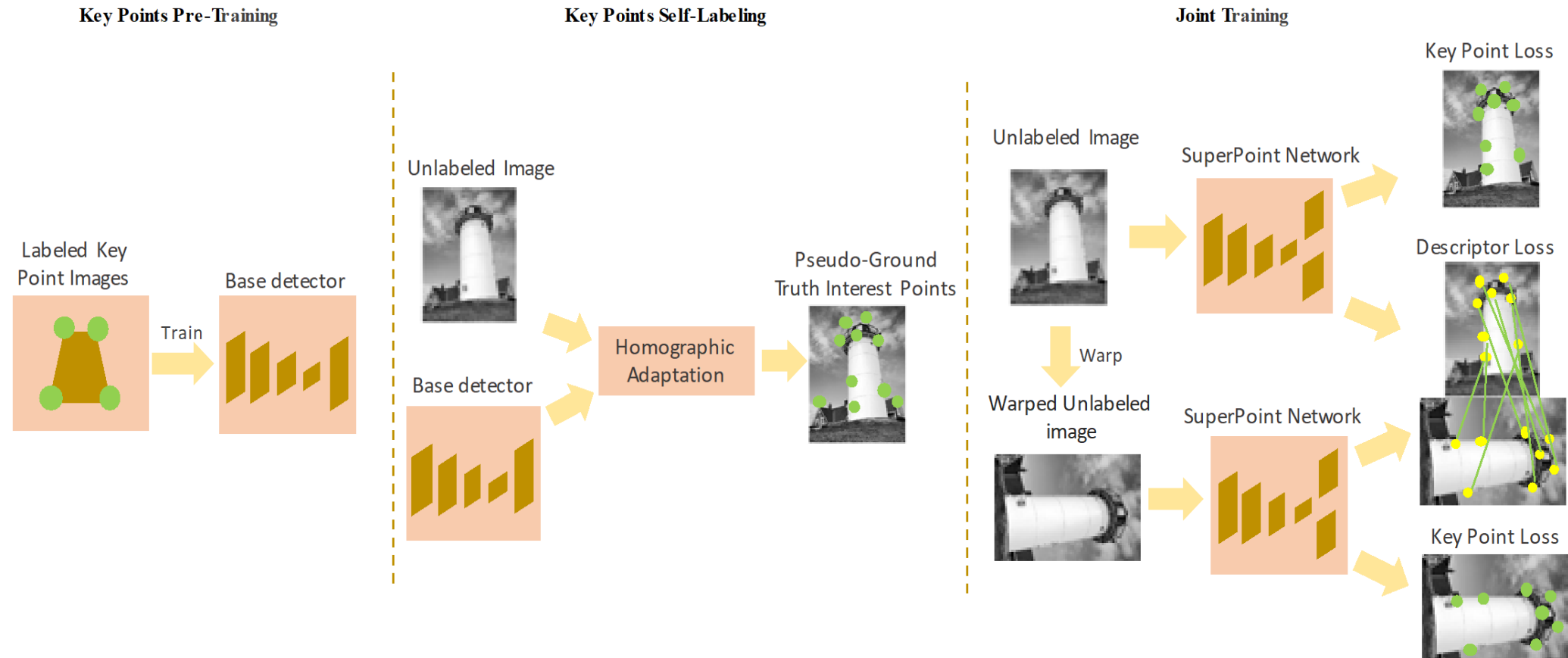
## In This Research:

- **Super point:** DeTone D, Malisiewicz T, Rabinovich A. Superpoint: **Self-supervised interest point detection and description**[C], 2018

Deep Learning  
based feature  
detection

# Feature Detection

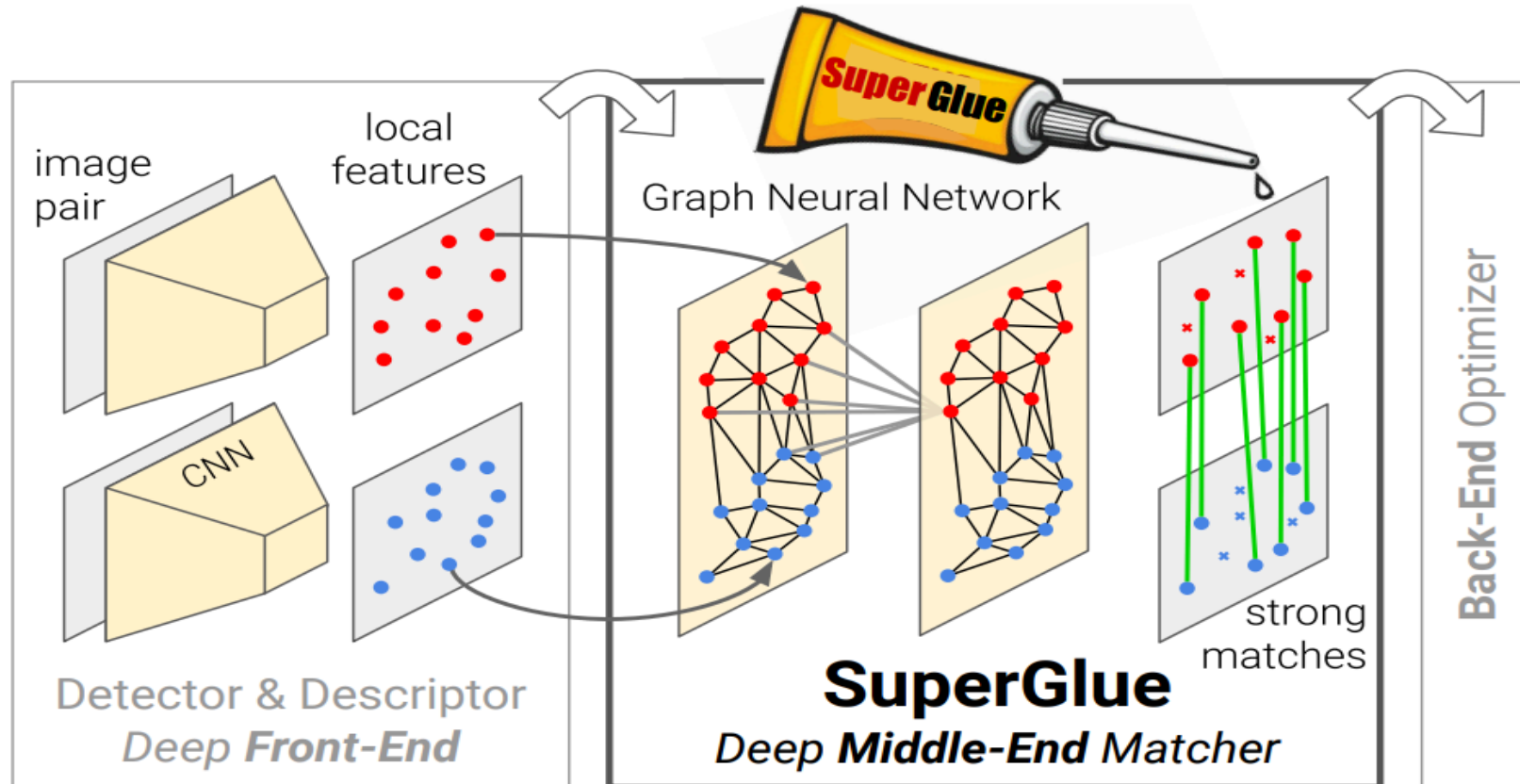
- A self-supervised framework for training interest point detectors and descriptors suitable for many multiple-view geometry problems in computer vision.





# Feature Matching

- **Super glue:** Sarlin P E, DeTone D, Malisiewicz T, et al. **Superglue: Learning feature matching with graph neural networks**[C], 2020.
- a neural network that matches two sets of key points by jointly finding correspondences and rejecting non-matchable points.



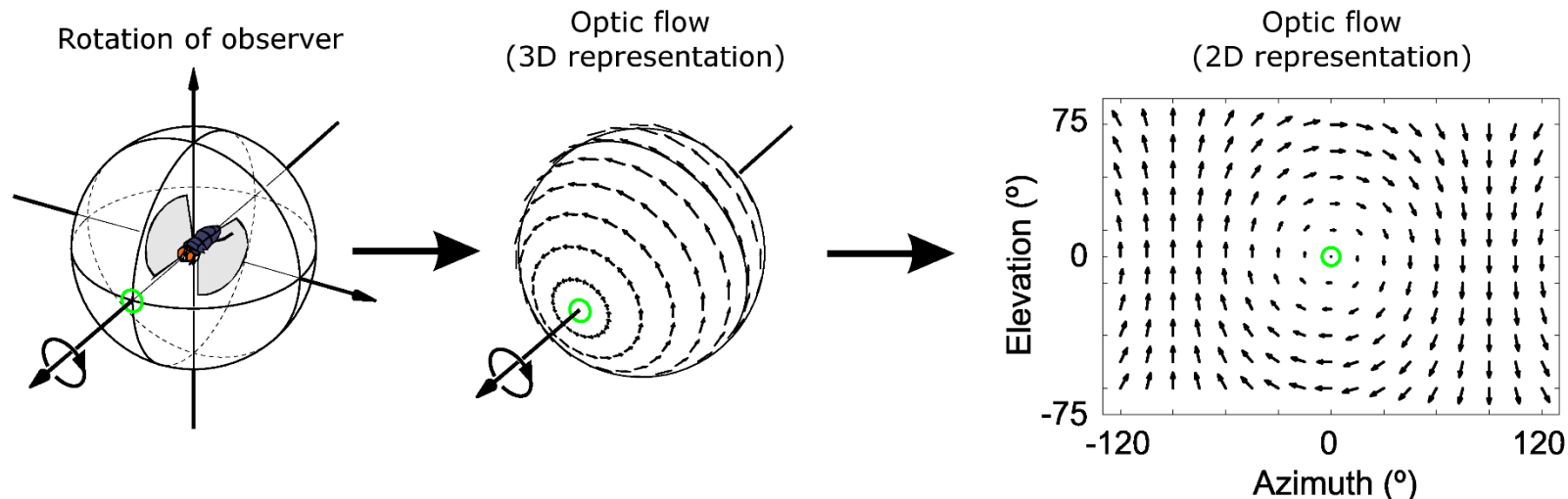
# Feature Tracking

- Kanade-Lucas-Tomasi (KLT) optical flow tracker is applied to traverse each frame of the stereo videos to find the matched key points.

Lucas B D, Kanade T. *An iterative image registration technique with an application to stereo vision*[J]. 1981.

Tomasi C, Kanade T. *Detection and tracking of point features*[J]. 1991.

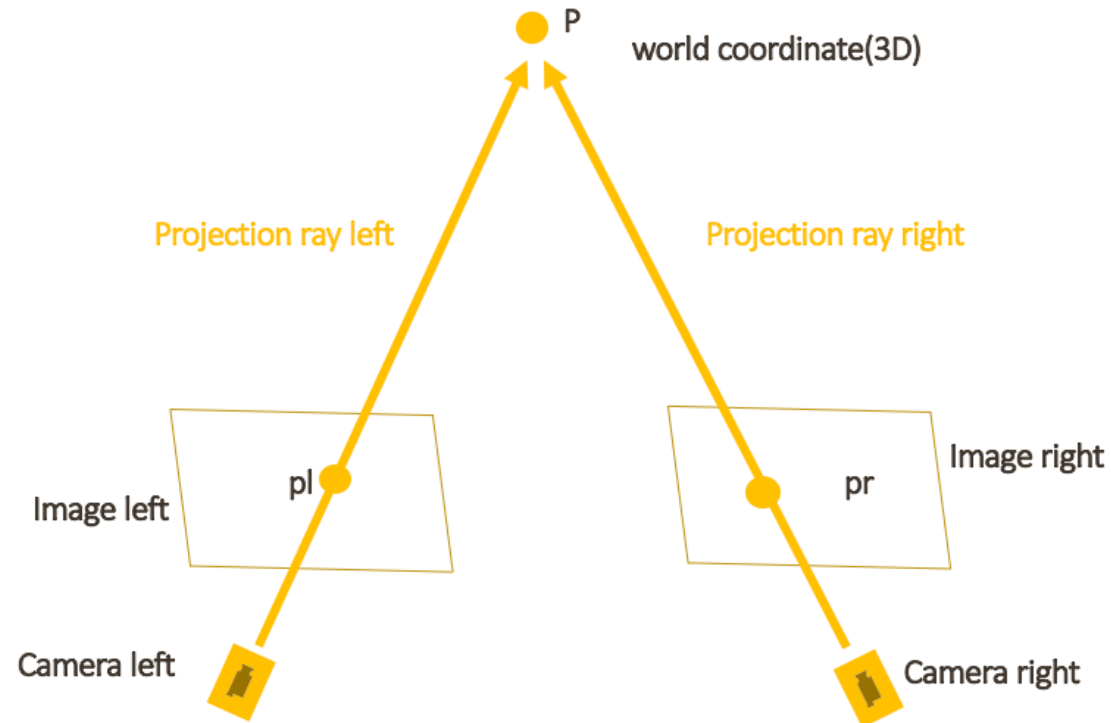
Shi J. *Good features to track*[C]//1994 Proceedings of IEEE conference on computer vision and pattern recognition. IEEE, 1994: 593-600.



# Triangulation

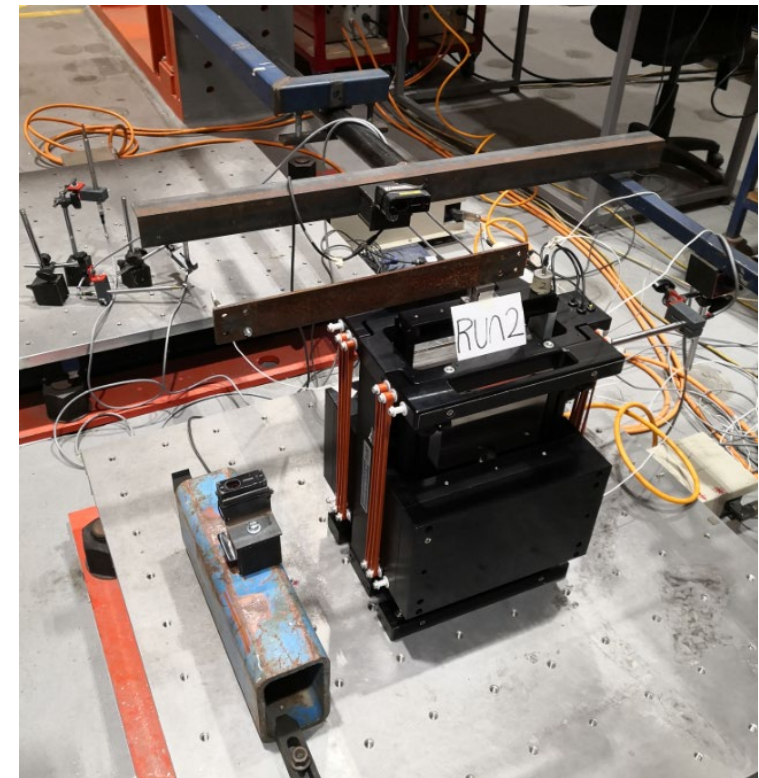
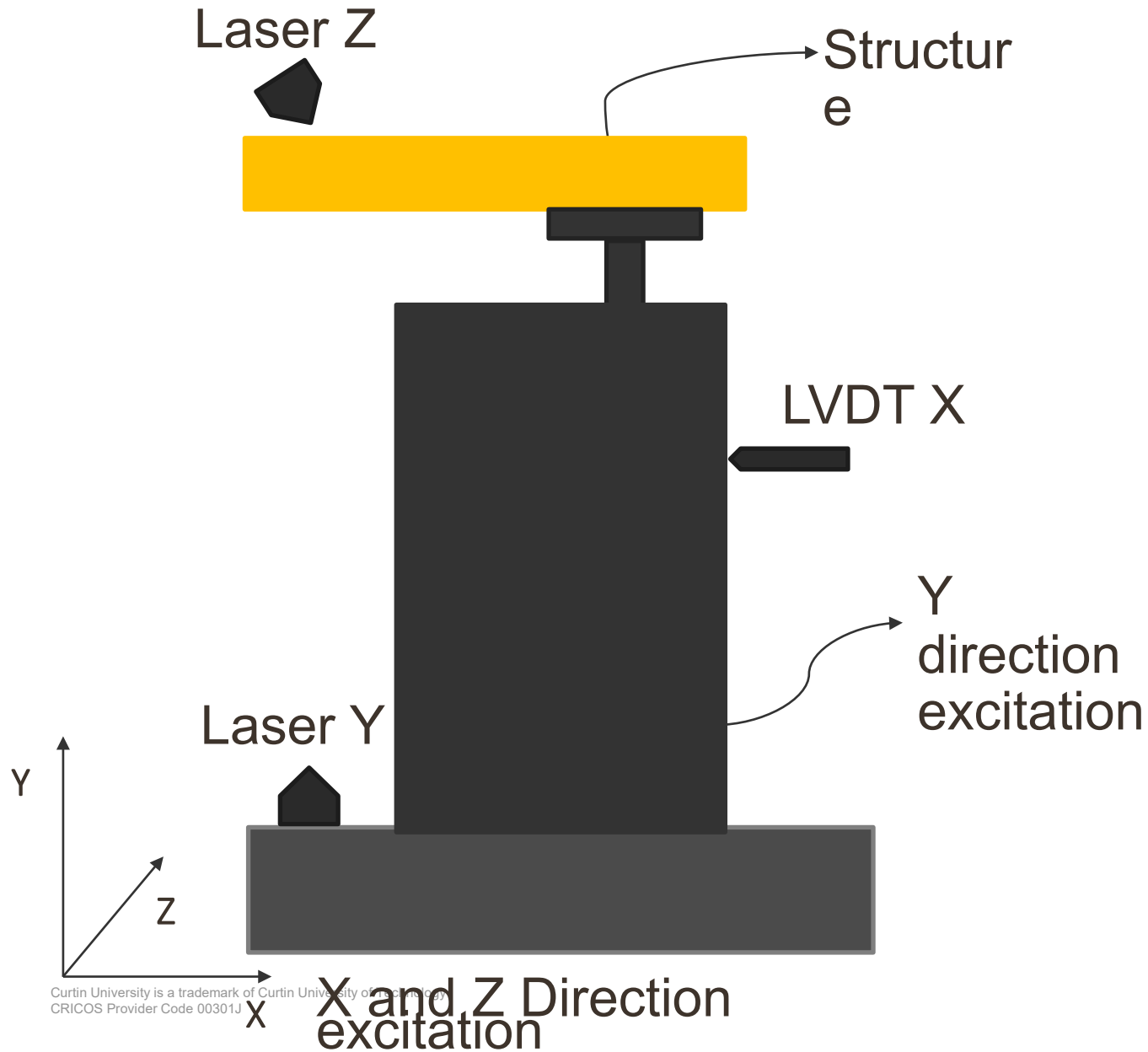
- Compute the position of a point in 3D space given **its image in two views** and the **camera matrices** of those views.

*Hartley, R. and A. Zisserman. "Multiple View Geometry in Computer Vision." Cambridge University Press, 2003*

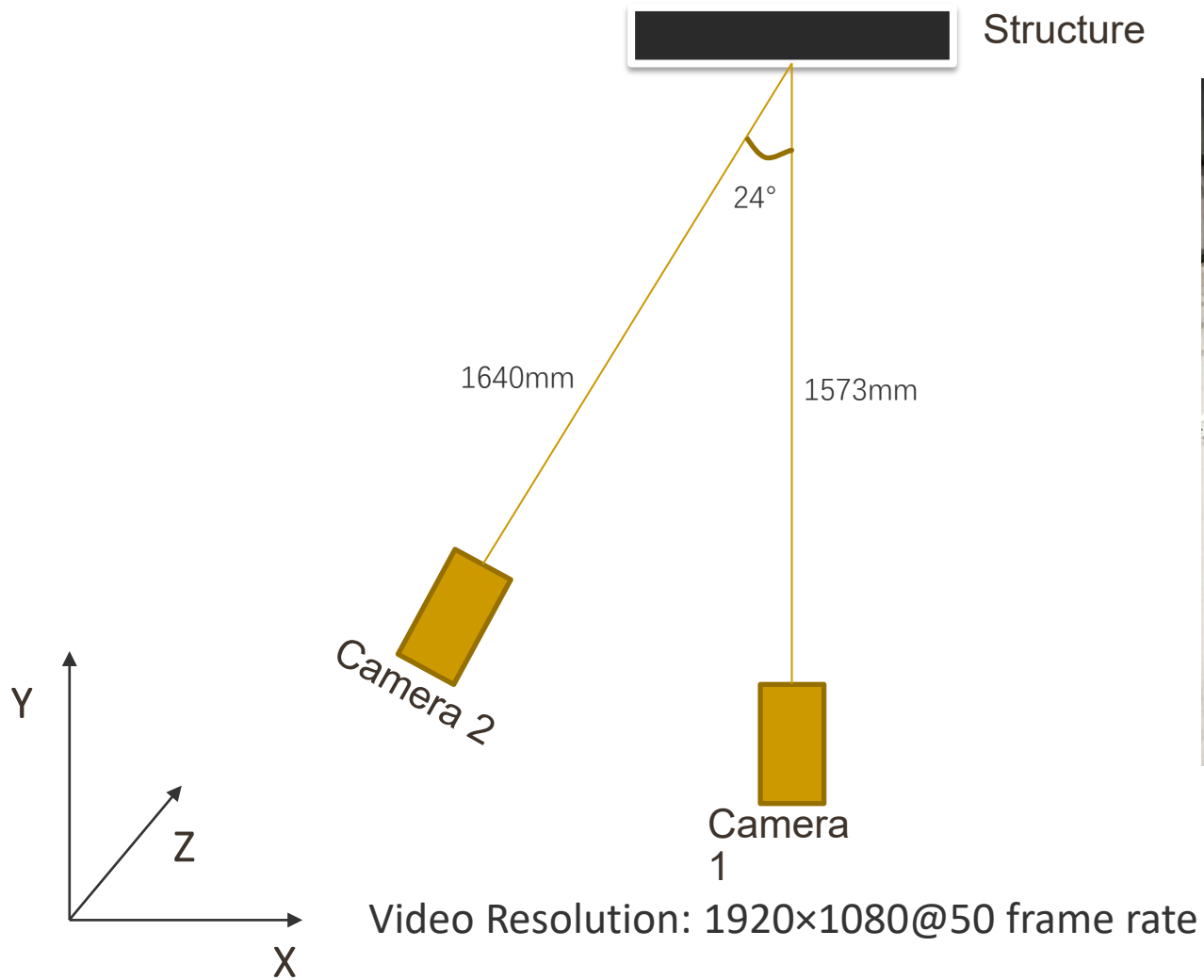




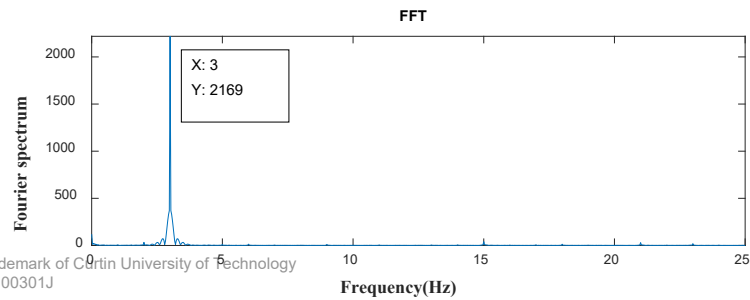
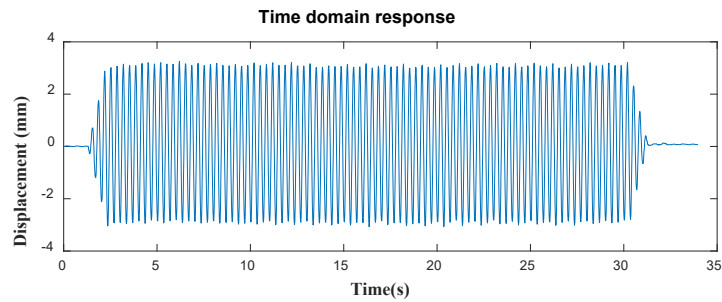
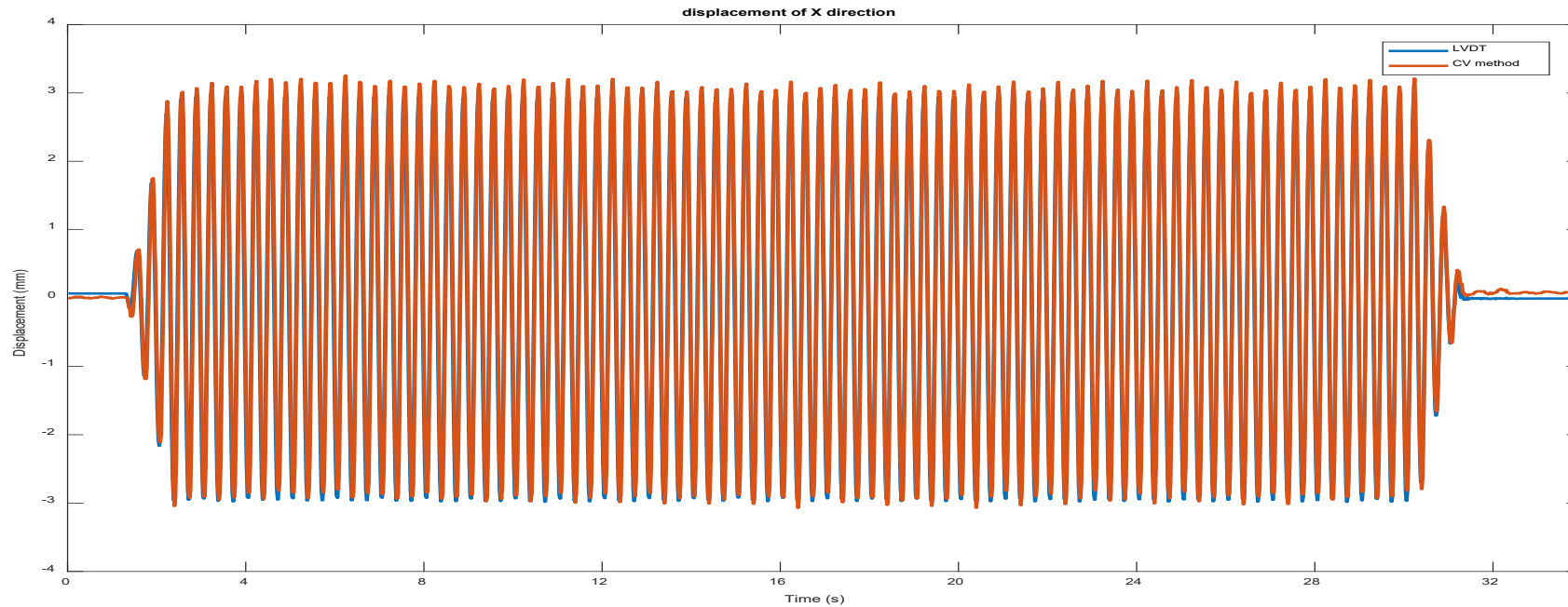
# 3.2 Laboratory validations



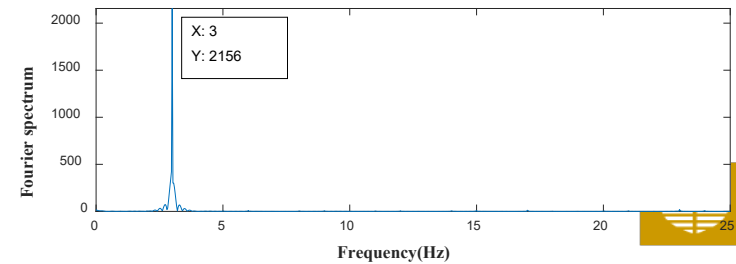
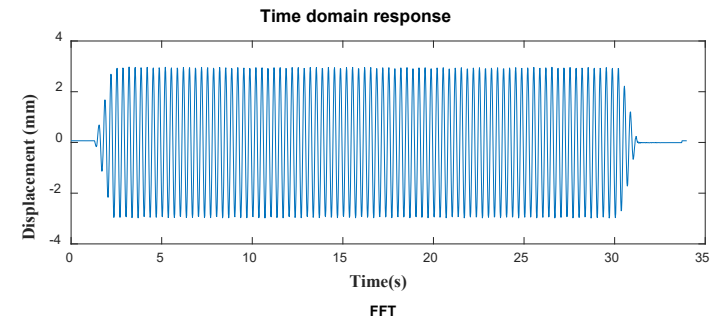
# relatively large movement



# Vibration displacement in X-direction

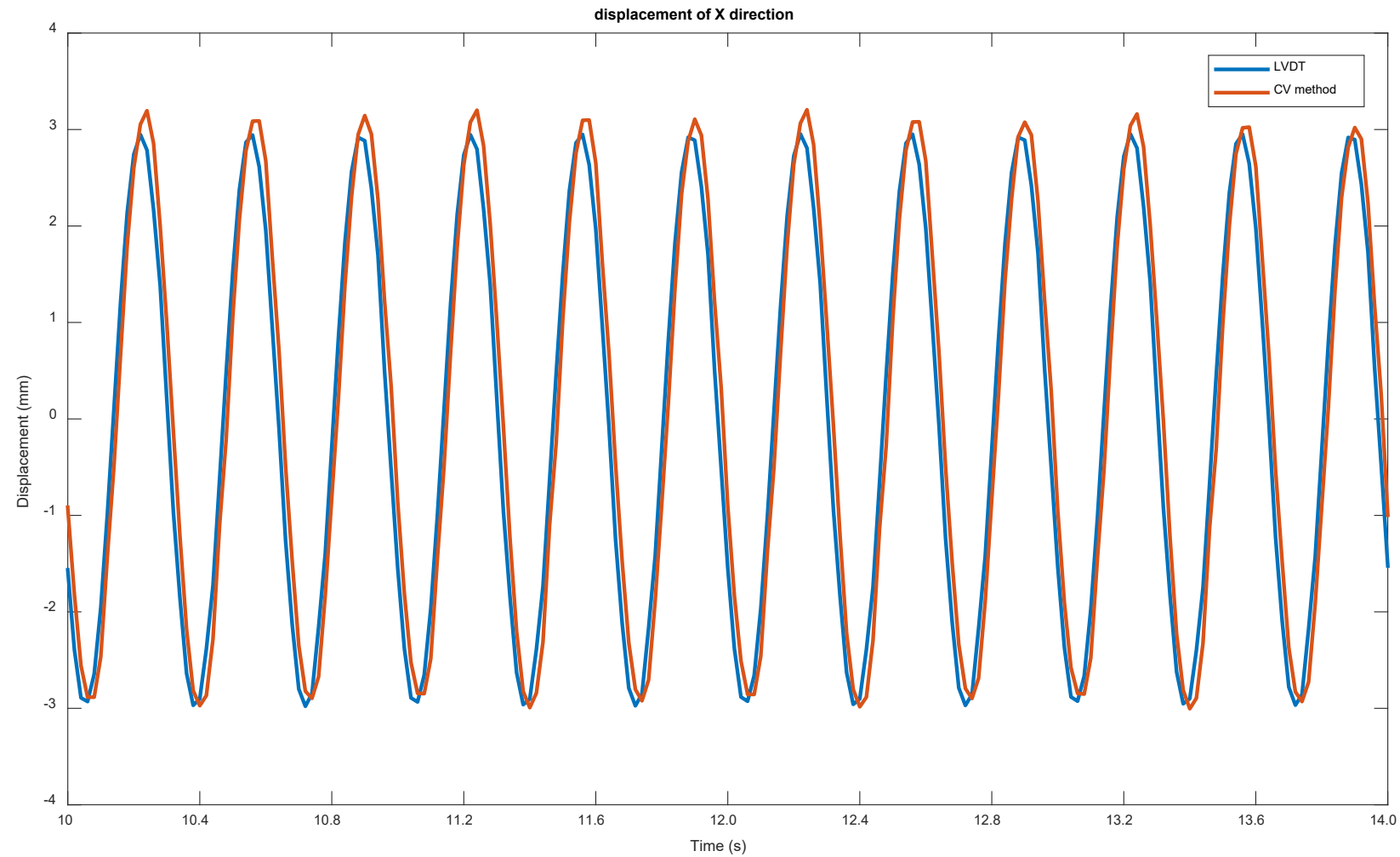


CV method



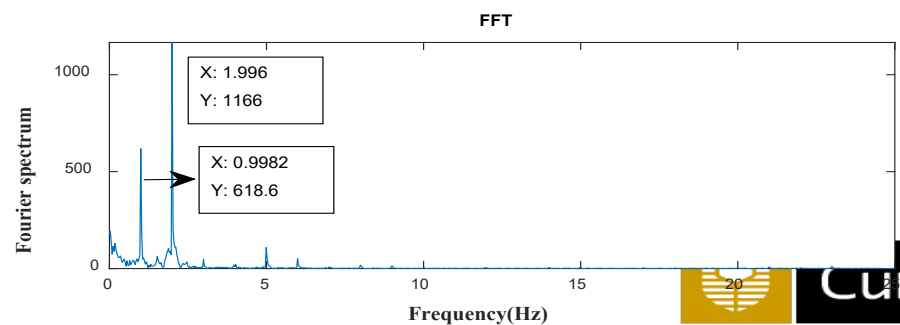
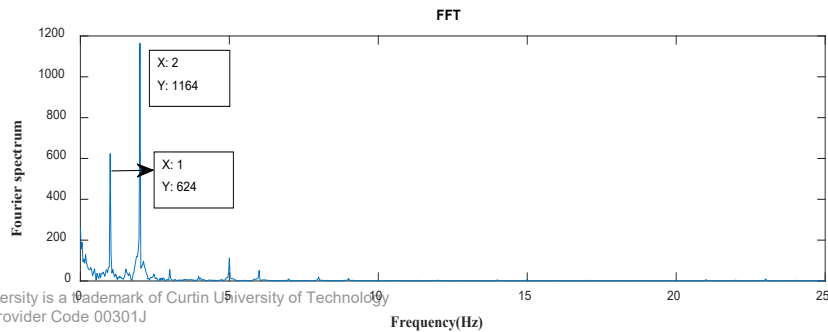
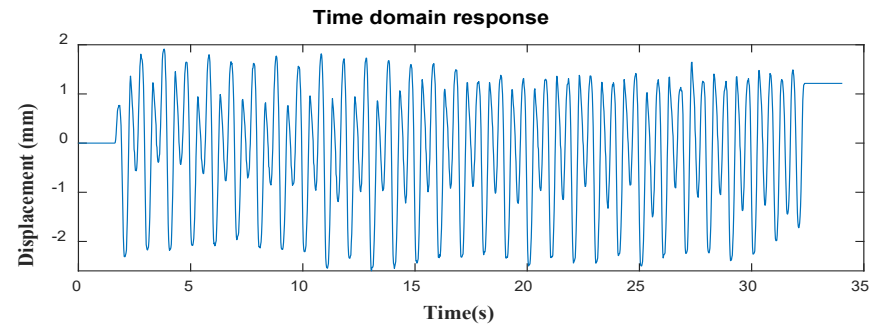
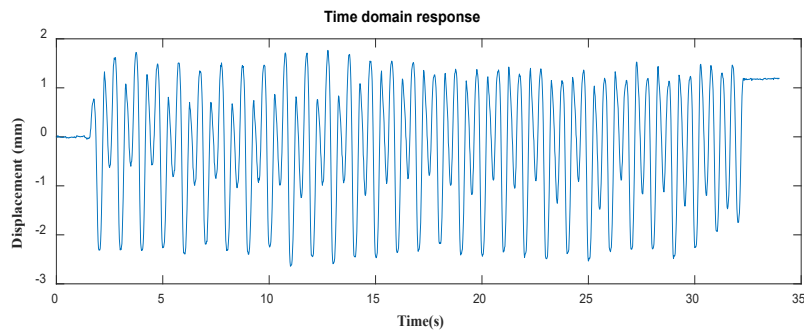
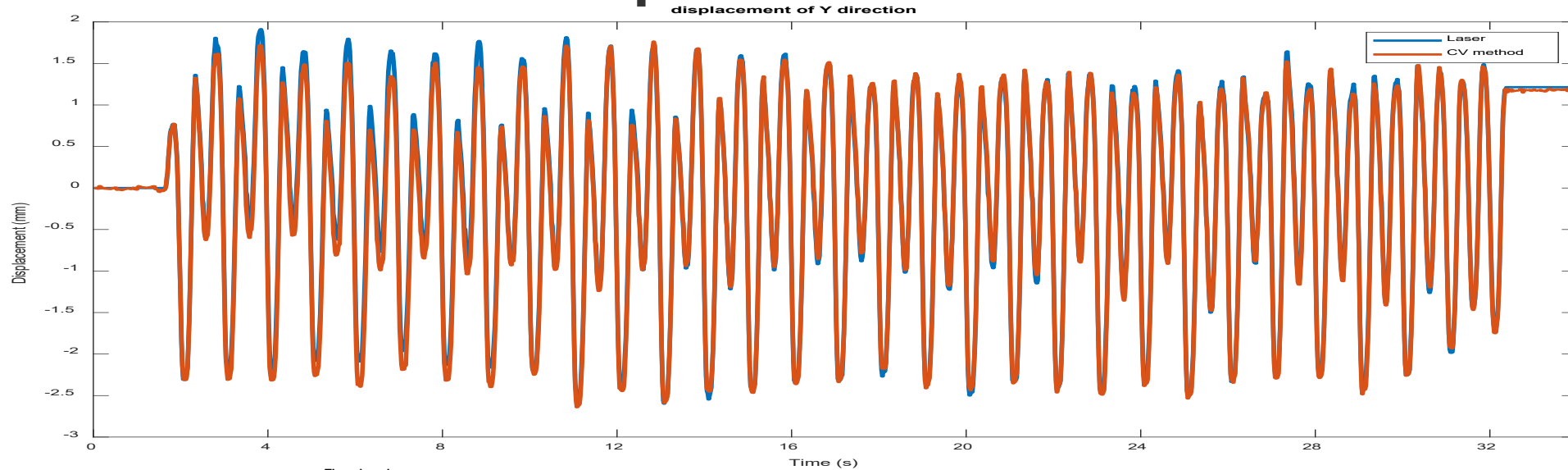
LVDT

# Vibration displacement in X-direction: ZOOM IN

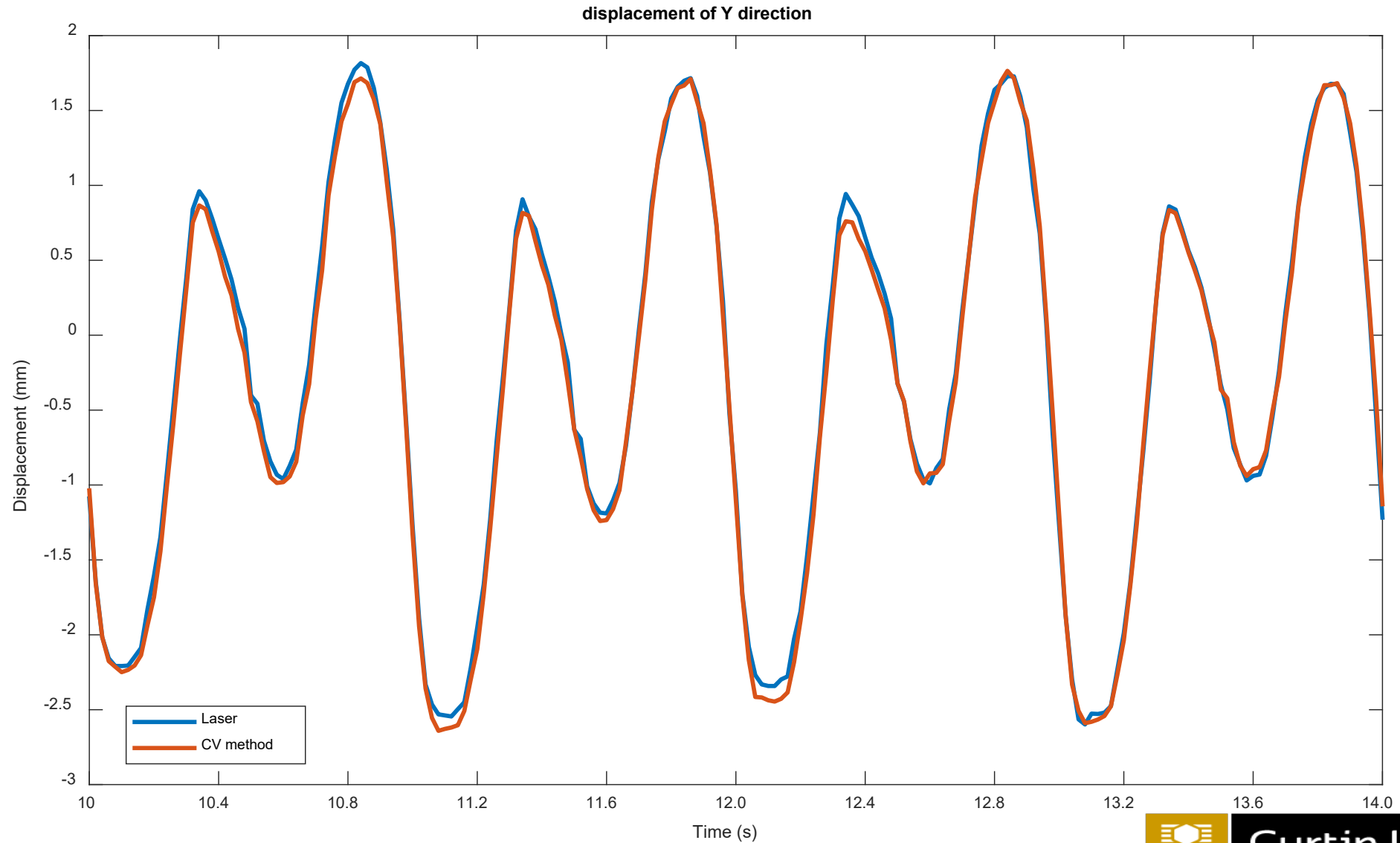




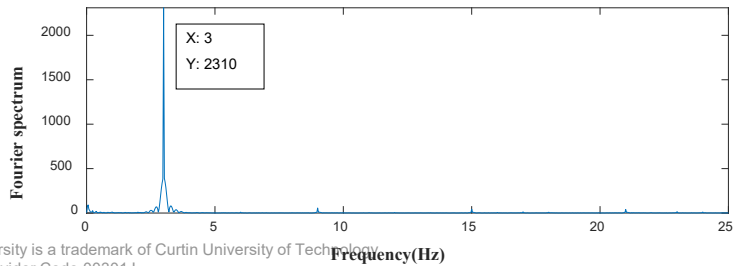
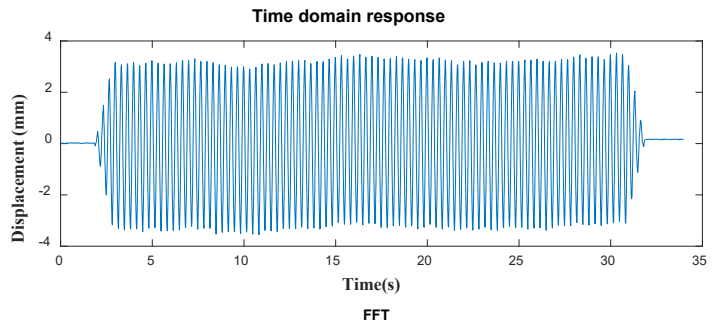
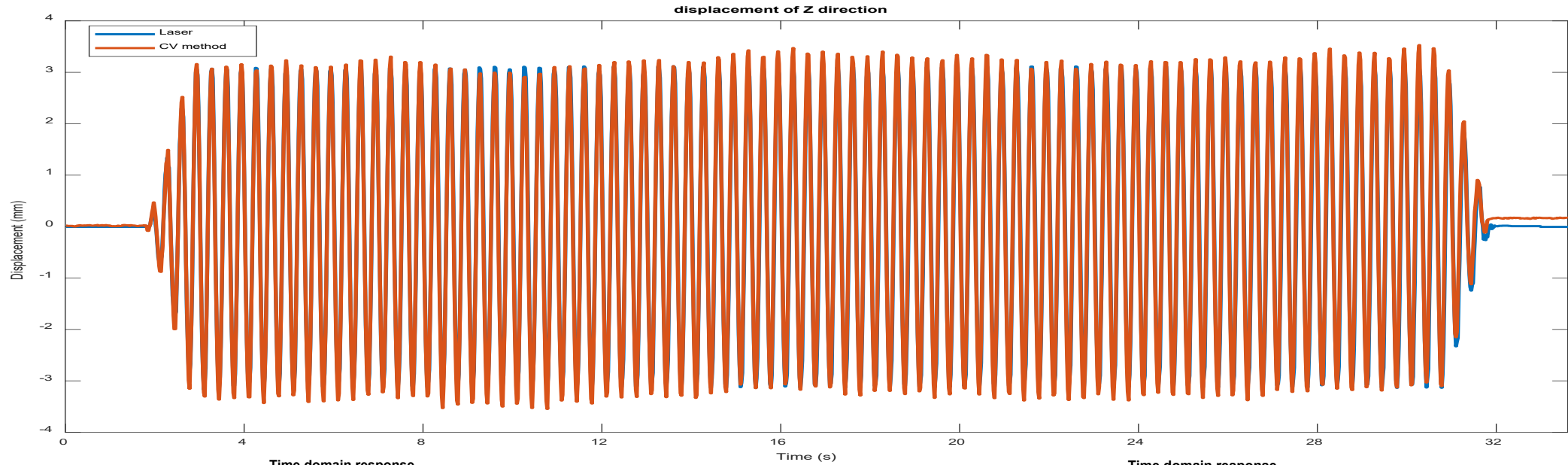
# Vibration displacement in Y-direction



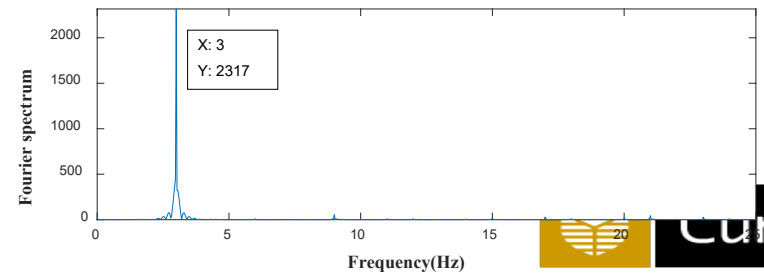
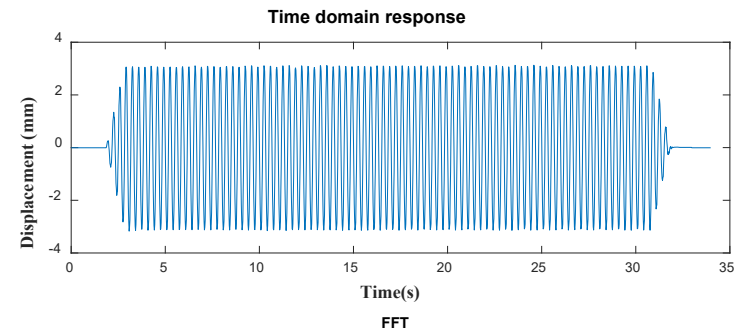
# Vibration displacement in Y-direction: ZOOM IN



# Vibration displacement in Z-direction: ZOOM IN



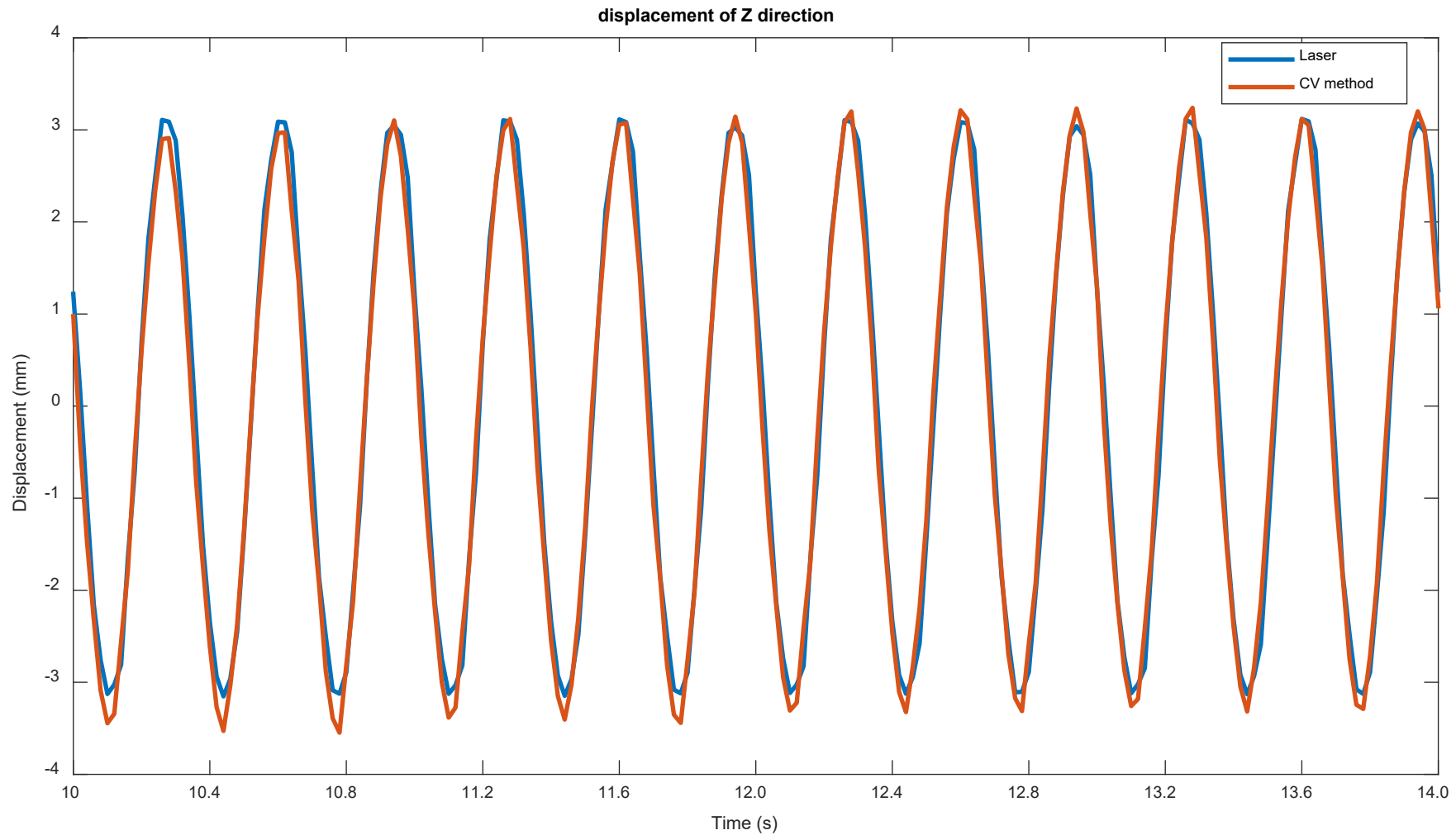
CV method



Laser

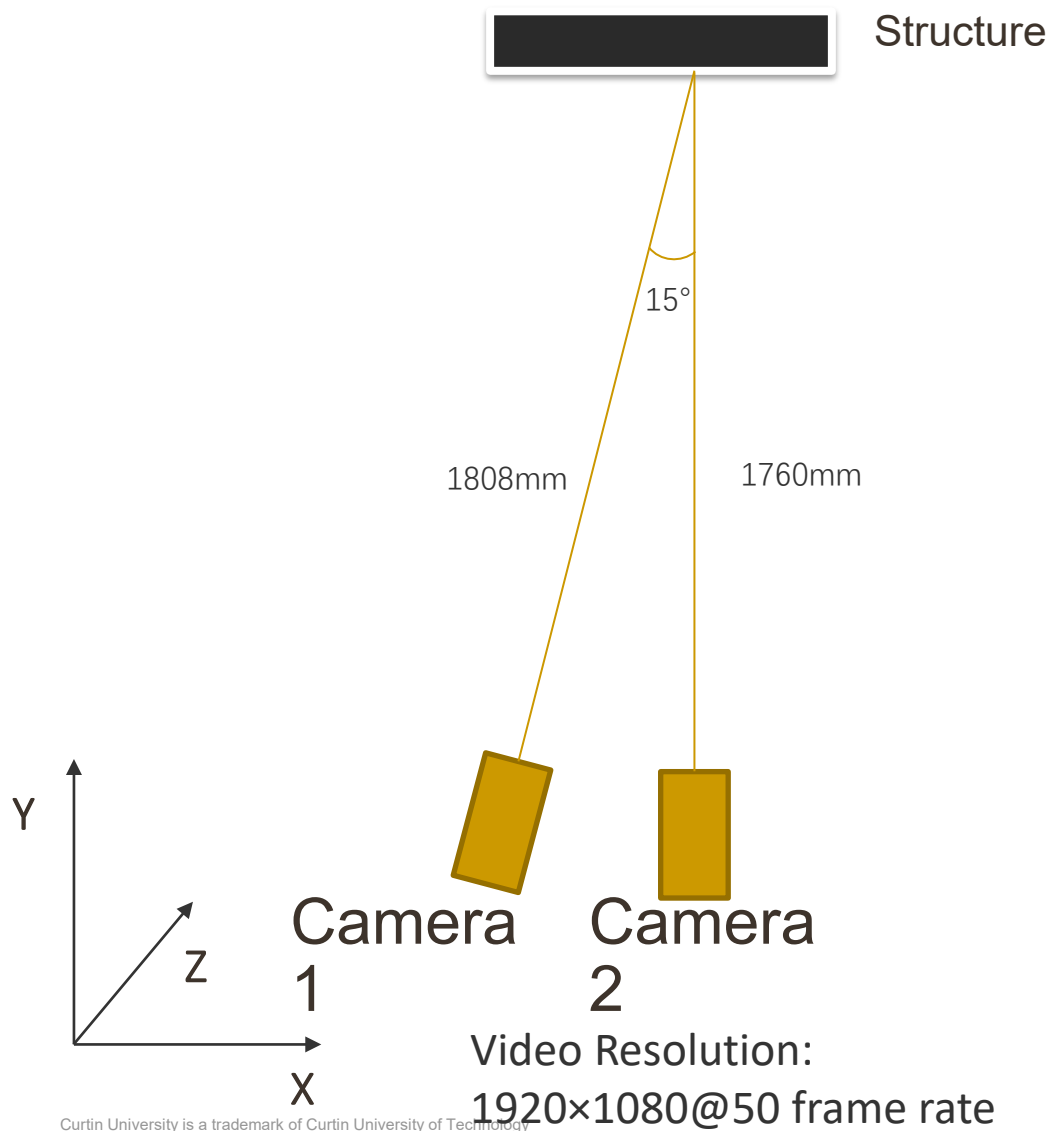


# Vibration displacement in Z-direction: ZOOM IN



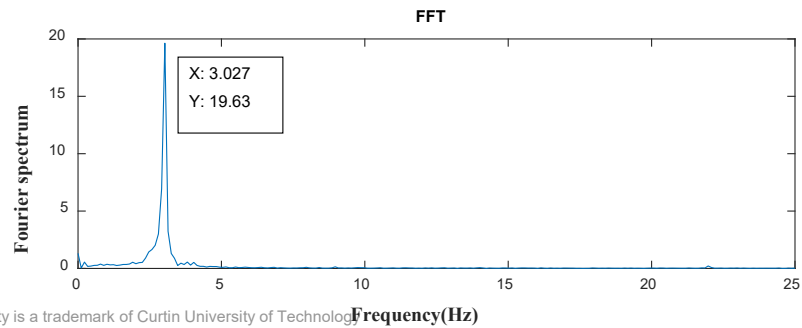
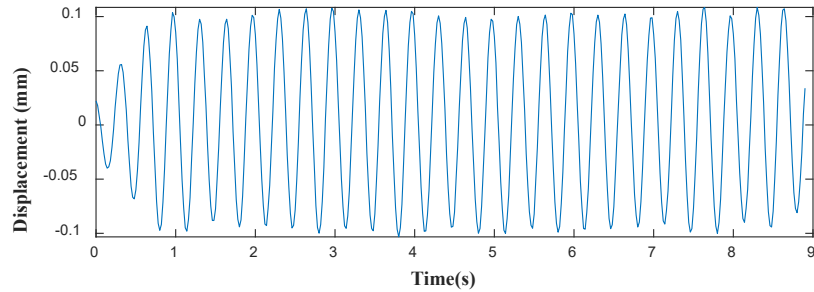
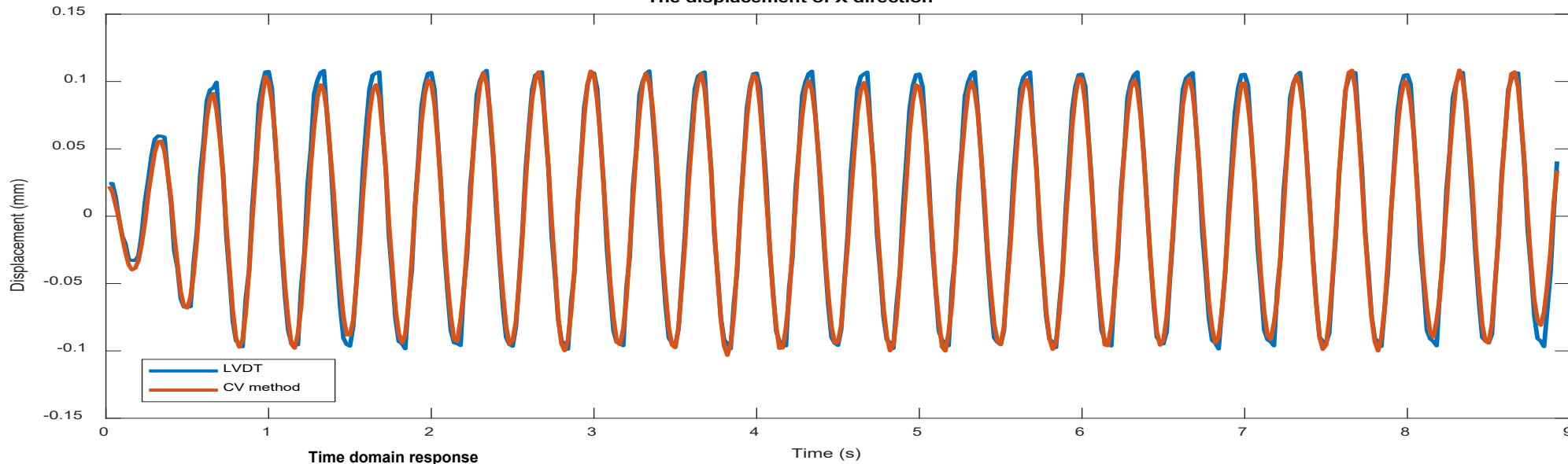


# Subtle 3D Displacement obtained with Motion Magnification

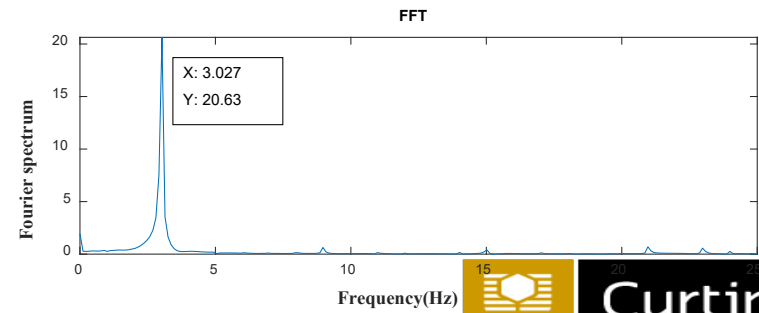
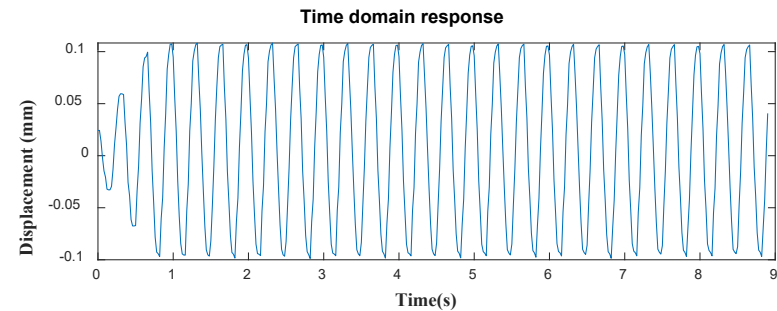


# Vibration displacement in X-direction

The displacement of X direction



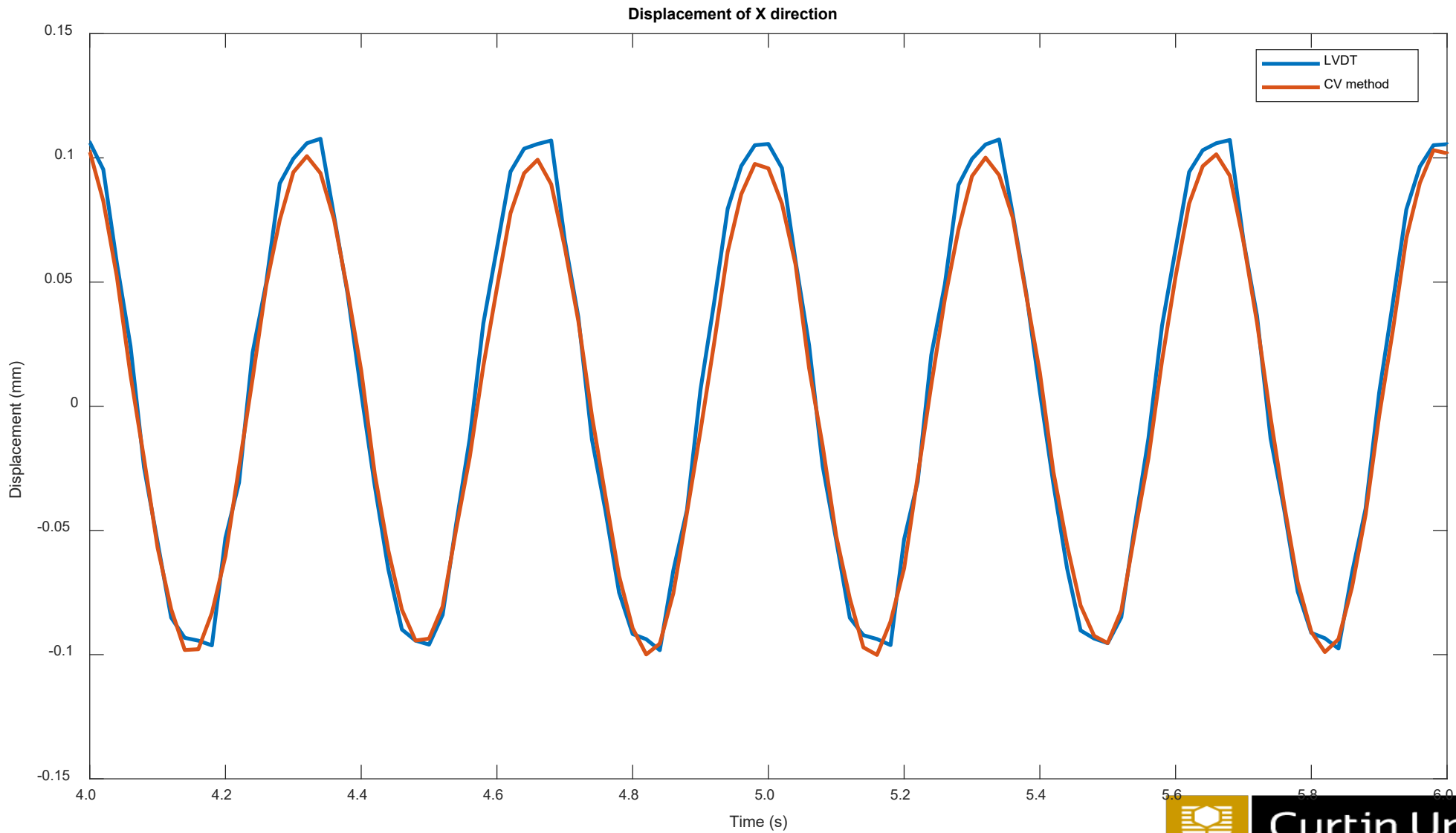
CV method



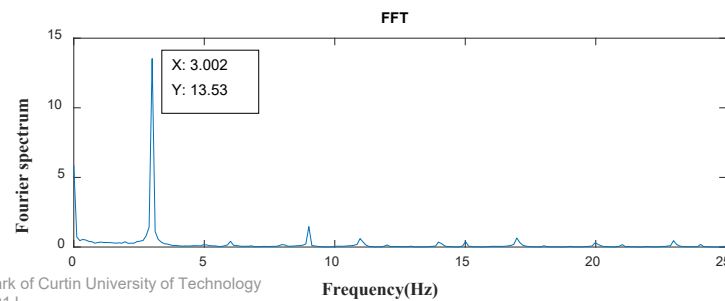
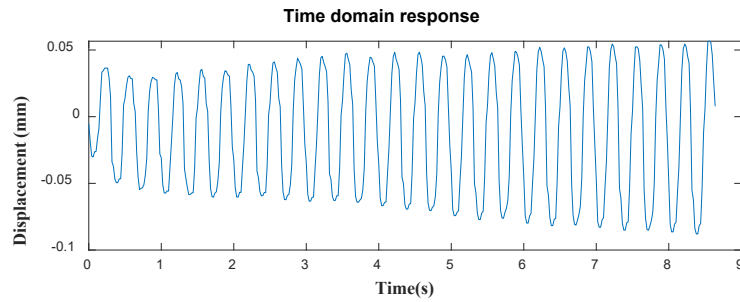
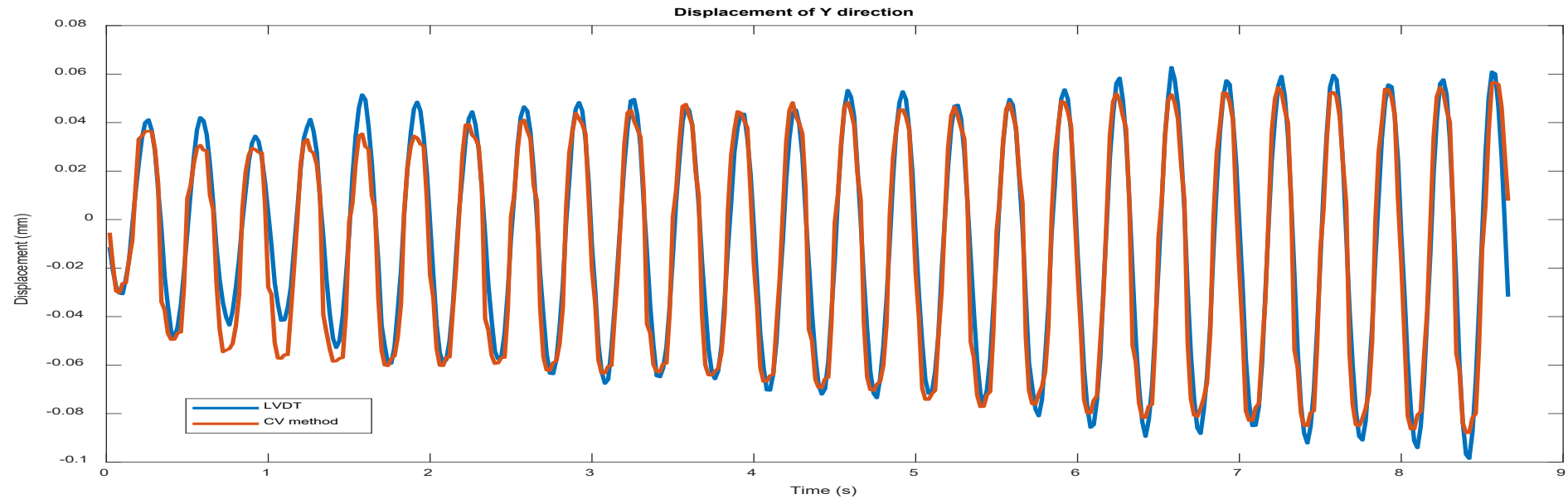
LVDT



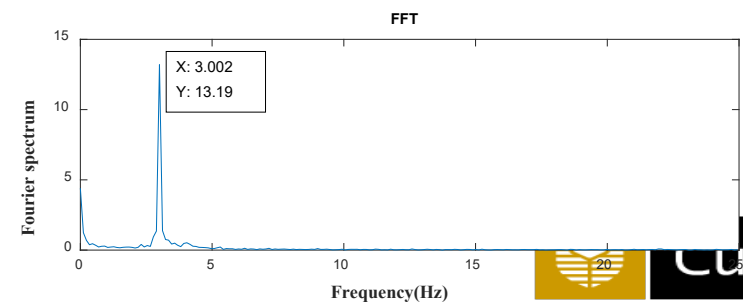
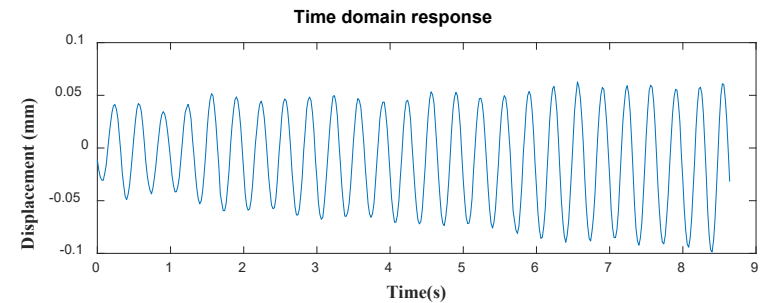
# Vibration displacement in X-direction: ZOOM IN



# Vibration displacement in Y-direction



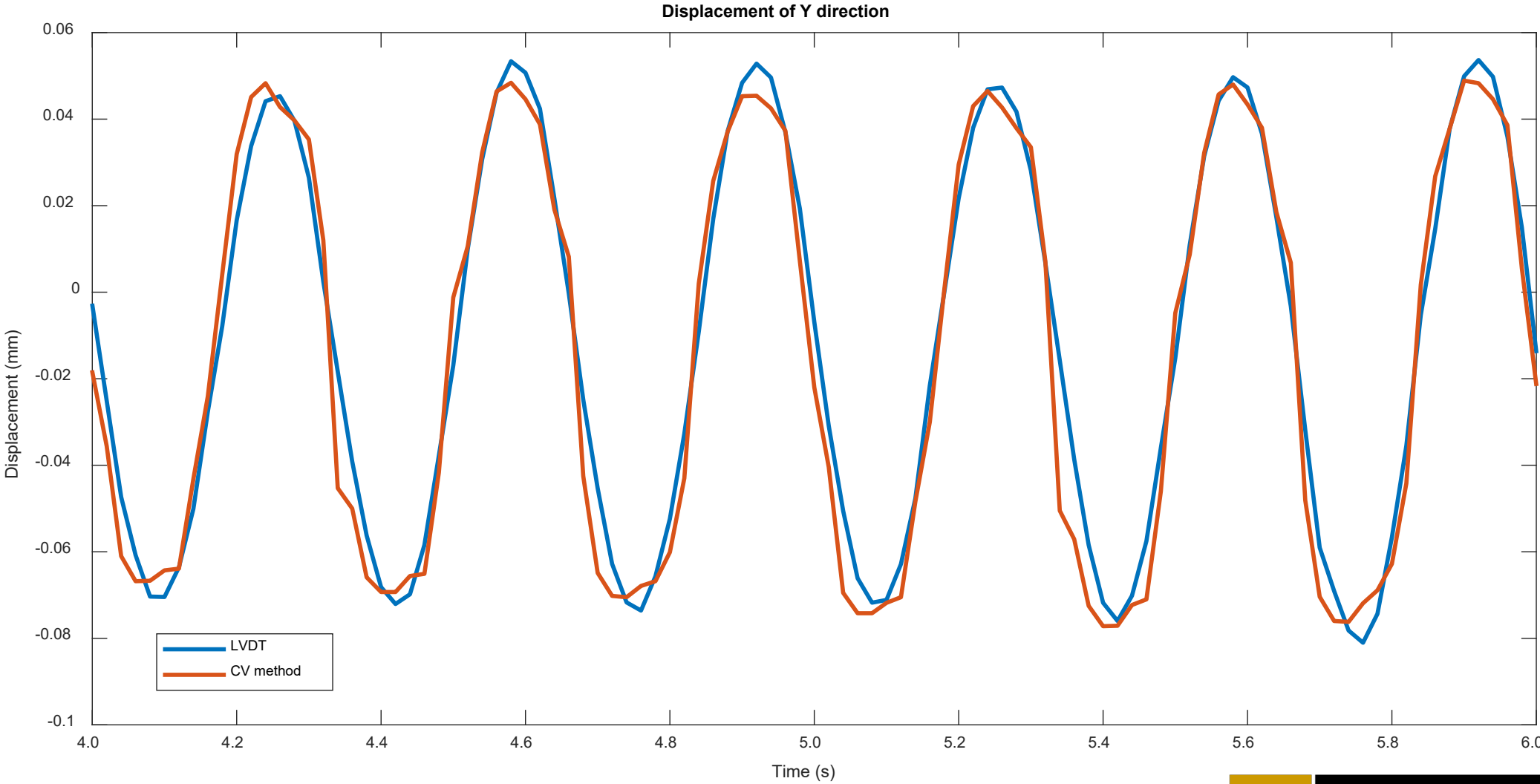
CV method



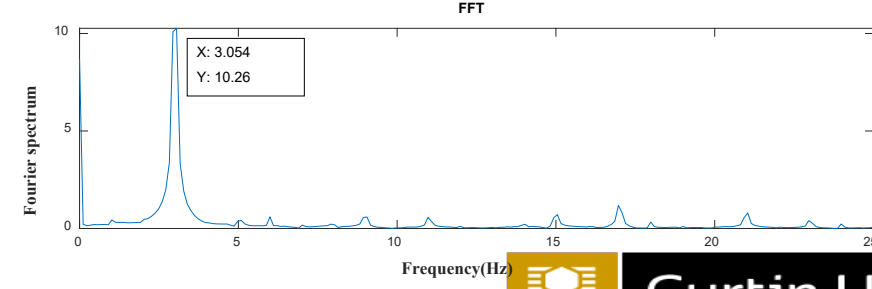
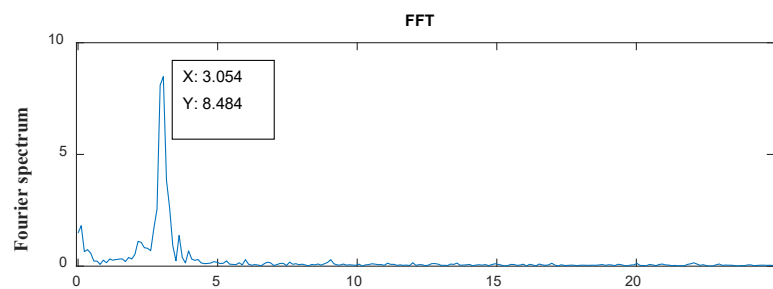
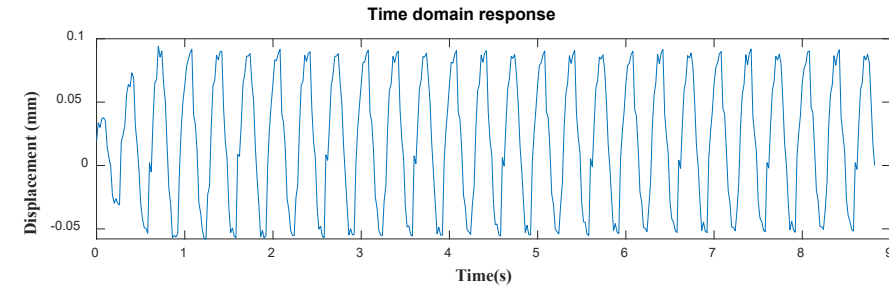
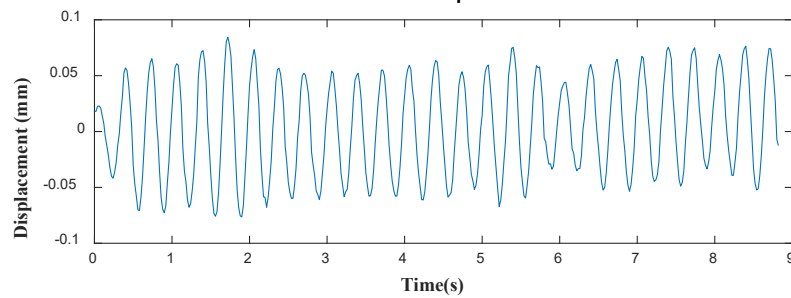
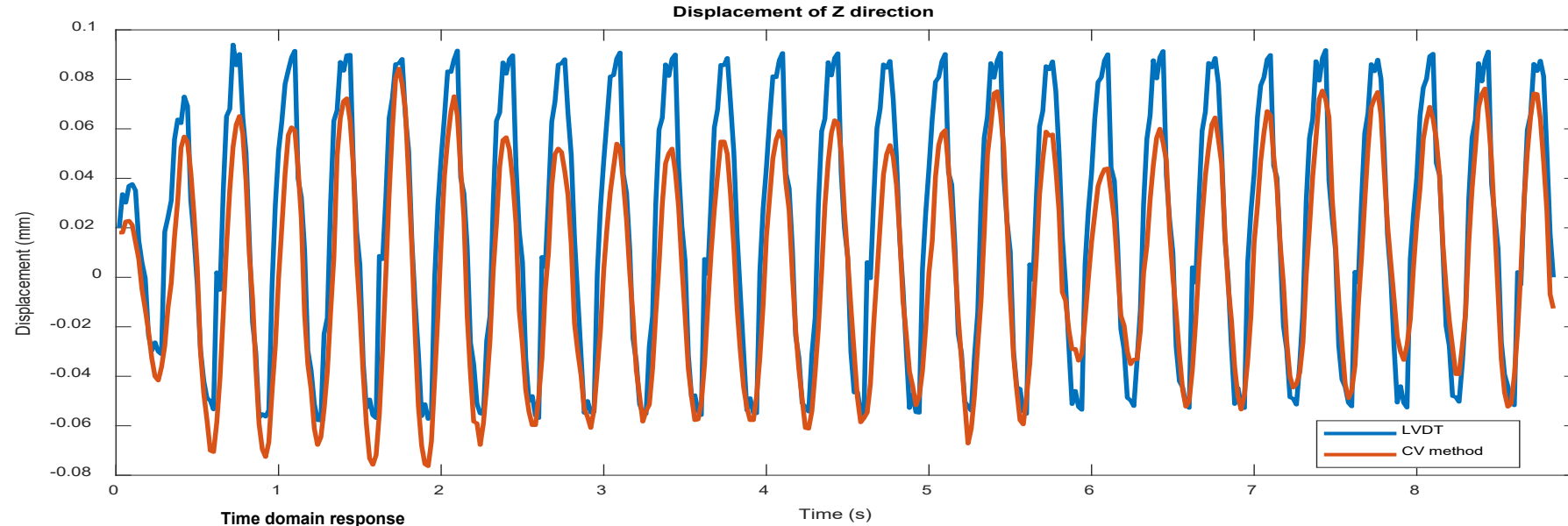
LVDT



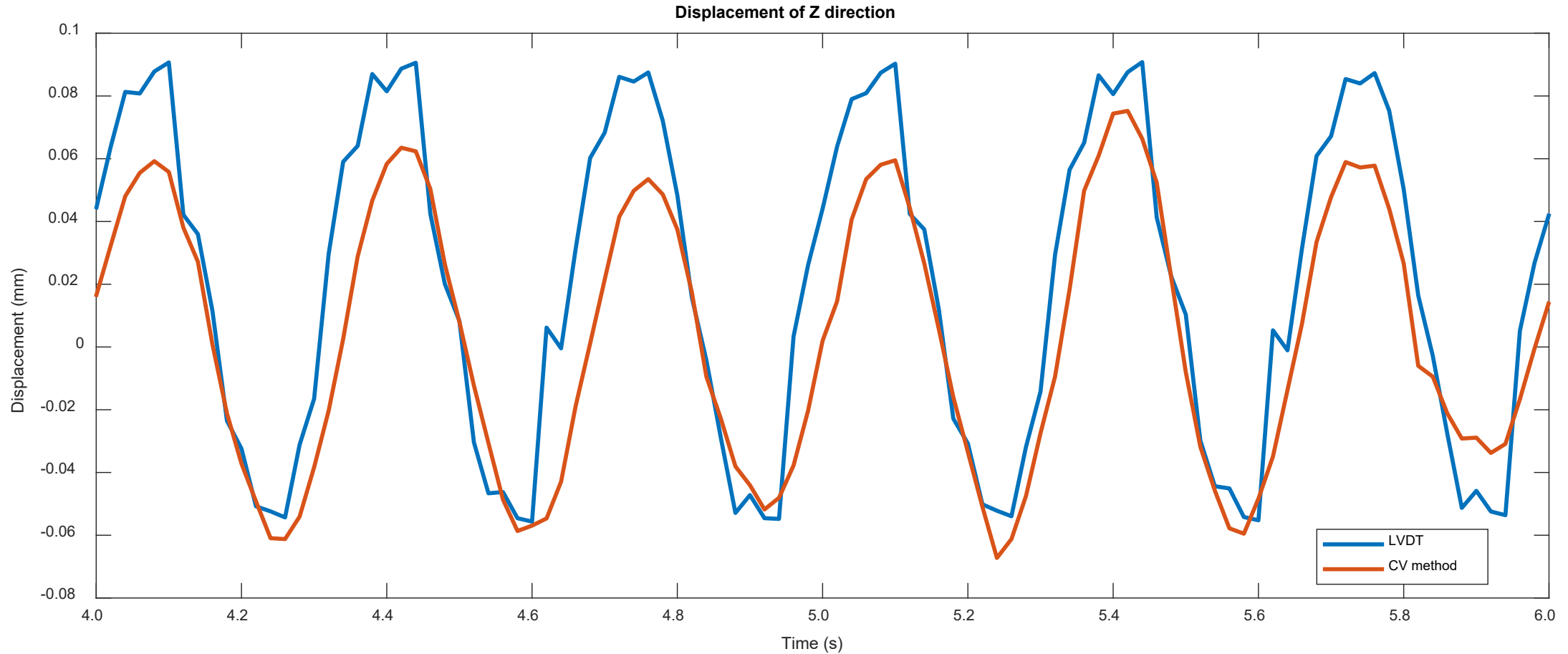
# Vibration displacement in Y-direction: ZOOM IN



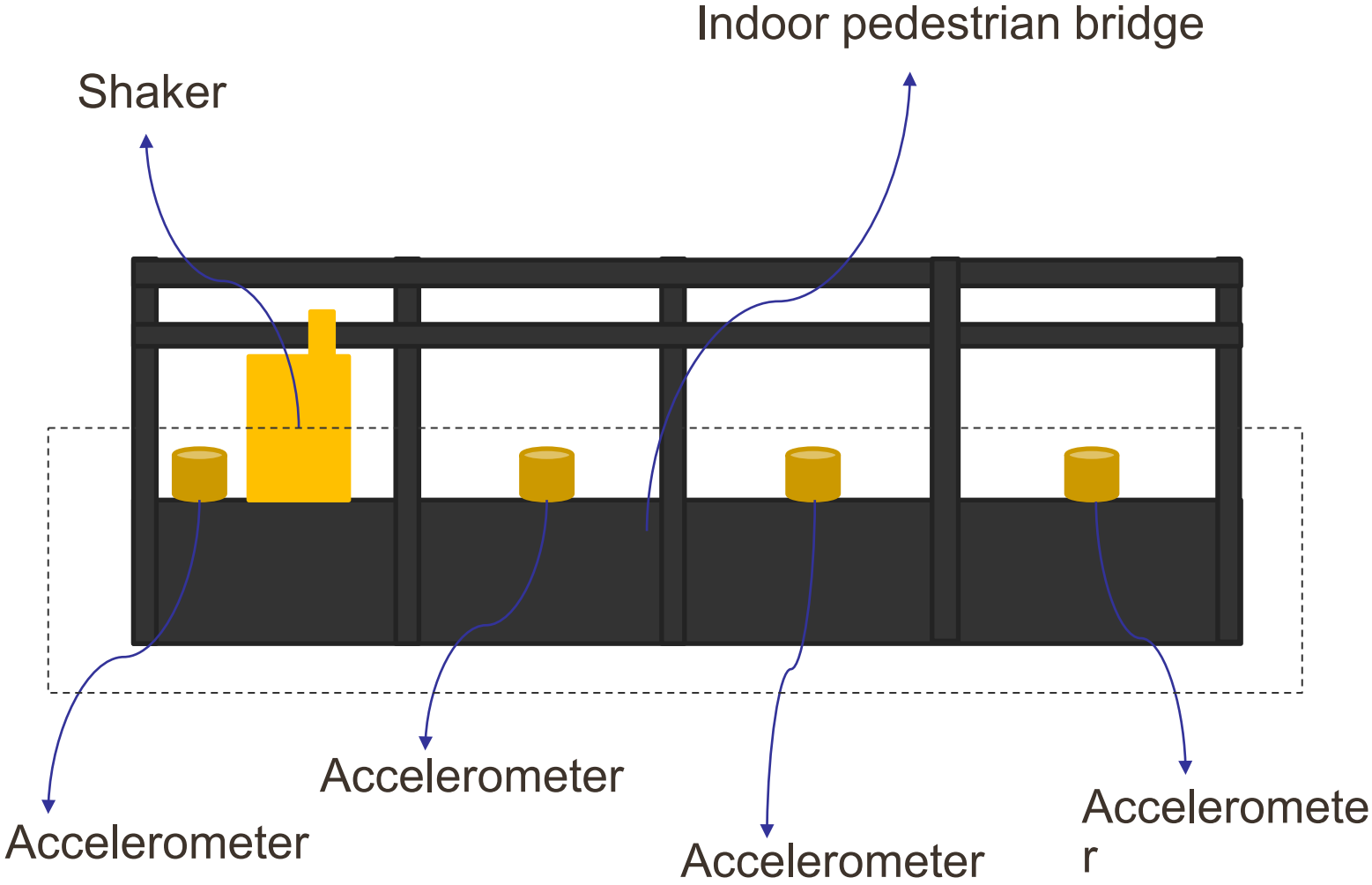
# Vibration displacement in Z-direction



# Vibration displacement in Z-direction: ZOOM IN

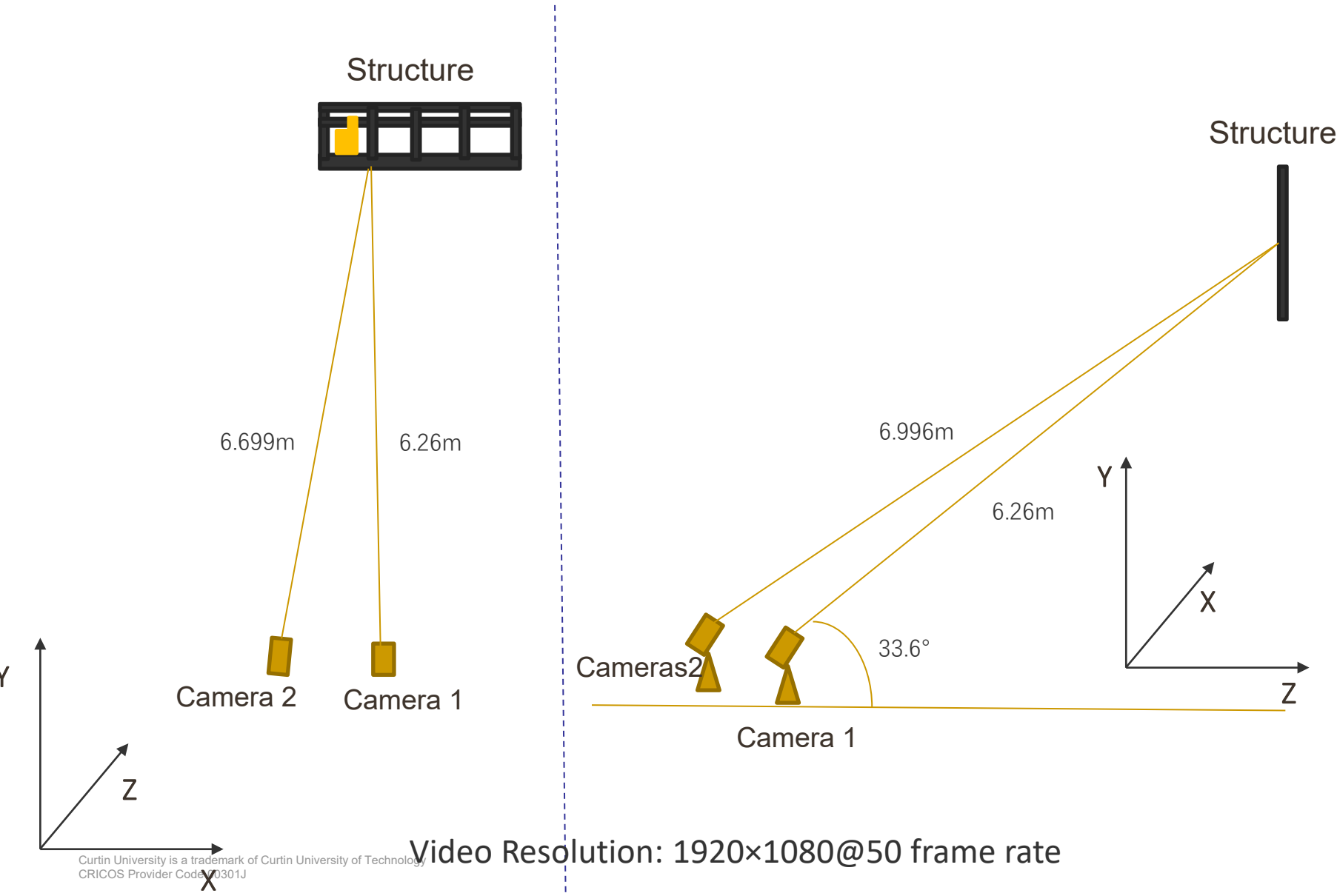


# 3.3. Application to a real engineering structure





# Indoor Pedestrian bridge



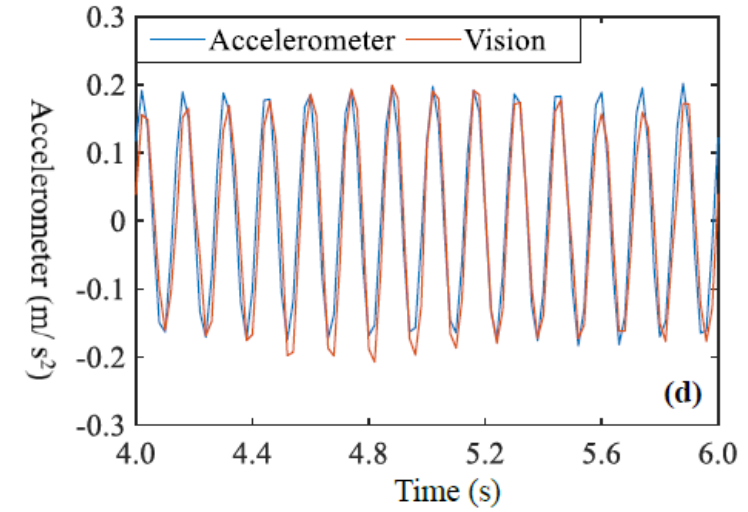
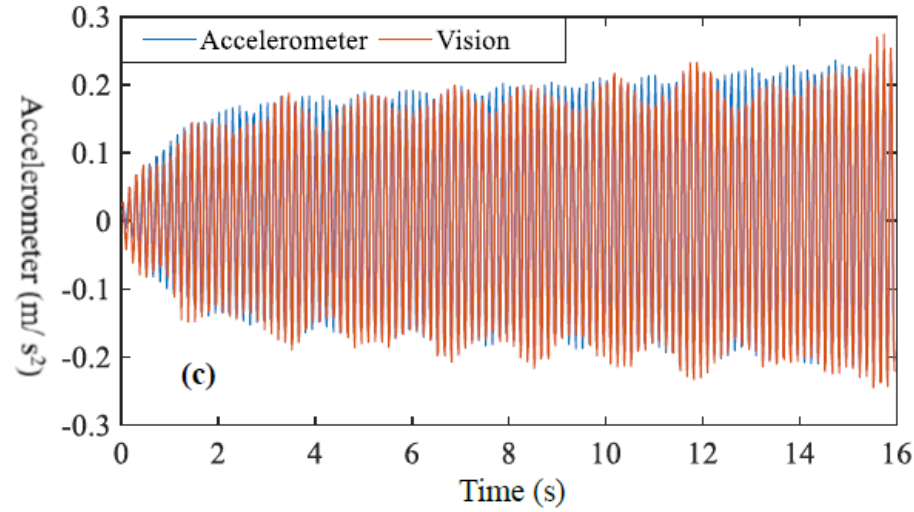
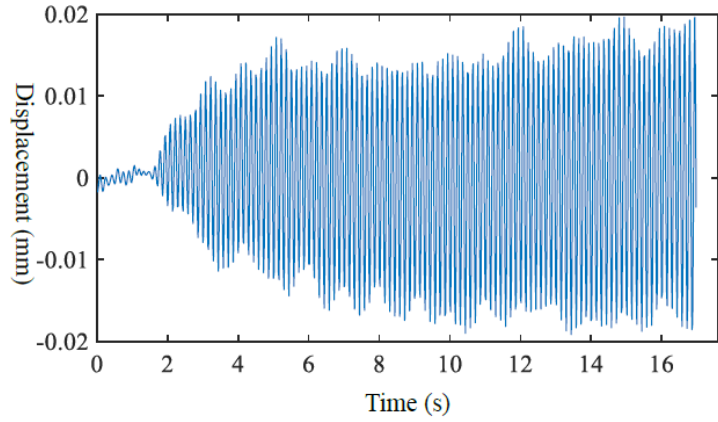
Video Resolution: 1920×1080@50 frame rate

Curtin University is a trademark of Curtin University of Technology  
CRICOS Provider Code 00301J

# Motion magnification for subtle vibration measurement

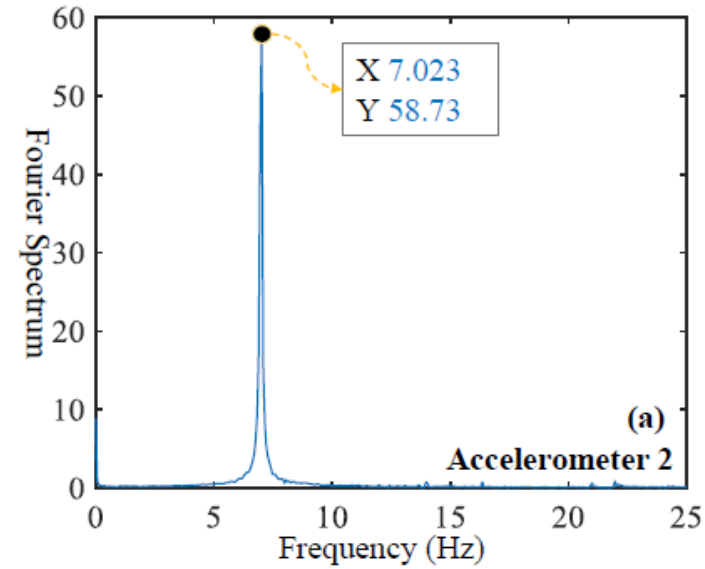
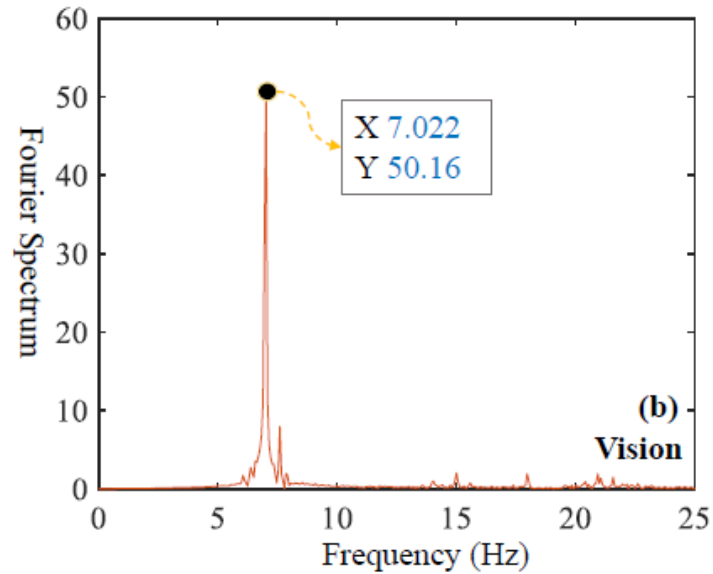


# Indoor Pedestrian bridge



Vibration Displacement

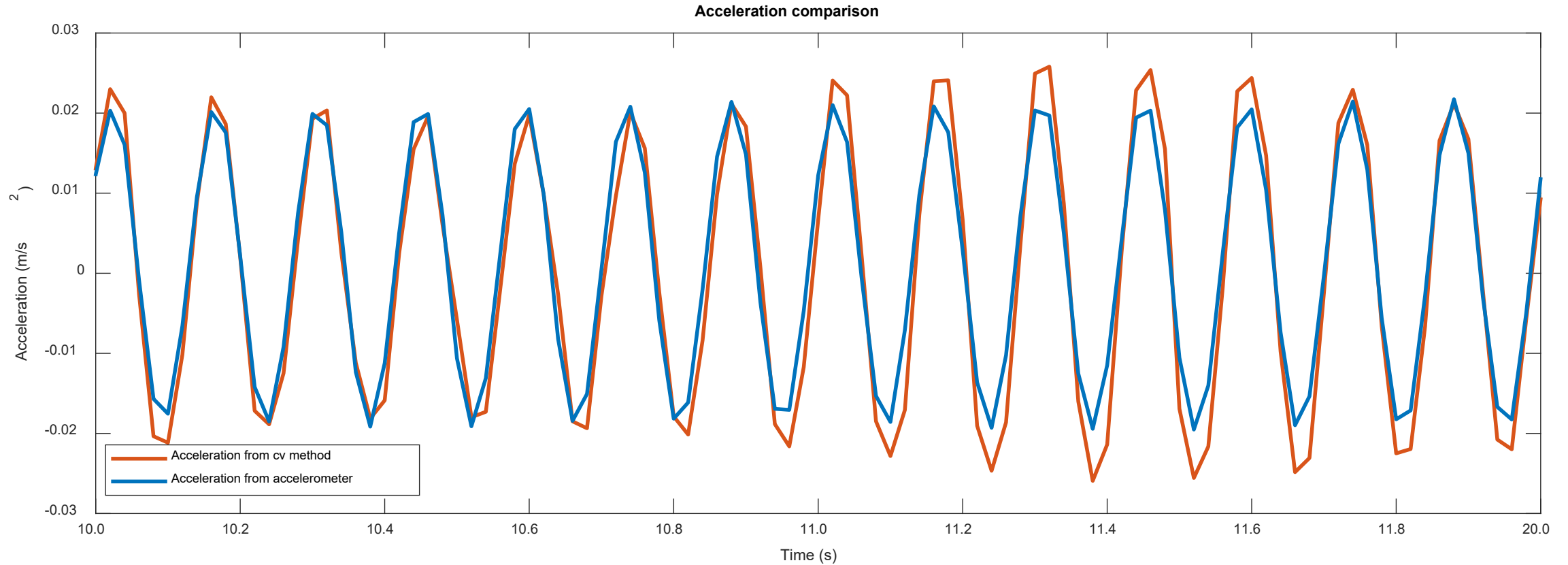
Vibration Acceleration



VISION method

Accelerometer

# Indoor Pedestrian bridge





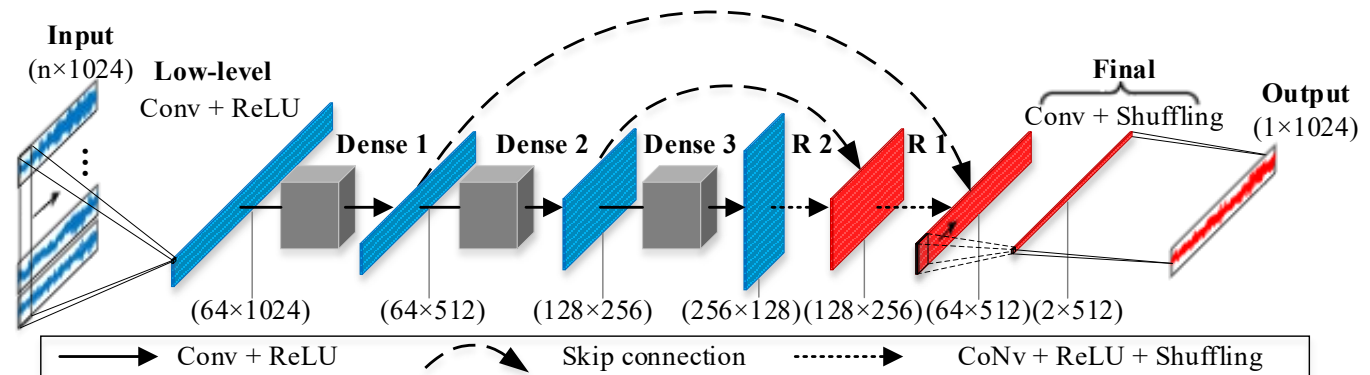
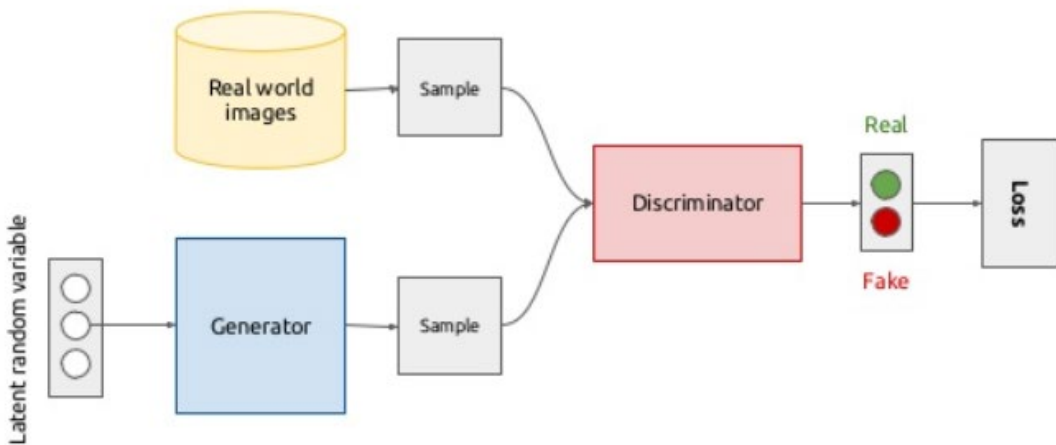
# Concluding remarks

- Developed a novel and accurate **Target-Free 3D** vision based approach for measuring vibration displacement measurement
- **Deep learning techniques** based feature detection and matching
- **3D subtle vibration displacement** measurement through motion magnification
- Can achieve an accuracy level of less than 0.1 mm
- Generally more challenging in obtaining the exact vibration displacement in depth direction from images/videos
- More investigations on the effect of distance and angle between cameras are ongoing

# 4 Generative Adversarial Networks (GAN) for Response Reconstruction

## Segment based GAN

- SegGAN consists of a bottlenecked generator and a segment-based discriminator
- Trained through an adversarial process
- Can capture both low-frequency (vibrational characteristics) and high-frequency structure (shifts of amplitude or instantaneous frequencies change) of data
- DenseNet with strong capability on feature extraction is used as generator

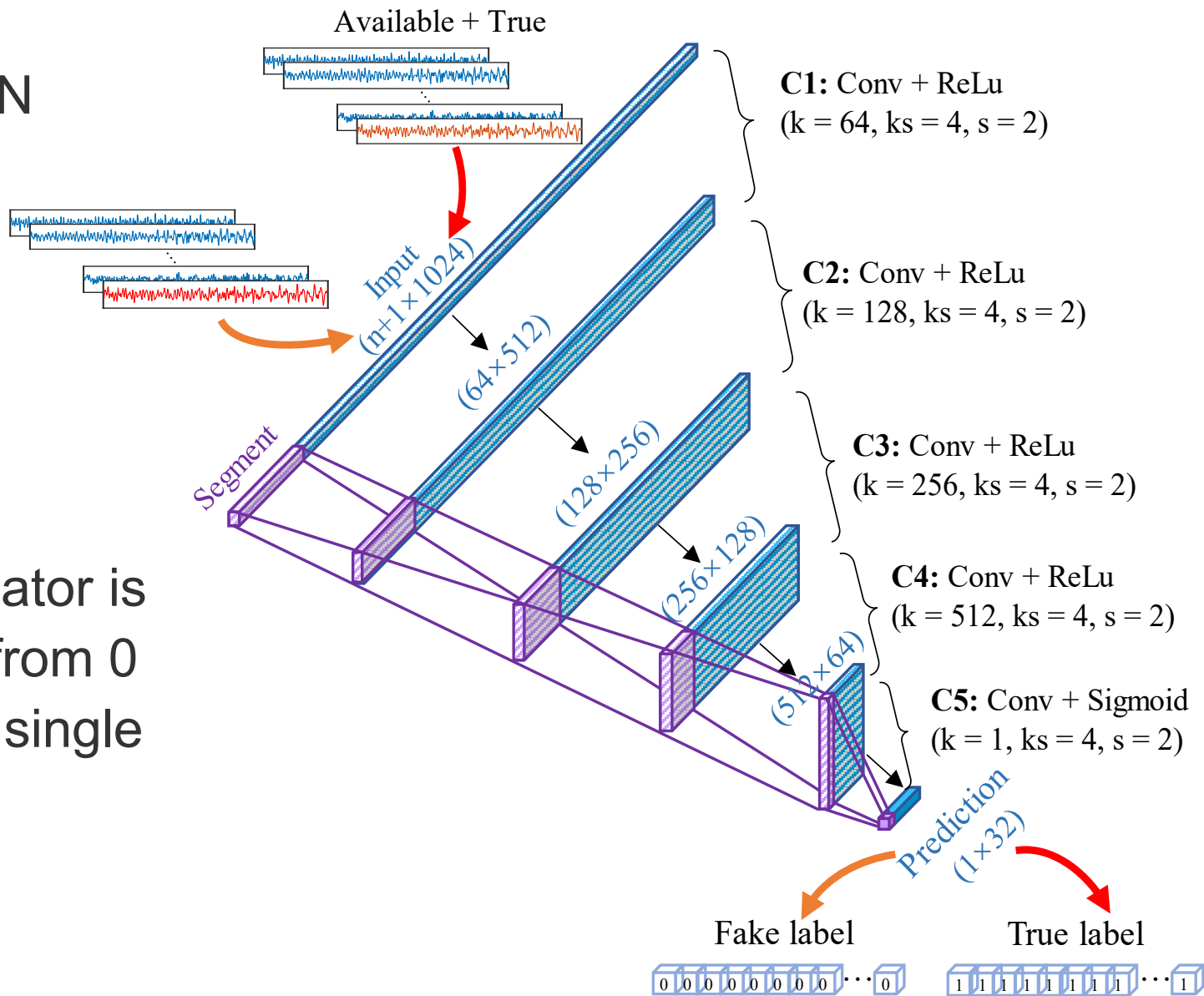


Architecture of DenseNet

## Conditioned discriminator

- Discriminator is a fully stacked CNN
- Aims to provide additional loss gradients to the generator for reinforcing high-frequency data structure learning
- conditioned input
- output of segment-based discriminator is an array contains scalars ranging from 0 to 1 (output of traditional GAN is a single number)

## Architecture of segment-based discriminator with conditioned input



# Objective of SegGAN

- Objective of SegGAN is to maximize the ‘truth’ of a reconstructed response through a discriminative training framework
- Trained supervised
  - Try to allocate a large value for true data
  - Try to allocate a small value for reconstructed data

$$\arg \min_G \max_D L_{SegGAN} = \mathbb{E}_{a,t} [\log D(a, t)] + \mathbb{E}_a [\log(1 - D(a, G(a)))]$$

- MSE loss has strong capability on learning low-frequency data features

$$L_{N-MSE} = \sum_{k=1}^n \frac{(t_k - G(a_k))^2}{t_k^2}$$

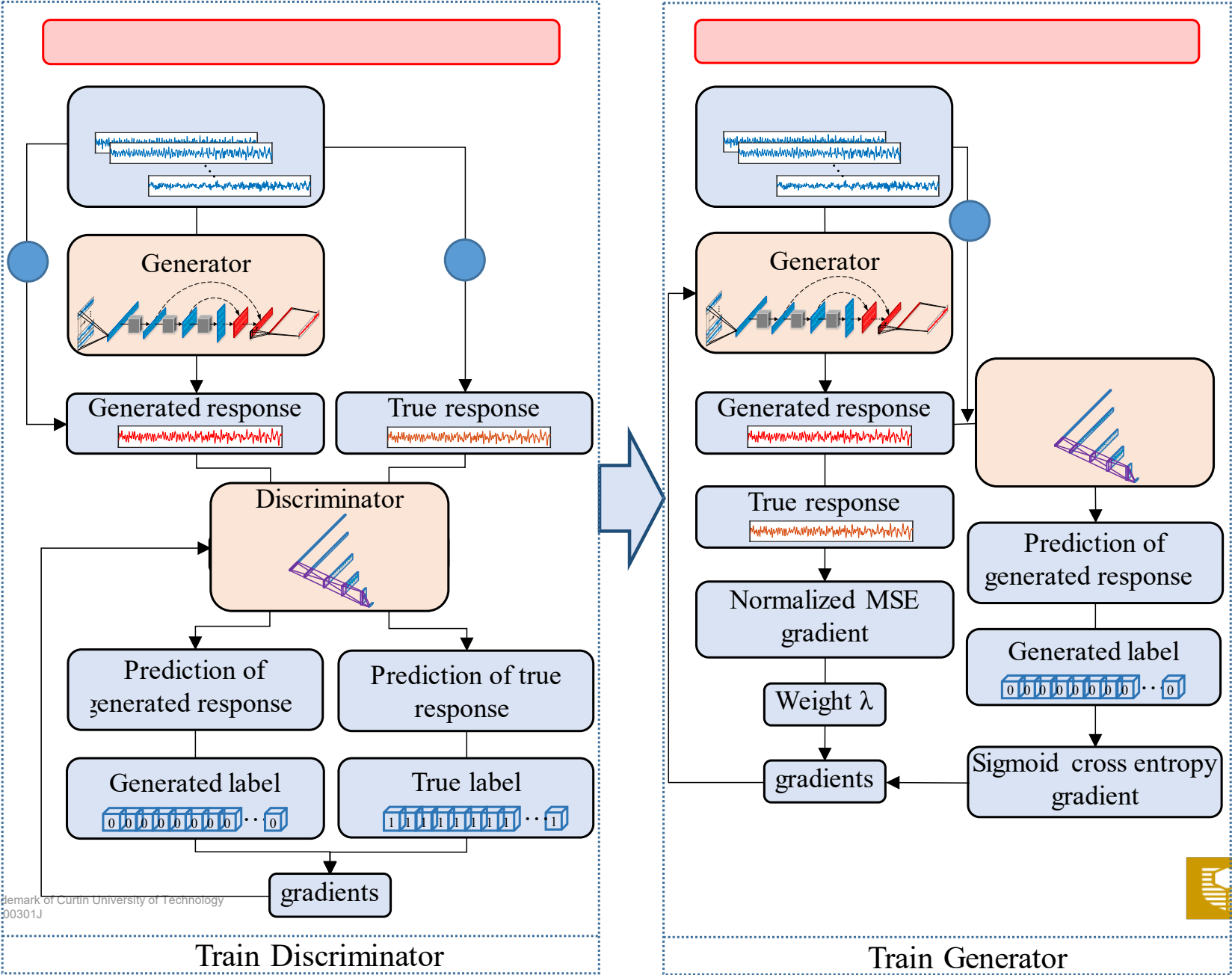
The target of the generator becomes producing responses to treat discriminator, meanwhile, to be close to the true responses in an MSE sense

The final objective function for the generator is expressed

$$L_G = \arg \min_G \max_D L_{SegGAN} + \lambda L_{N-MSE}$$



# Training process

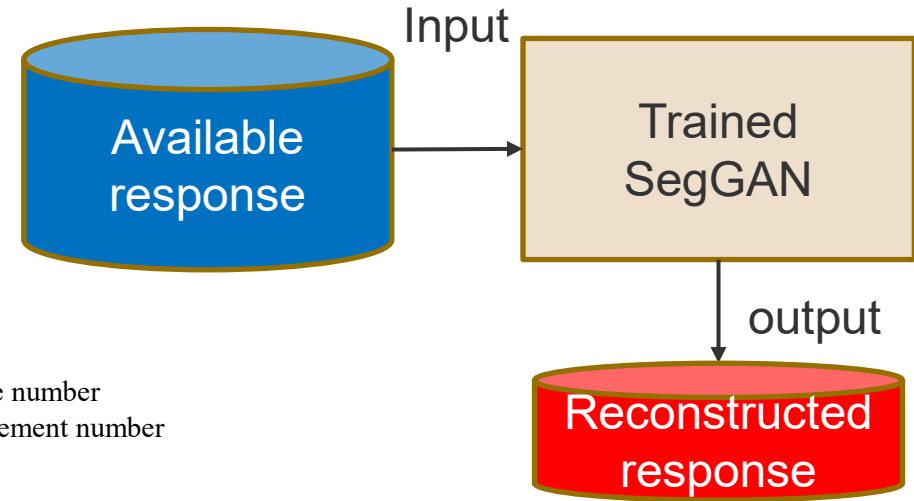
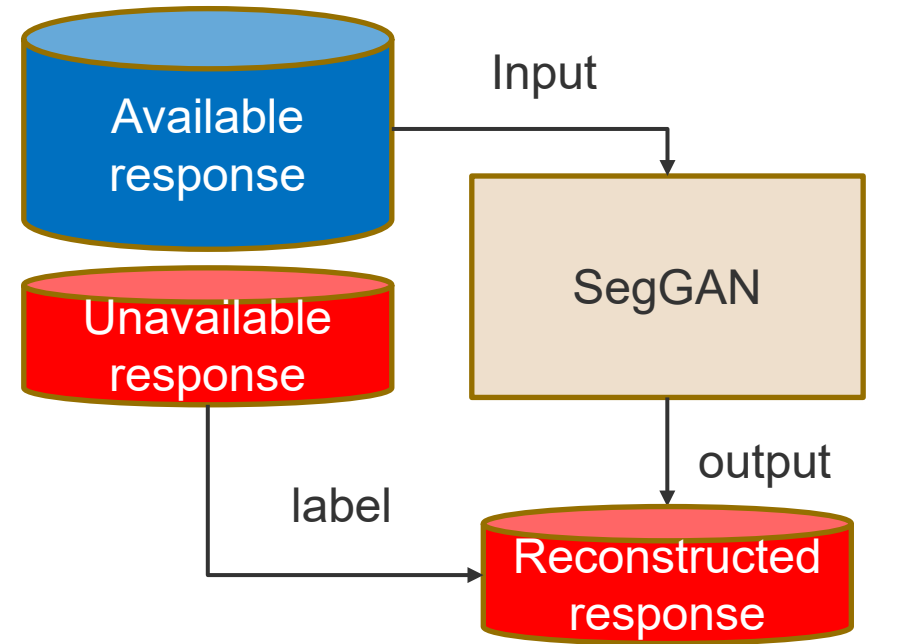
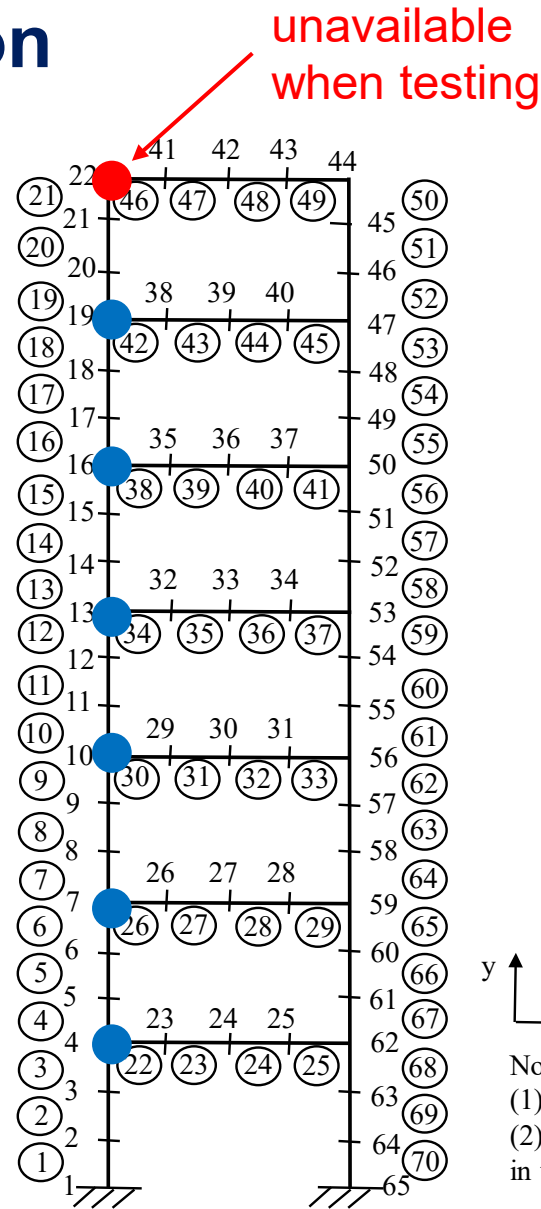
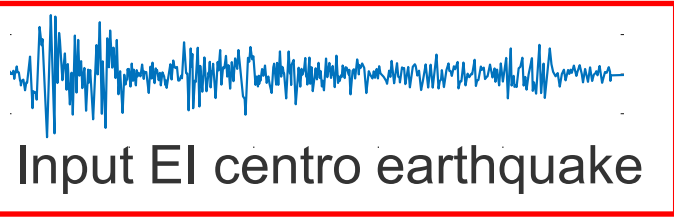


# Numerical validation with a frame structure

Training data:  
ambient excitation



Testing data:  
earthquake excitation

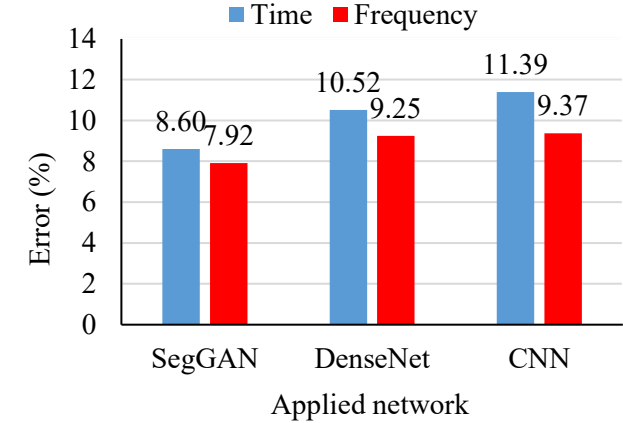
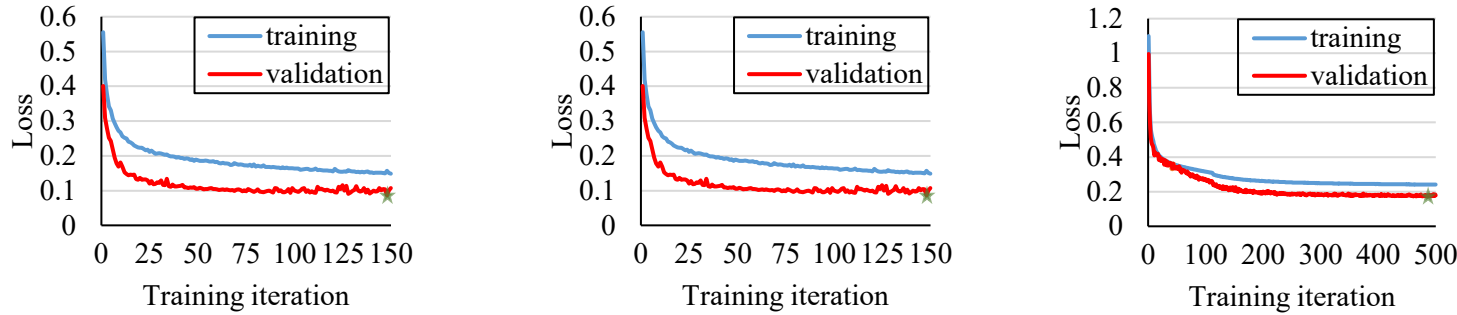


Use ambient response for training and earthquake response for testing

■ Results are compared with a traditional CNN and DenseNet

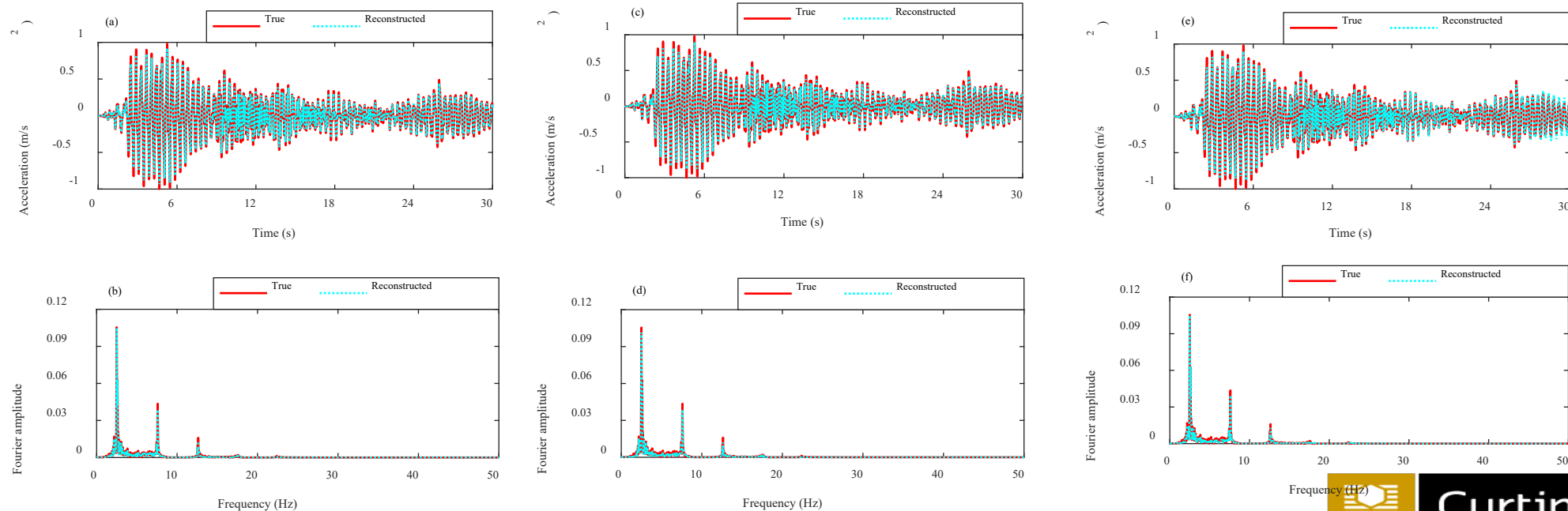
Reconstructed Response by SegGAN is more accurate

Training of SegGAN is more efficient



Training processes of (a) SegGAN (b) DenseNet and (c) CNN

Reconstruction errors



Comparison of true and reconstruction responses

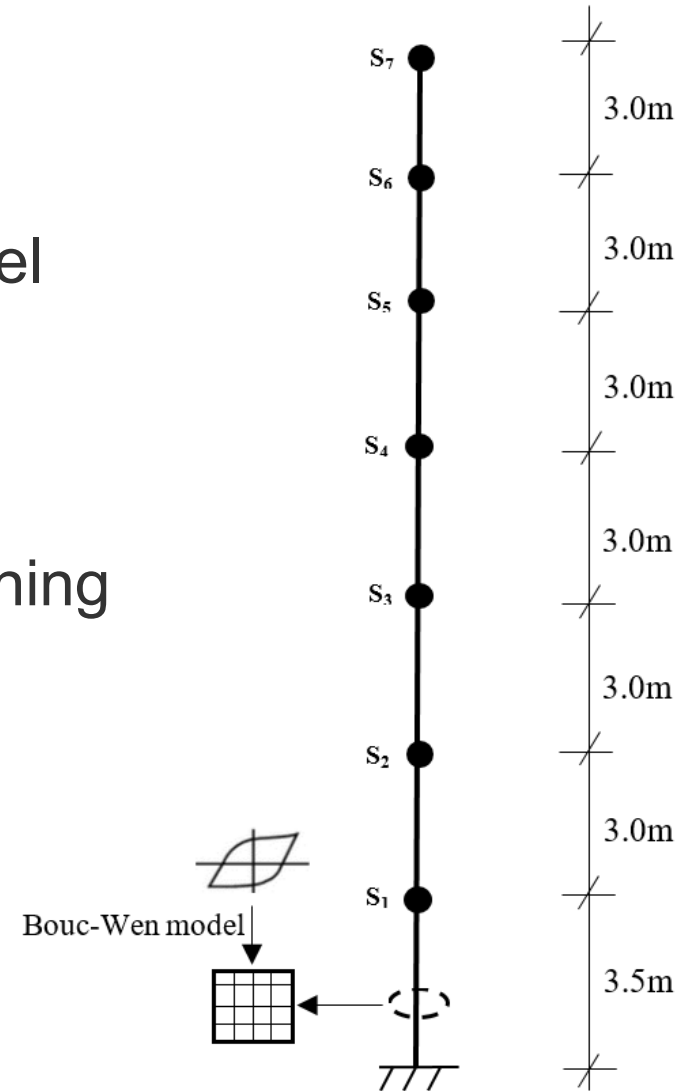
# Numerical validation with a nonlinear building model

## Testing setup

- The first story is assumed to have a nonlinear property following a Bouc-Wen hysteretic model

$$m\ddot{u}(t) + c\dot{u}(t) + f_{NL}[u(t), t] = f(t)$$

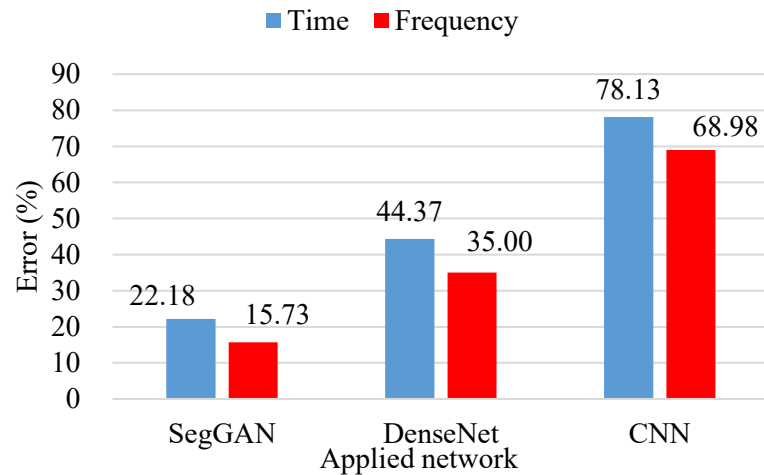
- Only 3 earthquake responses are used for training and 1 used for testing
- Top sensor become unavailable when testing



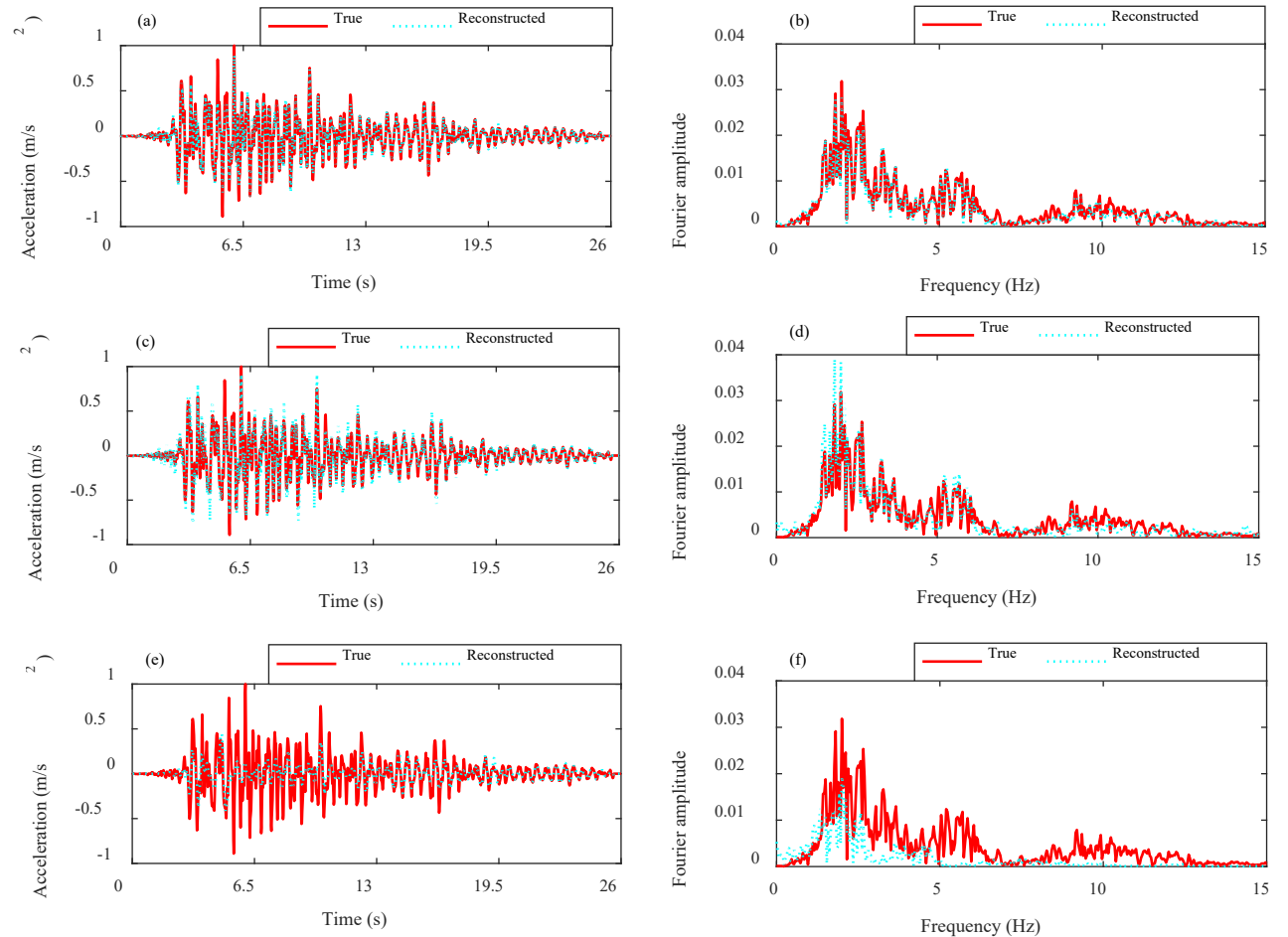


# Testing results

- SegGAN outperform other two networks
- SegGAN is more capable for extracting local changes than DenseNet



Reconstruction errors



Comparison of true and reconstruction responses

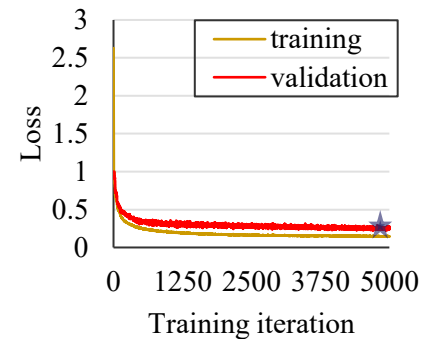
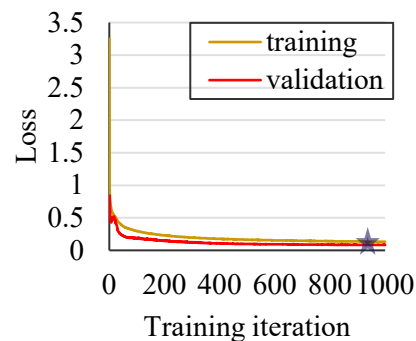
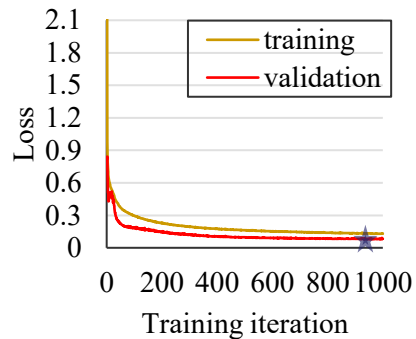
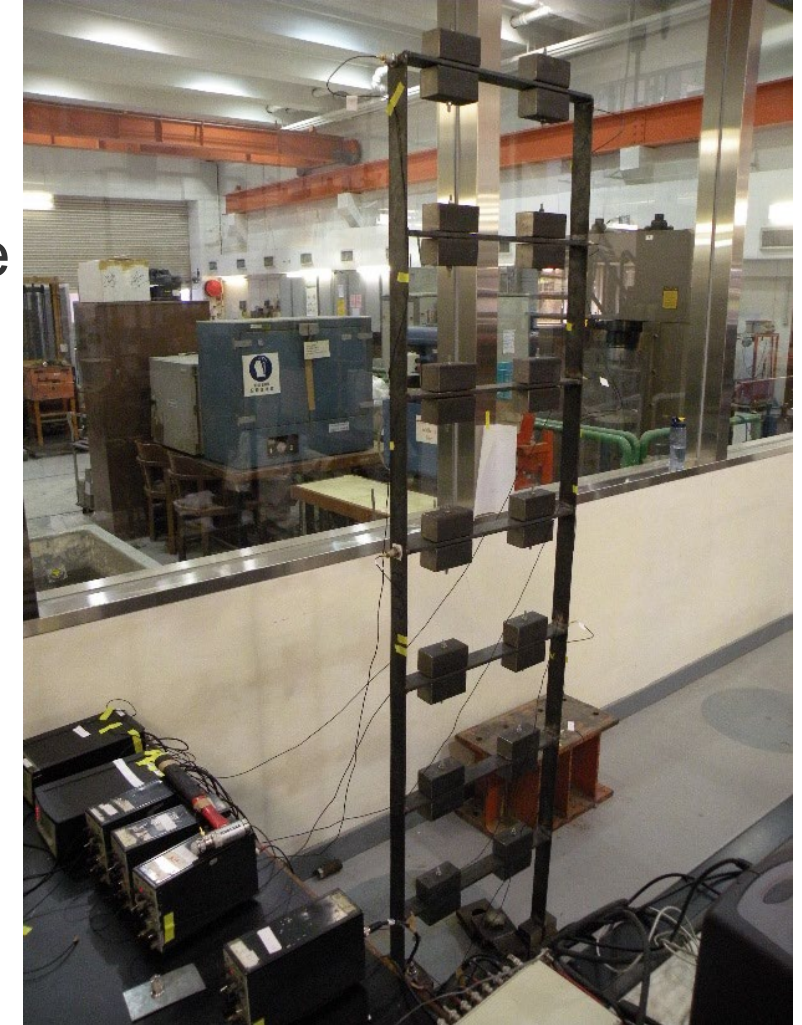
# Experimental validation

## Testing setup

- A seven-story frame structure
- Ambient response is used for training and earthquake response is used for testing

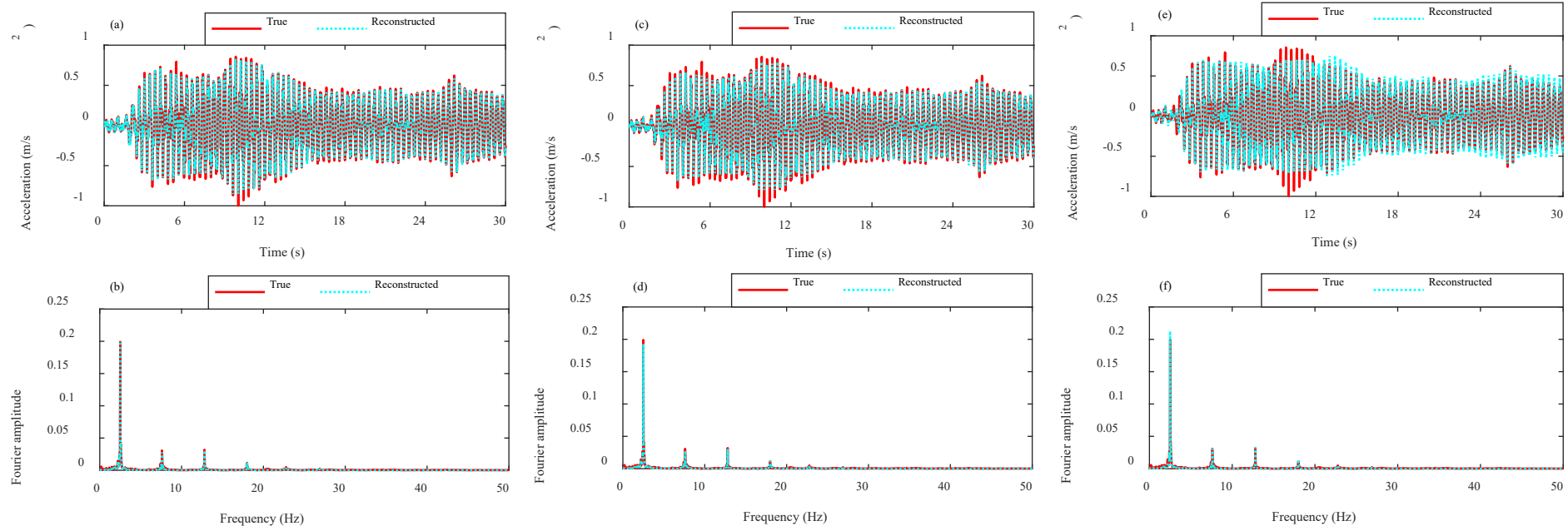
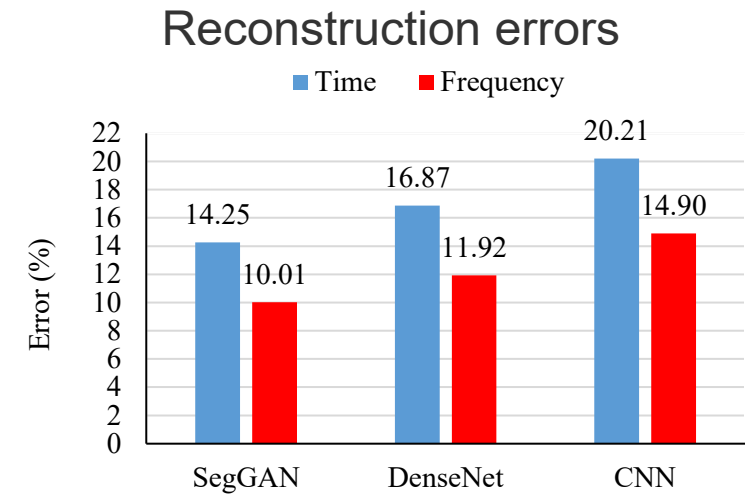
## Testing results

- Loss of SegGAN is lower and without overfitting



Training processes

- SegGAN performs better than DenseNet in reconstructing amplitude of responses contributing to the involved discriminator
- CNN is unable to extract the detail information of earthquake response and reconstructs response with averaging amplitudes



Applied network

Comparison of true and reconstructed earthquake responses

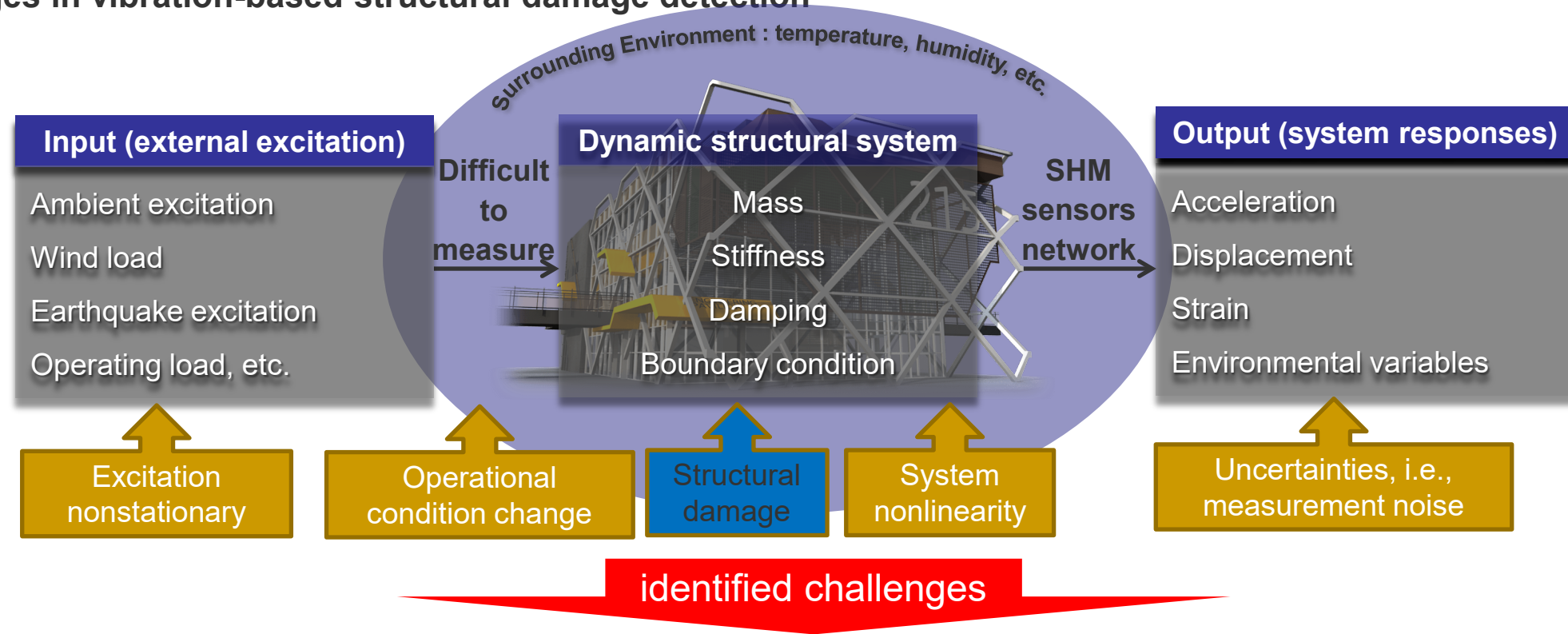
# Conclusion and discussions

- A SegGAN is proposed for reconstructing response under extreme loadings
- With efficient and accurate feature extraction, SegGAN outperforms the other two networks and produces distinguished reconstruction results in both time and frequency domains
- SegGAN in these studies effectively and automatically extracts linear and nonlinear response features from limited training data with measurement noise and varying environmental and operational conditions
- The advantages of less data requirement, complex environmental adaptability and automation leading this method applicable for real applications



# 5. Novel big data analytics for condition monitoring

- Challenges in vibration-based structural damage detection



- Challenge 1:** The change in modal parameters due to *temperature variation* could be contaminated by these induced by a *medium degree of damage*.
- Challenge 2:** Linear theory-based system identification or modal analysis methods might result in biased parameter estimation and inaccurate damage detect result due to the *excitation nonstationary, noise contamination* and *system nonlinearity*.



# Research Objective

- **Objective**: to develop reliable damage feature from vibration responses that are sensitive to structural damage but insensitive to **nonlinear effects**, **operational condition change** and **measurement noise**.

phase space-based manifold learning method for structural damage detection under changing environmental and operational conditions

## *Highlight:*

- *A novel structural damage detection approach under changing environmental conditions.*
- *The effectiveness and superiority are demonstrated on two real-world structures.*
- *It is sensitive to structural damage but insensitive to environmental conditions.*
- *The environmental effects can be efficiently characterized with only partial datasets.*

# Structural damage detection via phase space based manifold learning under changing environmental and operational conditions

## ■ Main contribution & significance

1. In the theory of phase space, the unobservable temperature spatial distribution can be view as a **hidden variable**, which manifested as a specific trajectory or distribution in the **phase space spanned by partial observable variables**;
2. Manifold learning is an efficient method to extract the inherent nonlinear relationship between modal frequencies and environmental.

## Methodology

### Phase space construction by using modal frequencies

$$f_n = \mathcal{F}_n(\lambda_n, G, K, M)$$

$$f_n = \mathcal{F}_n[\lambda_n(T), G(T), K(T), M, T] + e$$

$n$  : the  $n$ -th order modal frequency.

$\lambda_n$ : dimensionless parameter related to boundary constraint

$G$ : dimensionless parameter related to geometric structural

$K$  and  $M$ : stiffness and mass matrices

$T$ : non-uniform temperature distribution along the structure

$e$ : uncertainties caused by measurement noise and modelling errors.

### Manifold learning based DSF extraction

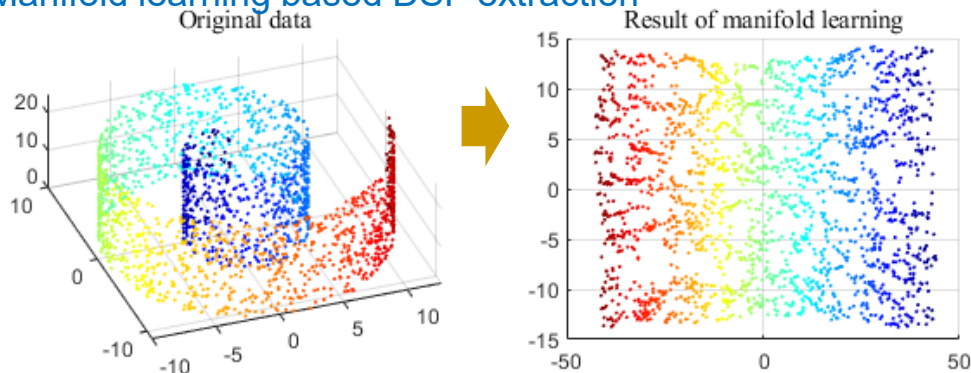


Fig.1 An illustrative example of manifold learning

## ■ Flowchart of the proposed method

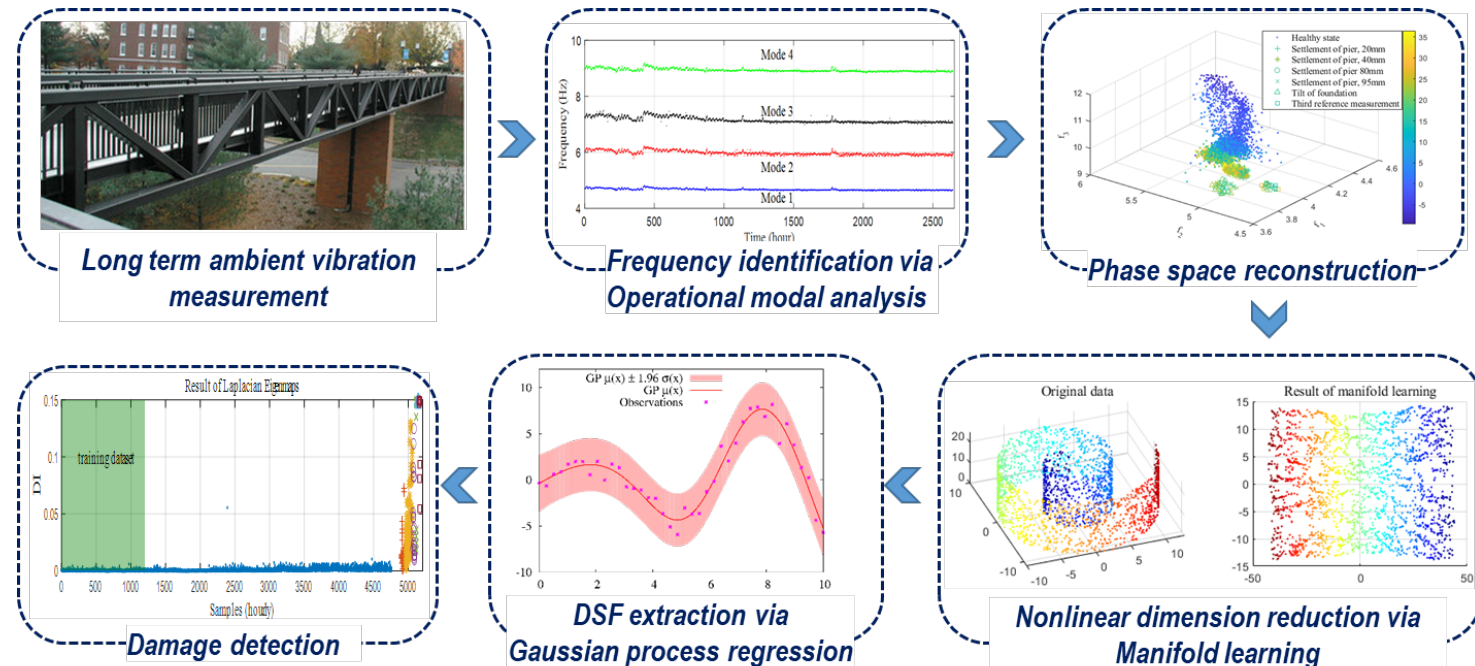


Fig.2 Flowchart of the proposed approach for structural damage detection from data obtained with varying environmental conditions



# Field Application 1: Dowling Hall Footbridge

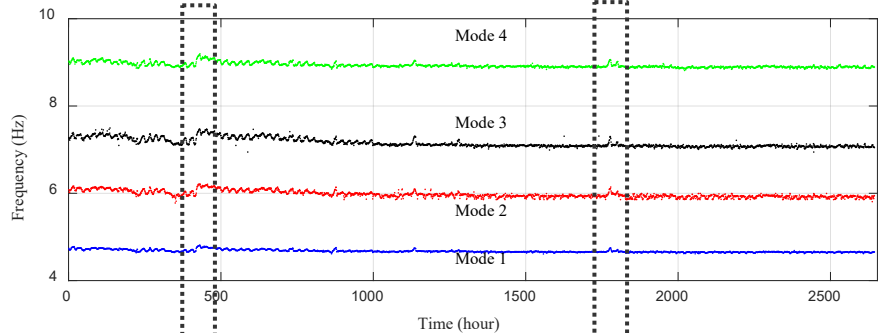
## 17 weeks Continuous Monitoring of the Dowling Hall Footbridge

- ✓ two-span continuous steel frame bridge



Fig.3 Overview of the Dowling Hall footbridge

### ✓ The first four order modal frequency & air temperature



First four natural frequencies during the monitored period

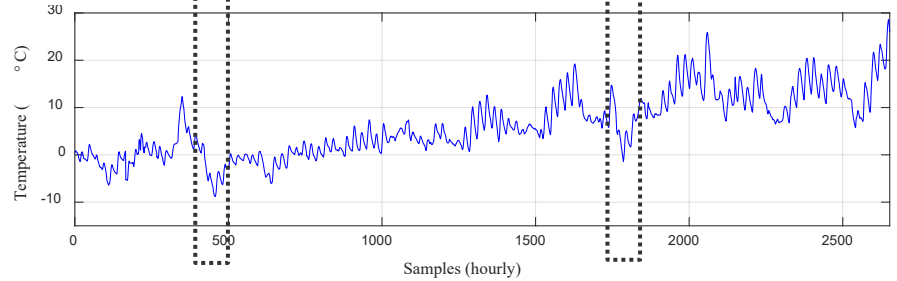


Fig.4 Air temperature variations during the monitored period

### ✓ Effect of live load on frequency

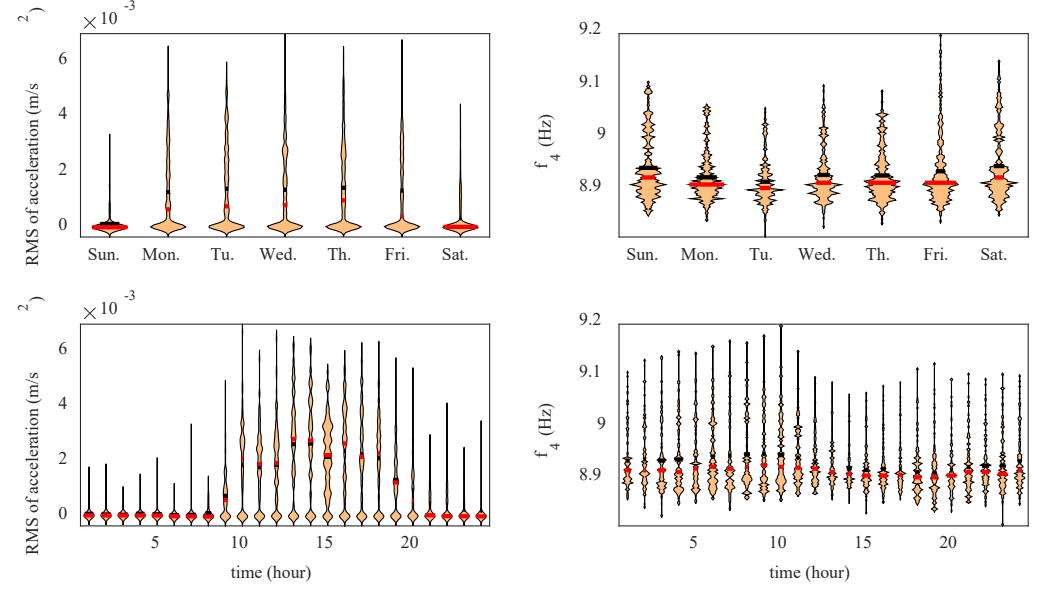
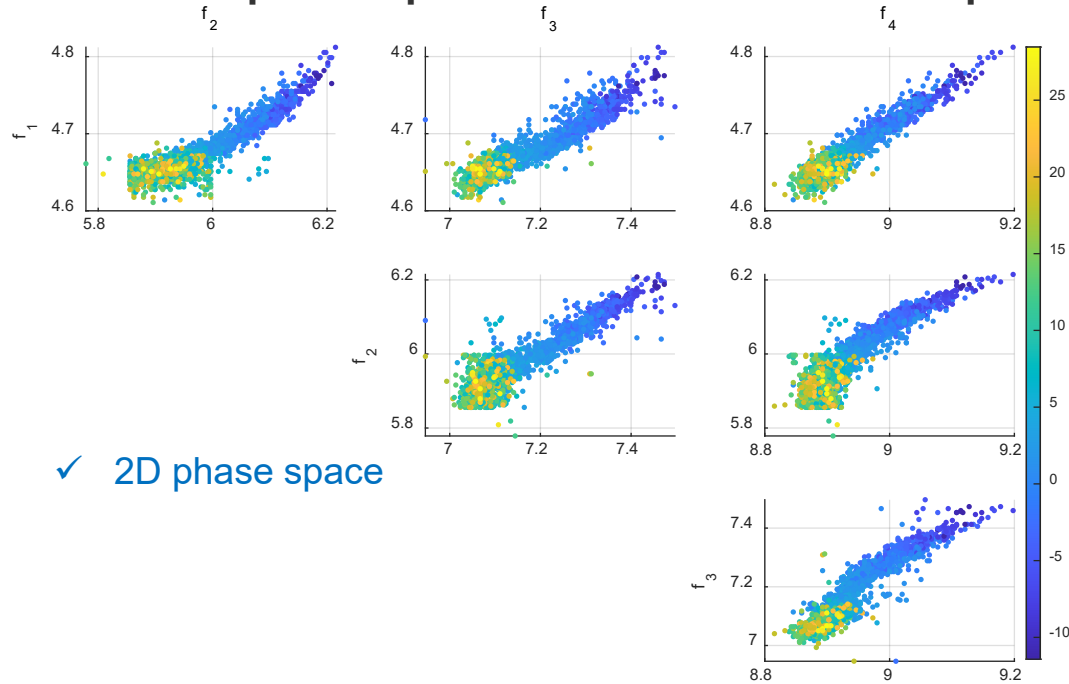


Fig.5 Effect of live load on natural frequency: (a) weekly RMS variation; (b) weekly frequency variation; (c) daily RMS variation; (d) daily frequency variation.

- The first four order frequencies obviously increased when the bridge experienced the lowest temperature.
- The frequency variations in the first four natural frequencies owing to environmental and operational effects are 4.18%, 7.02%, 7.34% and 4.16%, respectively.
- The weekly variation of the mean value of fourth order frequency is about 0.3%.

# Field Application 1: Dowling Hall Footbridge

## 2D and 3D phase space reconstruction via frequency observation



✓ 2D phase space

Fig.6 Visualisation of the relationships between the pairs of the first four natural frequencies. (The color bar denotes the environmental temperature)

✓ 3D phase space

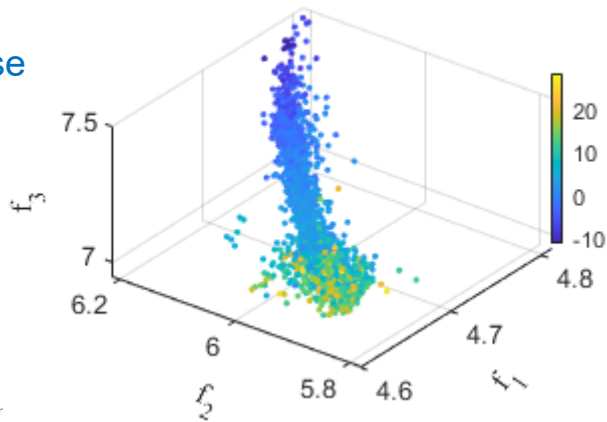


Fig.7 Visualisation of the nonlinear manifold of the Dowling Hall footbridge in the phase space spanned by the first three natural frequencies.

✓ Manifold structure extracted from 4D phase space to 3D phase space

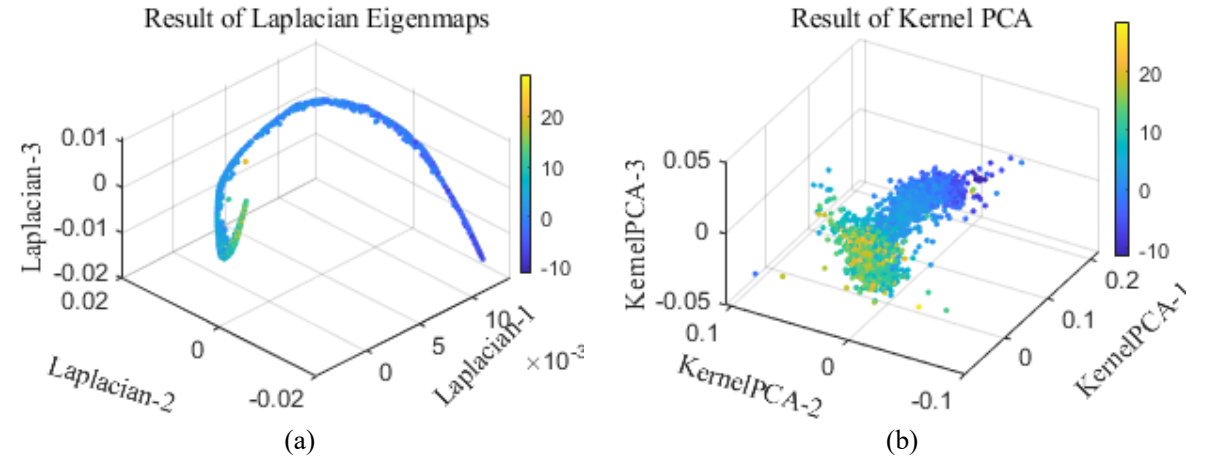


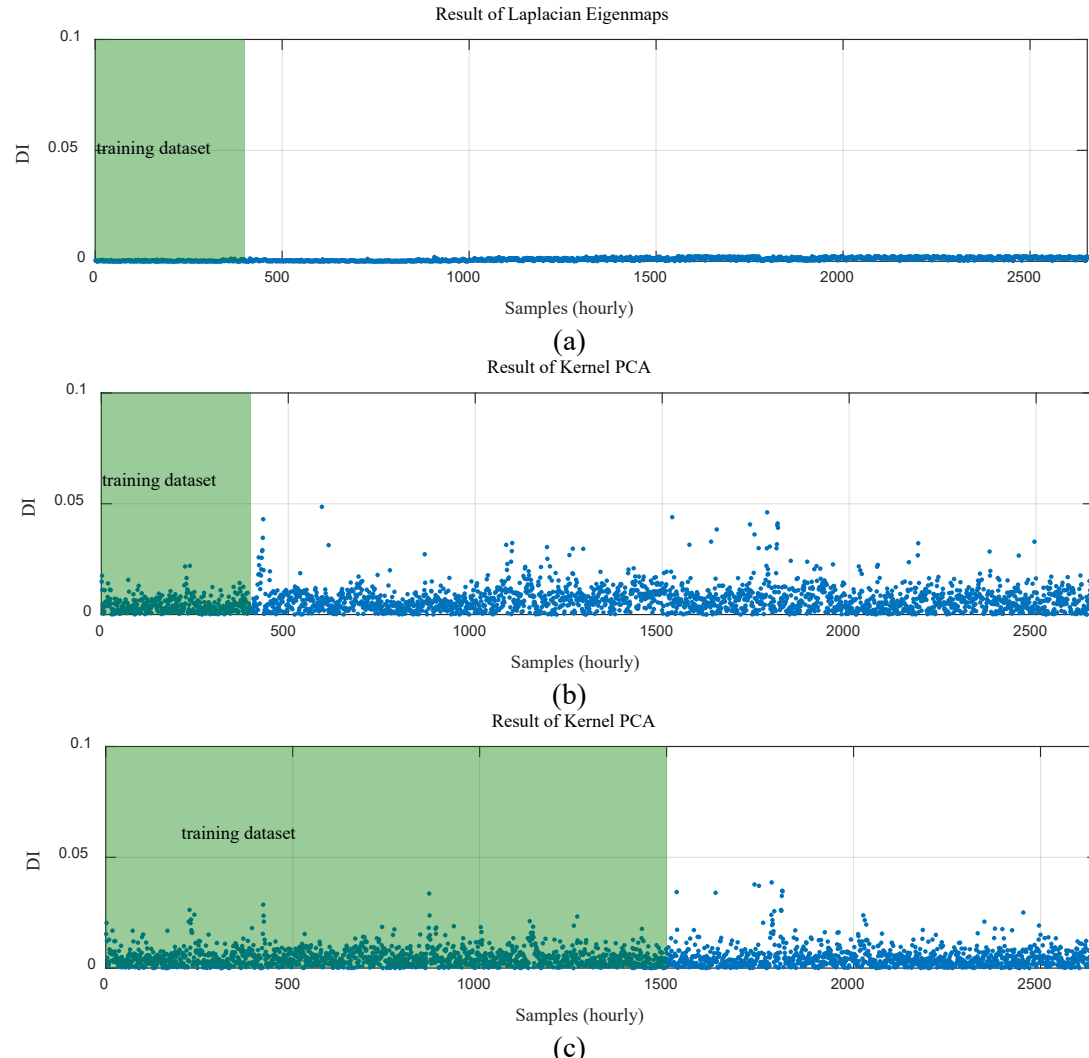
Fig.8 Manifold structures of the Dowling Hall Footbridge discovered by: (a) Laplacian Eigenmap method; (b) Kernel PCA method. (The color bar denotes the environmental temperature)

- Overall, the frequency is regularly distributed according to the temperature variation.
- A curve-like topologic structure is observed in a part of frequency pair, i.e.  $f_1$  vs  $f_2$ ,  $f_2$  vs  $f_4$  and  $f_3$  vs  $f_4$ . Linear relationship is observed in other frequency pairs.
- no distinct outlier cluster is found in the three-dimensional phase space.
- A better converged pattern is observed by using Laplacian Eigenmaps than that of the Kernel PCA method.

# Field Application 1: Dowling Hall Footbridge

## Condition assessment of the Dowling Hall Footbridge

### ✓ Identification results



- DI of Laplacian Eigenmaps is very stable and remain at the same level even though the temperature exceeded the training dataset. Meanwhile, significant fluctuation is observed in the DI of Kernel PCA at the samples interval 416 to 449, when the structure experienced the lowest temperature.
- The false positive alarms appeared in Fig. 9(b) owing to the extreme cold temperature, which, however, no longer exist in the results with more training samples as shown in Fig. 9(c). In addition, the overall amplitude of DI is also slightly decreased, which means that the environmental effects can be alleviated by including a wider range of temperature variations into the training datasets.
- However, it can be observed that larger damage index values are obtained for the testing sample, even when 1500 samples are used for training the Kernel PCA based method. Overall, no damage-induced outlier and very minor values are observed in the DI results calculated from the proposed approach, which is consistent with the ground truth.

Fig.9 DI results of Dowling Hall footbridge: (a) Laplacian Eigenmaps with 400 training data; (b) Kernel PCA with 400 samples; and (c) Kernel PCA with 1500 samples.



# Field Application 2: Z24 Bridge

## □ Nearly one year continuous Monitoring of the Z24 bridge

### ✓ Z24 progressive damage test scenarios

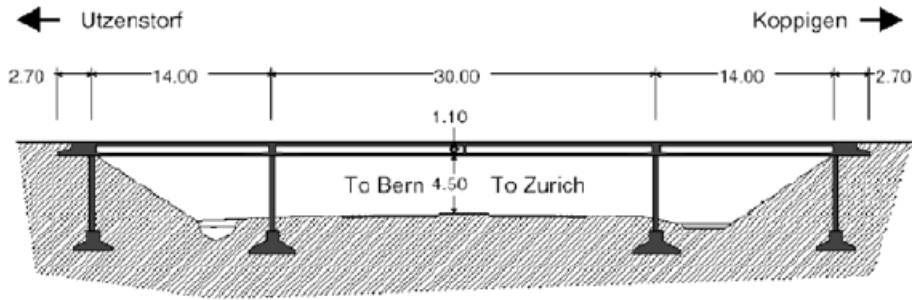


Table 1. Z24 progressive damage test scenarios [15]

Sequence	Date	Description	Samples No.
D0	11-Nov-1997 to 4-Aug-1998	Baseline state	1~6393
D1	10-Aug-1998	Settlement of pier, 20mm	6514~6557
D2	12-Aug-1998	Settlement of pier, 40mm	6572~6671
D3	17-Aug-1998	Settlement of pier, 80mm	6682~6705
D4	18-Aug-1998	Settlement of pier, 95mm	6726~6745
D5	19-Aug-1998	Tilt of foundation	6745~6765
D6	20-Aug-1998	New Reference Measurement	6769~6788
D7	25-Aug-1998	Spalling of Concrete (12 m <sup>2</sup> )	6874~6897
D8	26-Aug-1998	Spalling of Concrete (24 m <sup>2</sup> )	6898~6921
D9	28-Aug-1998	Landslide of 1 m at abutment	6962~6993
D10	31-Aug-1998	Failure of concrete hinges at abutment pier	7019~7028
D11	02-Sep-1998	Failure of anchor heads of post tensioning cables (1 head)	7066~7089
D12	03-Sep-1998	Failure of anchor heads of post tensioning cables (4 heads)	7090~7113
D13	07-Sep-1998	Rupture of tendons #1	7186~7209
D14	08-Sep-1998	Rupture of tendons #2	7210~7233
D15	09-Sep-1998	Rupture of tendons #3	7234~7257

### ✓ The first five order modal frequency & air temperature

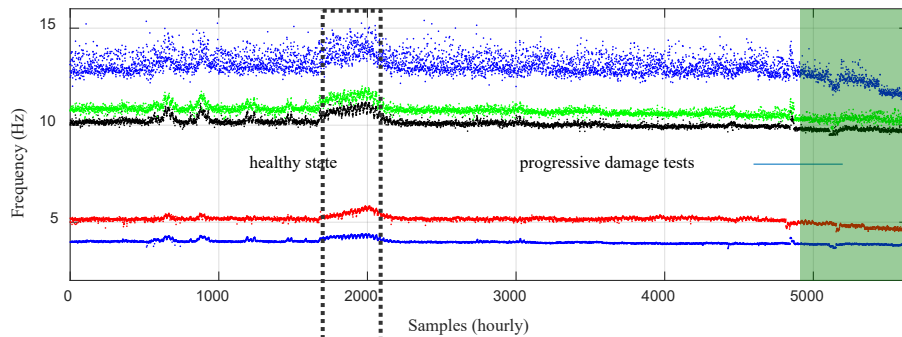


Fig.10 The first five natural frequencies during the monitoring period (the progressive damage scenarios are denoted by green background color)

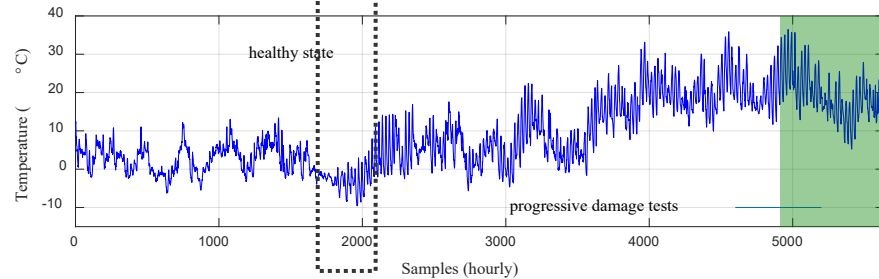
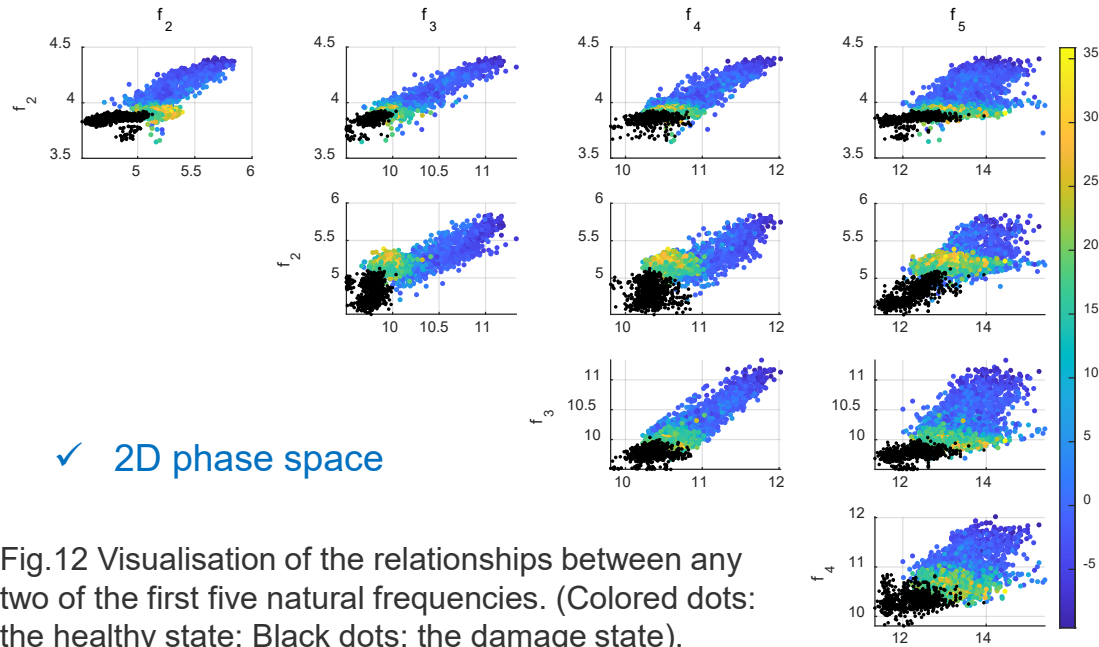


Fig.11 Air temperature measurements during the monitoring period

- Generally, the natural frequency is negatively correlated with the air temperature. Significant frequency fluctuations are observed in the samples from 1650 to 2300, owing to stiffness hardening caused by the soil-frozen effects, which is more obvious than the damage-induced frequency reduction in the first five natural frequencies;
- The environmental effects induced frequency variations of the first five natural frequencies under the healthy state are 17.22%, 20.34%, 14.69%, 15.34% and 22.09%, respectively.

# Field Application 2: Z24 Bridge

## 2D and 3D phase space reconstruction



## 3D phase space

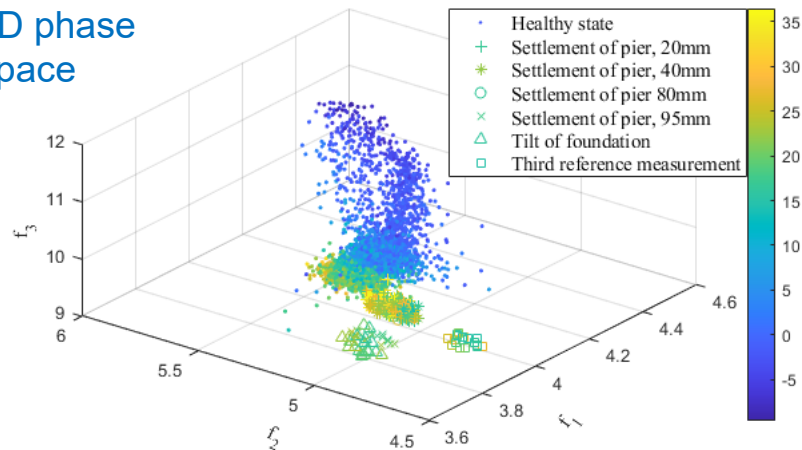


Fig. 13 Visualisation of the nonlinear manifold of Z24 bridge in the phase space spanned by the first three natural frequencies.

## Manifold structure extracted from 5D phase space

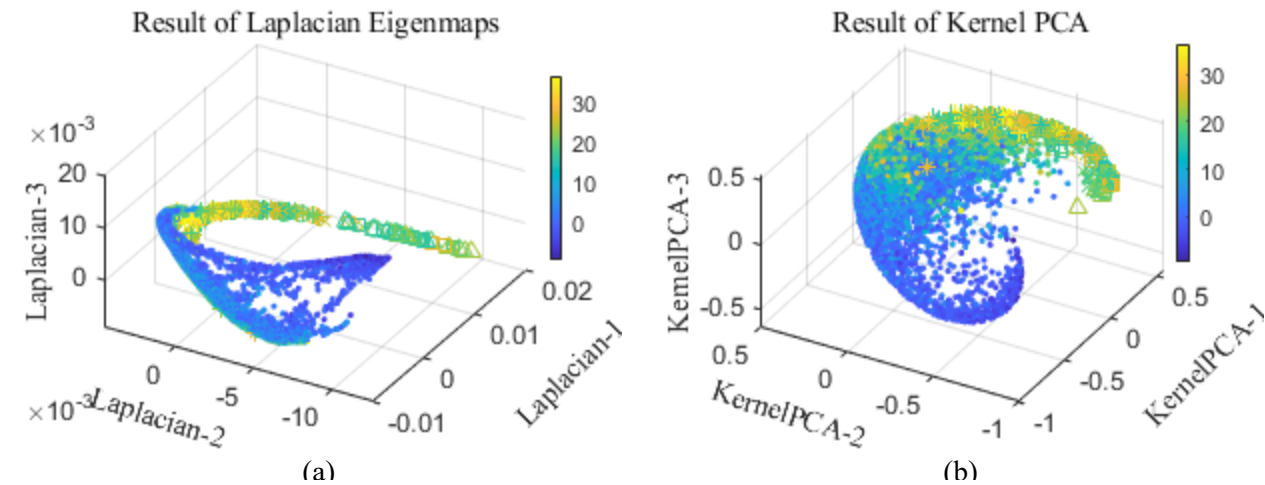


Fig. 14 Manifold structures of the Z24 bridge discovered by: (a) Laplacian Eigenmap method; and (b) Kernel PCA method.

- As shown in Fig. 12, the frequency observations corresponding to similar temperature conditions are distributed closely with each other
- The distribution of damaged states is overlapped with that of healthy state, which means that the 2D phase space spanned by any two of the five order frequencies is unable to separate the damage state with healthy state.
- The second modal frequency  $f_2$  is nonlinearly (bilinear) related with  $f_1, f_3, f_4, f_5$ , while the  $f_1, f_3, f_4$  appear to be nearly linearly related with each other. The distribution of damage states is well separated with that of the undamaged state in the 3D phase space, which means that the classification performance of structural condition changes can be improved in a higher dimensional observation space.
- The manifold identified by the Laplacian Eigenmaps is distributed along the temperature and convergent than that of Kernel PCA.

# Field Application 2: Z24 Bridge

## ✓ Identification results

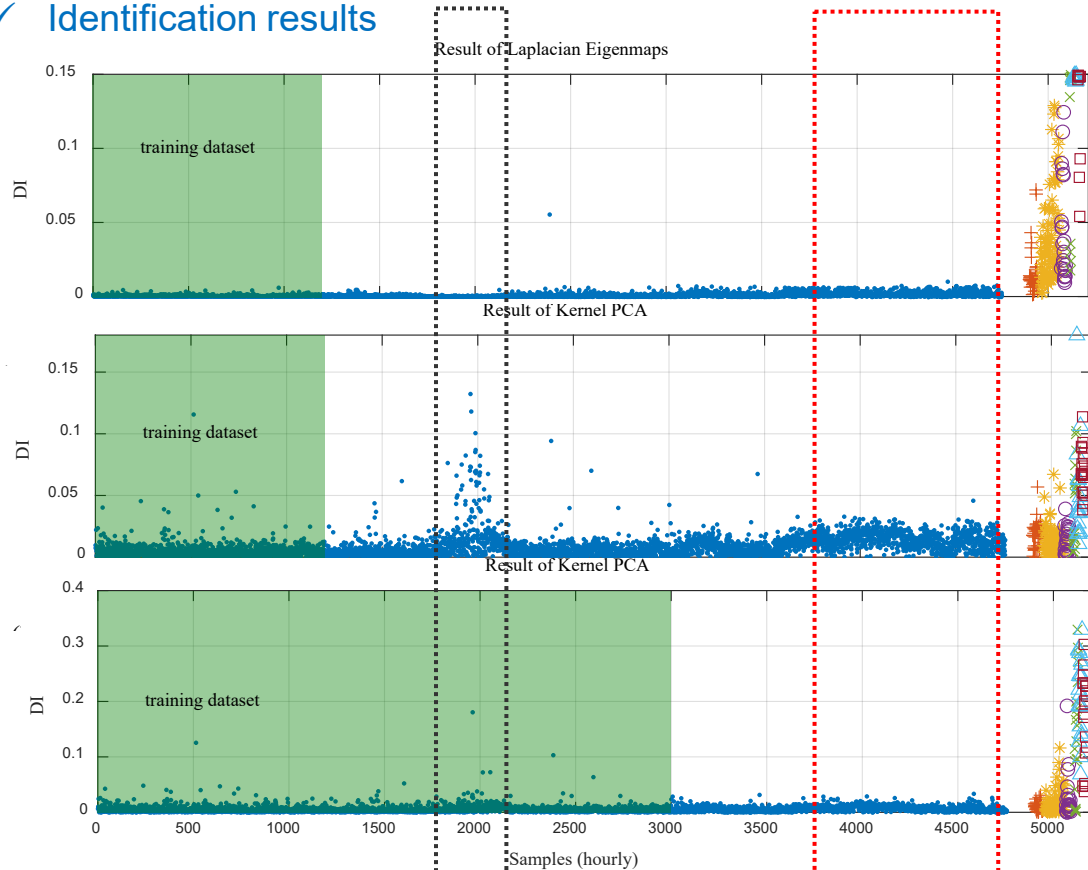
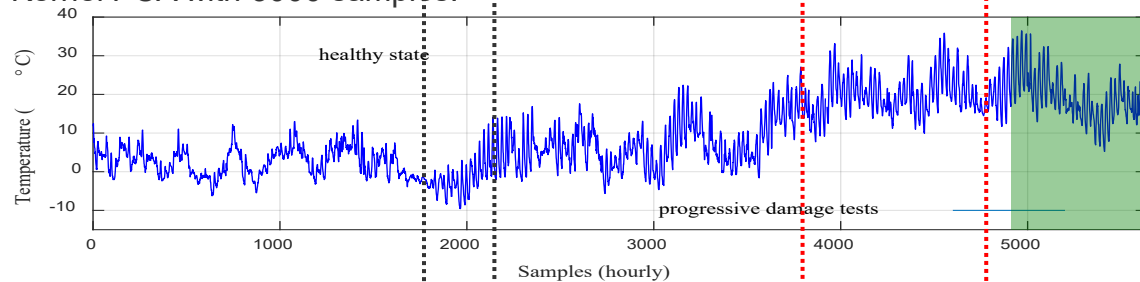


Fig.15 Comparison of damage detection results: (a) The proposed approach with training datasets of 1200 samples; (b) Kernel PCA with 1200 samples; and (c) Kernel PCA with 3000 samples.



- DI is very stable in the healthy states. No visible false positive alarm is occurred in the sub-zero and hot temperature.
- DI increased significantly as soon as the progressive damage scenarios is applied to the bridge.
- In Fig. 15(b), obvious peak around the sample 2000, when the temperature is cold than the lowest temperature used in the training data. the amplitude of false positive DI is at the same or even higher than that of damaged cases.
- The proposed method outperform most of the data-driven damage detection methods applied to Z24 bridge benchmark during in the past decade,
- The proposed method is sensitive to structural damage while insensitive to operational condition changes.



# 6 Engineering Applications



**NEWS**

[Just In](#) [Politics](#) [World](#) [Business](#) [Analysis](#) [Sport](#) [Science](#) [Health](#) [Arts](#) [Fact](#)

[Print](#) [Email](#) [Facebook](#) [Twitter](#) [More](#)

## Hundreds take to Perth's Matagarup Bridge for engineering test ahead of official opening

Updated 7 Jul 2018, 7:49am

PHOTO: More than 1,200 people in total will take part in stage one testing. (ABC News: Anna Hay)

**perth now**

[NEWS](#) [SPORT](#) [ENTERTAINMENT](#) [BUSINESS](#) [LIFESTYLE](#) [HAVE YOU HEAR](#)

[AFL](#) [CRICKET](#) [SOCCER](#) [BASKETBALL](#) [TENNIS](#) [NRL](#) [RUGBY](#) [MOTOR](#) [RACING](#) [MMA](#) [GOLF](#)

Click to unmute

0:00 / 1:14

Hundreds of people have volunteered to test Perth's new Matagarup bridge for the first time.

**Optus Stadium**

## Hundreds walk across Matagarup Bridge as part of "dynamic tuning" test

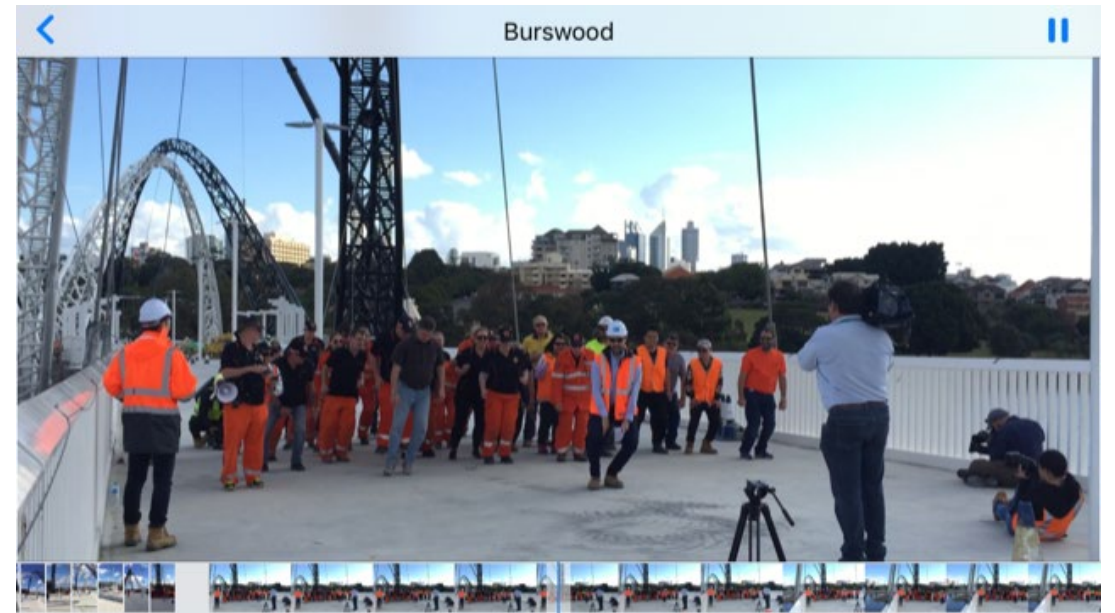
## Swan River Pedestrian Bridge Vibration Characteristics and Comfort testing







Crowds randomly walking on the bridge at Stage 1 test



Pedestrians walking on the bridge at a specific pacing rate



Pedestrians jumping and running on the bridge at a specific pacing rate



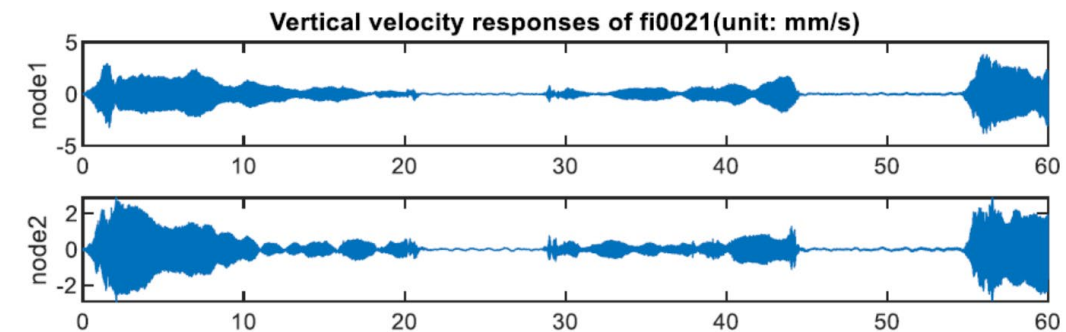
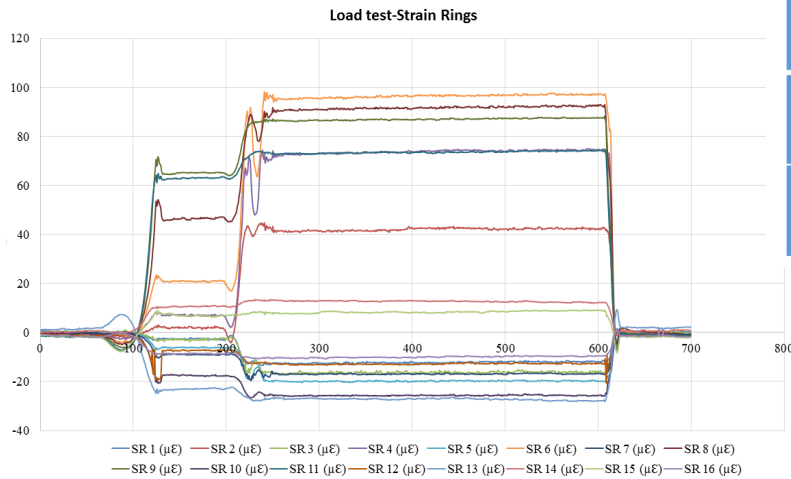


# load carrying capacity evaluation & construction induced vibrations monitoring



**Table1.** Comparison of the RF results between the original structure and the calibrated bridge model

Cases	1# Section	2# Section	3# Section	4# Section	5# Section
Initial FE model	1.58	1.14	1.35	1.14	1.51
Updated FE model	1.83	1.30	1.44	1.30	1.75



# 7. Conclusions

- Vision based binocular system for 3D vibration displacement measurement, and tiny 3D displacement responses can be obtained through motion magnification
- Only a single consumer-grade camera is used for displacement measurement and modal identification of relatively long simply-supported beams, and natural frequencies and mode shapes can be obtained.
- GAN is first used for dynamic response reconstruction of linear and nonlinear structures.
- Novel data analytics used for structural condition monitoring under varying environmental and operational conditions.

# Related publications in this talk

Shao, Y., Li, L., Li, J., An, S., & Hao, H. 2021. Computer vision based target-free 3D vibration displacement measurement of structures. *Engineering Structures*, 246, 113040.

Yanda Shao, Ling Li, Jun Li\*, Senjian An, Hong Hao, (2022), Target-free 3D tiny structural vibration measurement based on deep learning and motion magnification, *Journal of Sound and Vibration*, 117244.

Dong Tan; Jun Li; Hong Hao; Zhenhua Nie, Target-free vision-based approach for modal identification of bridges subjected to moving loads, *Engineering Structures*.

G. Fan, J. Li\*, H. Hao and Y. Xin, 2021. Data driven structural dynamic response reconstruction using segment based generative adversarial networks. *Engineering Structures*, 234, 111970.

Peng, Z., Li, J. \*, & Hao, H. (2022). Structural damage detection via phase space based manifold learning under changing environmental and operational conditions. *Engineering Structures*, 263, 114420.

Peng, Z., Li, J.\*, Hao, H., (2022), Data Driven Structural Damage Assessment using Phase Space Embedding and Koopman Operator under Stochastic Excitations, *Engineering Structures*, 255, 113906.





# Thank you for your attention and comments!

Dr. Jun Li, Associate Professor  
ARC Future Fellow

Centre for Infrastructure Monitoring and Protection  
School of Civil and Mechanical Engineering  
Curtin University, Australia  
Email: [junli@curtin.edu.au](mailto:junli@curtin.edu.au)